STEREOSELECTIVE CATIONIC POLYMERIZATION OF VINYL ETHERS THROUGH ASYMMETRIC ION-PAIRING CATALYSIS

Travis Peter Varner

A dissertation submitted to the faculty of the University of North Carolina at Chapel Hill in partial fulfillment of the requirements for the degree of Doctor of Philosophy in the Department of Chemistry in the College of Arts and Sciences.

Chapel Hill
2021

Approved by:

Frank Leibfarth

Jeffrey Johnson

Marcey Waters

Jeffrey Aubé

Wei You

ABSTRACT

Travis Peter Varner: Stereoselective Cationic Polymerization of Vinyl Ethers
Through Asymmetric Ion-Pairing Catalysis
(Under the direction of Frank Leibfarth)

I. Background and Introduction

The thermomechanical properties of macromolecules can be directly linked to their tacticity, the relative stereochemistry of repeat units. Herein, the importance of polymer tacticity and strategies for stereoselective polymer synthesis are described. A brief discussion on stereoselective coordination–insertion, coordination–addition, anionic, and cationic polymerization methodologies is included.

II. Mechanistic Insight into Using a Chiral Lewis Acid

We recently demonstrated asymmetric ion pairing catalysis as an effective approach to achieve stereoselective cationic polymerization of vinyl ethers through the use of a chiral Lewis acid. Herein, we provide a deeper understanding of stereoselective ion-pairing polymerization through comprehensive experimental and computational studies. These findings demonstrate the importance of ligand deceleration effects for the identification of reaction conditions that enhance stereoselectivity.

III. Substrate Scope and Copolymerization Using a Chiral Lewis Acid

An evaluation of monomer substrates with systematic variations in steric parameters and functional group identities established key structure−reactivity and structure—property relationships for stereoselective polymerization facilitated by our chiral Lewis acid. This methodology also allowed for successful stereoselective copolymerization, enabling the systematic tuning of both glass transition and melting temperature in copolymers derived from alkyl vinyl ethers. Collectively, these

results highlight the diverse material properties and expanded chemical space that can be accessed by this method.

IV. Catalyst and Monomer Chirality

Catalyst and monomer chirality were thoroughly probed in the cationic polymerization of vinyl ethers enabled by both our chiral Lewis acid system, as well as a novel single component Brønsted acid system based on an imidodiphosphormidate (IDPi) scaffold. In the context of investigating the axial chirality of both catalyst scaffolds, we found that using differing enantiomeric ratios of either catalyst did not result in a change to polymer tacticity. Subsequent studies expanding the monomer scope to include enantioenriched vinyl ethers were then performed, enabling the systematic studying of match-mismatch effects within a polymerization.

V. Using Chiral Hydrogen Bond Donors

Herein, we report the targeted binding of triflate anions with chiral squaramides for the stereoselective cationic polymerization of vinyl ethers. Kinetic investigations reveal a ligand deceleration effect, while temperature dependent stereoselectivity analyses confirm the need for low reaction temperatures. Further, this work represents the first example of anion binding catalysis applied to cationic polymerization, thereby introducing a new mechanistic framework for the continued exploration of stereoselective polymerizations as a whole.

To forging a life worth living

ACKNOWLEDGEMENTS

I'd like to begin by thanking my advisor, Frank Leibfarth, for taking a chance on me. I joined the lab as a naïve chemist who essentially knew nothing about polymers. A few years later, I taught a class on them, and now, I am preparing to defend a Ph.D. on their synthesis. It takes a strong, motivated, thoughtful, and enthusiastic mentor to have enabled that most ambitious crossover event in history. I'm grateful to have grown as a critically thinking researcher, an empowering teacher, and an overall stronger person under his mentorship.

Of course, the lab also comprises many other individuals. I am so grateful for everyone's friendship, scientific support, emotional support, and above all, their constant willingness to go to Linda's for tots. In particular, I am grateful for the original members of the lab: Sally Lewis, Marcus Reis, Jill Williamson Alty, and Aaron Teator. These individuals have seen me at my scientific lowest, and they have always gone out of their way to lend a helpful hand, a listening ear, or a dank meme. Our glow-up from #KenanTrash to #CaudillCash is truly something to be celebrated. I treasure all of the great moments shared with them, and I am honored to have them as friends.

Prior to graduate school, I was incredibly fortunate to have learned from the greatest and goofiest professors that College of Charleston had to offer: Justin Wyatt, Richard Himes, Amy Rogers, and Neal Tonks. Their enthusiasm and approach for education is contagious. They taught me how to ask the important questions and follow those questions through to answers. Teaching someone how to learn is the greatest lesson imaginable, and I'm thankful for receiving this instruction from these individuals. The way they believed in me and built my confidence has inspired me to enter into a career focused on education and mentorship. To this day, I find myself repeating phrases they would often say. My favorite is the following: "It's called research for a reason. If everything worked the first time, it would just be called search."

As I've grown over the past several years, it has become readily apparent the need for a solid core group of friends. I've been so lucky to have established this group of people. To start, Nick Taylor. It's almost scary how much our paths have remained connected (ie: how obsessed he is with me)—from being roommates in two different states to working in the same lab to having hoods right beside each other. He has provided me with so many laughs (especially in the kitchen), and I'm grateful for our friendship. Also in the Triangle area, I am a better person for having befriended Brianna and Richard Eisenreich and Chrissy and Justin Crute. I look forward to many more nights filled with Avalon and contemplating the intricacies of Minnesotan culture. During my time at the College of Charleston (#CougarNation), I made the friends of a lifetime in Ben Stephens, Jamie Claire, Kristin Hoecker, Alexis Violette, Nathan Adamson, Colleen Quass, Dillon Presto, and Elsa Cousins. I have so many amazing memories with these people at Bro House, Ascot Alley, SSMB, Folly Beach, Addlestone, CFB, Juanita's, and all across the Southeast. I know that wherever life takes us, we will remain connected (through embarrassing pictures and in the double bond). To conclude, I go back to the beginning of childhood, where Andrew Carter and Jared Westmoreland emerged as the best friends every kid dreams about having. I cherish all of our memories together and I am thankful for their continued presence in my life.

My family has always stood in unwavering support of me. To my Mom and Dad, nothing that I could say here would even come close to capturing how thankful I am for every single sacrifice they have made to give me a better life. My brother, Kyle Varner, is a model for what all brothers should strive to be. He has always had my back, doing everything he can to look out for me. I am so grateful that he has Heather and Ryan in his life, and I look forward to every moment we get to spend together. Any success that I have is really a success for my entire family. Even though I don't say it often enough, I love and miss them all dearly.

And finally, I would not be anywhere near the person I am today without the unending love and support from my wife, Paige Varner. Every single day, I wake up thankful for all that she is and all that she does. I cannot help but smile every time I think of her, and I am grateful that we have chosen each other as partners in life. On the hardest days in lab, my spirits are lifted by listening to our wedding playlist and knowing that I get to come home to her and Bourbon. I thank her for being my biggest cheerleader, and I look forward to continuing to build our lives together.

TABLE OF CONTENTS

LIST OF FIGURES

LIST OF ABBREVIATIONS AND SYMBOLS

(*S*)-MBVE	(*S*)-2-methylbutyl vinyl ether
(*S*)-SBVE	(*S*)-sec-butyl vinyl ether
°C	degrees Celsius
^{13}C NMR	carbon nuclear magnetic resonance spectroscopy
^{1}H NMR	proton nuclear magnetic resonance spectroscopy
^{31}PNMR	phosphorous nuclear magnetic resonance spectroscopy
Å	Angstrom
AcOVE	acetoxy ethyl vinyl ether
Al	aluminum
Ar	aryl
BF3·OEt_2	boron trifluoride etherate
BINOL	1,1′-bi-2-naphthol
BzOVE	benzoyloxy ethyl vinyl ether
C	catalyst
CAP	coordination–addition polymerization
CCl_4	carbon tetrachloride
$CDCl_3$	deuterated chloroform
CF_3	trifluoromethyl
CH_2Cl_2	dichloromethane
Đ	dispersity
DFT	density functional theory
DSC	differential scanning calorimetry
E_a	activation energy
eq	equivalents

Et_2O	diethyl ether
Et_3N	triethylamine
EtOAc	ethyl acetate
EtOH	ethanol
EVE	ethyl vinyl ether
f_{AcOVE}	molar feed ratio of AcOVE present prior to initiation
f_{Bu}	molar feed ratio of *n*-butyl vinyl ether present prior to initiation
f_{BzOVE}	molar feed ratio of BzOVE present prior to initiation
f_{Et}	molar feed ratio of ethyl vinyl ether present prior to initiation
f_{MOPhOVE}	molar feed ratio of MOPhOVE present prior to initiation
f_{MOVE}	molar feed ratio of MOVE present prior to initiation
f_{PhOVE}	molar feed ratio of PhOVE present prior to initiation
f_{ROVE}	molar feed ratio of ROVE present prior to initiation
F_{AcOVE}	mole fraction of AcOVE incorporated into polymer
F_{Bu}	mole fraction of n-butyl vinyl ether incorporated into polymer
F_{BzOVE}	mole fraction of BzOVE incorporated into polymer
F_{Et}	mole fraction of ethyl vinyl ether incorporated into polymer
F_{MOPhOVE}	mole fraction of MOPhOVE incorporated into polymer
F_{MOVE}	mole fraction of MOVE incorporated into polymer
F_{PhOVE}	mole fraction of PhOVE incorporated into polymer
F_{ROVE}	mole fraction of ROVE incorporated into polymer
g	gram
G	Gibbs free energy
GPC	gel permeation chromatography
h	hour

H	enthalpy
HCl	hydrochloric acid
$Hg(OAc)_2$	mercury acetate
HSQC	heteronuclear single quantum coherence
Hz	hertz
iAVE	isoamyl vinyl ether
iBVE	isobutyl vinyl ether
IDPi	imidodiphosphorimidate
iPP	isotactic poly(propylene)
*i*Pr	isopropyl
iPVE	isopropyl vinyl ether
IR	infrared
J	coupling constant
k	rate
kcal	kilocalorie
kg	kilogram
k_{obs}	observed rate constant
M	molar
m	*meso* diad
r	*racemo* diad
M	monomer
Me	methyl
MeCy	methylcyclohexane
MeOH	methanol
mg	milligram

$MgBr_2$	magnesium bromide
$MgSO_4$	magnesium sulfate
MHz	megahertz
min	minute
mL	milliliter
mM	millimolar
MMA	methyl methacrylate
mmol	millimole
M_n	molar mass
mol	mole
MOPhOVE	2-methoxy-4-methyl-phenoxy ethyl vinyl ether
MOVE	2-methoxy ethyl vinyl ether
N	normal
N_2	nitrogen gas
NaOH	sodium hydroxide
nBVE	*n*-butyl vinyl ether
nPrVE	*n*-propyl vinyl ether
NR	no reaction
OAc	acetate
OcVE	octyl vinyl ether
OMe	methoxide
OTf	triflate
P	polymer
PA	(*R*)-3,3’-bis(3,5-bis(trifluoromethyl)phenyl)-1,1’-binaphthyl phosphate
PDA	photodiode array

Ph	phenyl
PhMe	toluene
PhOVE	phenoxy ethyl vinyl ether
ppm	parts per million
PVE	poly(vinyl ether)
R	often used to denote a “generic” residual substitution
RDS	rate-determining step
RI	refractive index
RMA	butyl, hexyl, or isodecyl methacrylate
ROVE	any substituted oxyethylene vinyl ether
RT	retention time
S	entropy
SiO_2	silicon dioxide
$SnCl_2$	tin (II) chloride
$SnCl_4$	tin (IV) chloride
T	temperature
T	temperature
TADDOL	α,α,α’,α’-tetraaryl-1,3-dioxolane-4,5- dimethanol
*t*BuLi	*tert*-butyllithium
tBVE	*tert*-butyl vinyl ether
TEA	triethylamine
T_g	glass transition temperature
THF	tetrahydrofuran
Ti	titanium
T_m	melting temperature

TMS	trimethylsilyl
UV	ultraviolet
v/v	volume:volume ratio
VE	vinyl ether
α	alpha
β	beta
βMMBL	β-methyl-α-methylene-γ-butyrolactone
γ	gamma
δ	chemical shift
Δ	delta
λ	wavelength

CHAPTER 1: BACKGROUND AND INTRODUCTION

1.1 Importance of the Control of Tacticity

This chapter was adapted in part with permission from *ACS Macro Lett.* **2020,** *9*, 1638−1654.[1]

Much research effort in the field of polymer science has focused on obtaining synthetic control over polymer structure (**Figure 1.1**). In the past several decades, synthetic chemists have developed multiple methods of controlled polymerization to regulate molecular weight and dispersity. These strategies for precision polymer synthesis have enabled the realization of more complex polymer compositions, including block copolymers, comb copolymers, and bottle brush copolymers. By expanding the synthetic toolbox amenable to polymer chemists, the structure space of material properties has likewise dramatically expanded as well. While these past successes are certainly worthy of celebration, it is also important to note that advancements in the control of one aspect of polymer structure, tacticity, has lagged far behind.

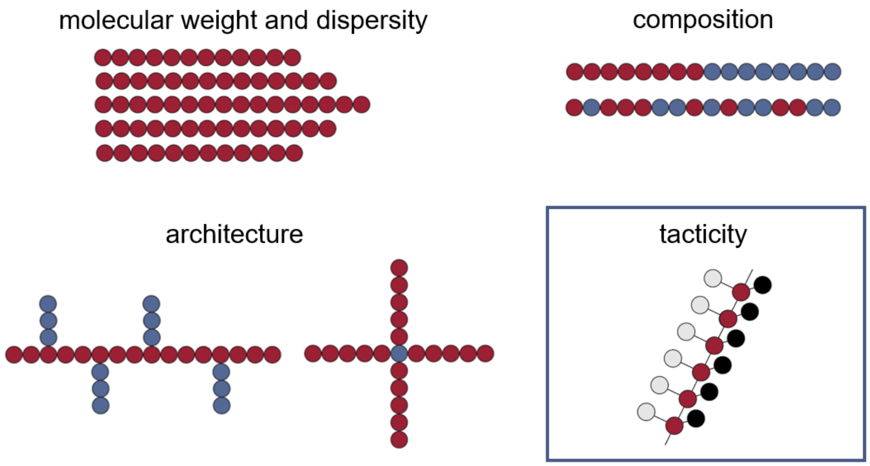

Figure 1.1. Aspects of polymer structure that can be controlled synthetically.

The stereochemical architecture, or tacticity, of a polymer is often a primary determinant of its material properties. As an illustrative example, atactic polypropylene is a viscoelastic fluid of little utility, whereas isotactic polypropylene (iPP) is a low-cost thermoplastic used in automotive, packaging, and structural applications at a volume exceeding 50 million metric tons annually.[2] However, with the exception of iPP and a handful of other polymers, detailed and systematic studies of how main-chain stereochemistry influences physical and mechanical properties are lacking.[3] This is largely a consequence of the lack of stereoselective polymerization methodologies that result from the challenges of biasing facial addition at each monomer enchainment event.

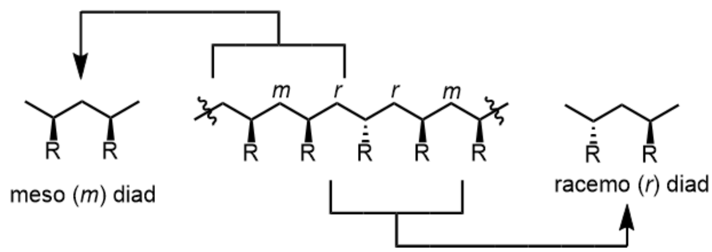

Figure 1.2. The Bovey formulism used to describe polymer tacticity, where *meso* diads (*m*) and *racemo* diads (*r*) are used to indicate enchainment that leads to isotactic diads and syndiotactic diads, respectively.

1.2 Coordination—Insertion Polymerization

By far, the most noteworthy example of stereoselective polymerization is coordination–insertion polymerization. Its use to synthesize iPP represents the largest volume application of asymmetric catalysis.[4] Even though industrial iPP production is still dominated by heterogeneous catalysts, the discovery of homogeneous single-site transition metal catalysts for stereoselective α-olefin polymerization has provided key mechanistic insight into the origin of stereocontrol.[5–8] This fundamental understanding has enabled the tailoring of catalyst coordination environment to precisely control polyolefin microstructure, leading to a dazzling array of thermomechanical properties from only a few α-olefin building blocks.[9–11] The coordination–insertion polymerization mechanisms often utilized to synthesize isotactic poly(α-olefins) rely on the symmetry and ligand geometry of an organometallic complex covalently bound to the growing polymer chain end to facially bias each monomer addition event.[12] By fine tuning the ligands, polyolefins with >99% *mmmm* (see **Figure 1.2** regarding the Bovey formulism used to describe polymer tacticity) can be produced through enantiomorphic site control, whereby the catalyst controls each monomer facial addition event.[13]

This type of stereocontrolled polymerization methodology can be amenable to minor changes in the alkyl substitution of α-olefin monomers. Despite these impressive advances, a long-standing goal has been to incorporate polar functionality into polyolefins to enhance their interfacial properties.[14,15] An intrinsic challenge arises from the irreversible binding of Lewis basic heteroatoms with the electrophilic early transition metal catalysts traditionally used for stereoselective α-olefin polymerization, which often precludes copolymerization with polar monomers.[16] Numerous research groups have investigated protecting group strategies to allow for the copolymerization of polar monomers with their non-polar hydrocarbon analogues. Trimethylsilyl groups, aluminum species, and borane monomers have been utilized to incorporate polar repeat units after post-polymerization reactions.[14] However, these methods generally require the synthesis of exotic monomers containing a several carbon spacer between the polar group of interest and the olefin. In addition, the overall incorporation of these polar monomers is generally less than 5% due to a significant reactivity mismatch with nonpolar olefins.

In attempts to circumvent the need for a protecting group approach, late transition metal catalysts (typically nickel or palladium) that are more amenable to the direct copolymerization of polar vinyl comonomers with ethylene or α-olefins have been explored.[15,17–19] Detailed mechanistic insight elucidating the effects of modulating ligand stereoelectronics has enabled the synthesis of linear, high-molecular weight polyolefins bearing polar functionality. Yet, the incorporations of repeat units bearing Lewis basic functionality are routinely low. Furthermore, efficient control of polymer tacticity while incorporating a variety of polar monomers remains a staggering hurdle.

1.3 Coordination–Addition Polymerization

Despite the limitations of interfacing heteroatom-containing polar monomers with the catalysts used for the coordination–insertion polymerization of nonpolar α-olefins, one research thrust that has seen considerable success is coordination–addition polymerization (CAP). The use of highly active, electron-deficient single-site metal catalysts with enolizable monomers (*e.g.*, methacrylates, acrylamides, etc.) results in a substrate-directed change in mechanism. In the case of CAP, conjugate addition is the key step that facilitates monomer enchainment. For reference, a generic mechanism for CAP is shown in **Figure 1.3**. Coordination of a vinyl monomer, such as methyl methacrylate (MMA), to the cationic ester enolate complex **1.1** is followed by fast intramolecular Michael addition to generate eight-membered ester enolate chelate **1.2**.[20,21] This complex serves as the resting state during the propagation catalytic cycle. Next, a rate-determining associative displacement of the coordinated ester in **1.2** results in ring-opening of the chelate and subsequent coordination of an additional MMA molecule to regenerate the active species.

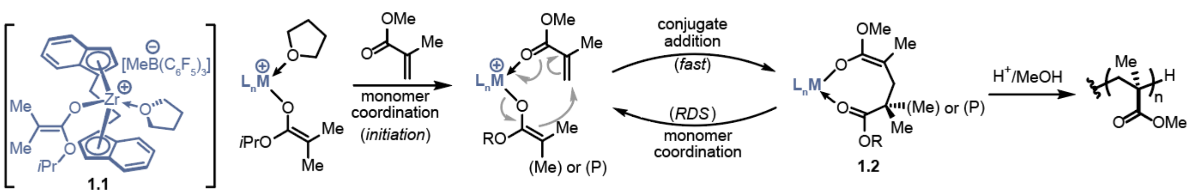

Figure 1.3. The isotactic coordination–addition polymerization of methyl methacrylate using catalyst **1.1**. R = Me or *i*Pr. P = polymer. RDS = rate-determining step.

An array of catalysts has been investigated in stereoselective CAP, with lanthanide- and group IV-based metallocene complexes generally exhibiting the most success. To achieve stereoselectivity in coordination–insertion polymerization, there must be a strong bias for one enantioface of a prochiral α-olefin monomer to react because a stereocenter is set immediately upon monomer insertion.[22] In CAP, however, monomer enchainment yields a prochiral ester enolate chain-end, and the stereochemistry is not set until that chain-end reacts with another prochiral monomer.[23,24]

The symmetry of the catalyst complex is crucial for designing a stereoselective coordination–addition strategy. Although there are exceptions,[25–29] C_2-symmetric[30–36] and C_1-symmetric[28,33,37–40] complexes predominantly engender isotactic polymers, while C_{2v}-symmetric[37,40] and C_s-symmetric complexes[41,42,51,52,43–50] typically give rise to syndiotactic polymers. Steric interactions between the ligands, chain-end, and monomer may all help to facilitate a transition state the leads to stereoselectivity.[23,24,39,53–59] One particularly privileged catalyst scaffold is the C_2-symmetric ethylene-bridged-*ansa*-zirconocenium ester enolate **1.1** (**Figure 1.3**). This complex has been shown to polymerize various methacrylate,[20,35,60–62] acrylamide,[36,56,63,64] and methacrylamide[56] monomers to yield highly-isotactic (≥94% *mm*) polymers via enantiomorphic site control.

By probing the mechanism of this process, CAP has recently made several more significant advancements in the past decade focused on chemoselectivity, stereocomplexation, and biorenewable monomers. Leveraging the requirement for activation of the carbonyl to facilitate conjugate addition, methacrylates and acrylamides bearing pendant vinyl groups have been shown to undergo chemoselective vinyl addition exclusively through the respective methacrylate or acrylamide moiety.[61,65] The unreacted vinyl group has subsequently been explored as a handle for post-polymerization functionalization.[59,61,66]

In addition to chemoselectivity, stereoselective CAP has also provided interesting materials through stereocomplexation. Stereocomplexed poly(MMA) exists as a triple-helix structure (a double helix of isotactic poly(MMA) surrounded by a single helix of syndiotactic poly(MMA)) formed through van der Waals interactions.[67–71] This supramolecular structure exhibits a significantly higher crystallinity and T_m when compared to its individual stereoregular components.[67,68,71] Chen and coworkers recently used a mixture of C_2- and C_s-symmetric zirconocene bis(ester enolate) catalysts in one pot to combine both synthesis and fabrication of stereocomplexed poly(MMA) into a rapid single-step method.[60] Polymer chain exchange between reactive centers was not evident, and real-time dynamic light scattering indicated that efficient stereocomplexation had occurred *in situ* as polymer chains were growing. More recently, stereoselective living CAP and stereocomplexation have been employed to generate thermoplastic elastomers.[62] Using catalyst **1.1**, isotactic ABA triblock copolymers were synthesized with stereocomplexing isotactic poly(MMA) composing the two “hard” end-blocks and non-stereocomplexing isotactic poly(RMA) (where RMA is butyl, hexyl, or isodecyl methacrylate), composing the “soft” mid-block. Subsequent blending of the triblock copolymer with syndiotactic poly(MMA) resulted in the generation of stereocomplexes that aggregate the end-blocks to form crystalline domains and act as strong physical crosslinks.

Finally, recent advances in stereoselective CAP have resulted in an expanded monomer scope that includes biorenewable monomers,[72] particularly the biomass-derived β-methyl-α-methylene-γ-butyrolactone ($_{\beta}$MMBL). This cyclic monomer gives rise to a glassy thermoplastic with greater organic solvent resistance than polymers formed from acyclic methacrylates. A variety of rare-earth[58,73] and group 4[57,74] metal complexes yield highly isotactic (91–99% *mm*) poly($_{\beta}$MMBL) while demonstrating varying polymerization activity. The obtained materials exhibited increasing T_g values concomitant with increasing degrees of stereoselectivity, with the highest tacticity examples (*i.e.*, 99% *mm*) reaching a T_g of 304 °C (**Figure 1.4**). The observed substrate dependence of the method combined with support from computational studies suggest that the formation of an isotactic microstructure chiefly originates from steric interactions involving the methyl group on the β-carbon of the coordinated monomer and the last inserted $_{\beta}$MMBL unit of the chain.

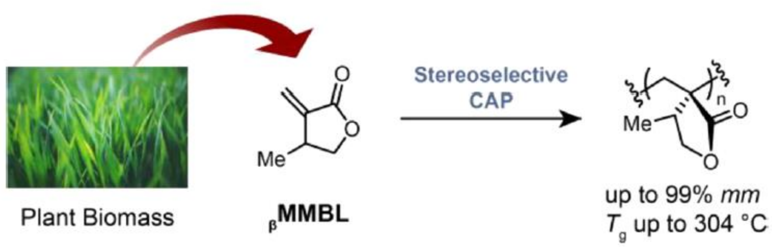

Figure 1.4. Stereoselective CAP of the biomass derived $_{\beta}$MMBL and obtained high performance materials.

1.4 Anionic Polymerization

The overwhelming majority of stereoselective anionic polymerizations rely on a chain-end control mechanism for stereoinduction, whereby the stereochemistry of the last enchained monomer unit heavily biases the facial addition of each subsequently enchained monomer (**Figure 1.5**). In one of the most notable examples, *tert*-butyllithium (*t*BuLi) is used as an initiator.[75] Equimolar quantities of $MgBr_2$ formed during the preparation of the *t*BuLi initiator actually proved to be the key to obtaining high isospecificity (97% *mm*). The magnesium Lewis acid was hypothesized to coordinate to the Lewis basic carbonyls present near the chain end found, encouraging *meso* diad formation via chain-end control.[76] More recently, Al-based additives,[77–85] chiral ligands,[86,87] and even chiral initiators[88–90] have been utilized to synthesize stereoregular polymer structures from anionic polymerization.

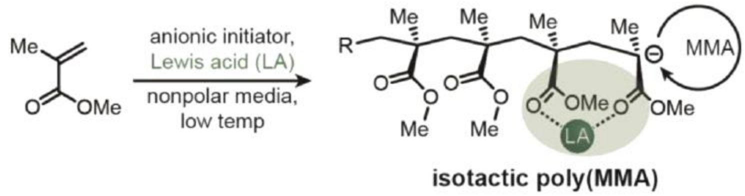

Figure 1.5. Illustration of anionic polymerization via chain-end controlled stereoselective propagation.

1.5 Cationic Polymerization

To put into perspective the difficulty associated with achieving the stereoselective cationic polymerization of prochiral polar vinyl monomers, it is helpful to analyze the propagating chain-ends of common vinyl polymerization mechanisms. (**Figure 1.6**). Coordination–insertion polymerization of α-olefins, which represents the most widely developed stereoselective vinyl polymerization method, features a covalent, organometallic chain end with a well-defined ligand environment. Ligand geometry of the transition metal sterically biases facial addition of incoming monomers to achieve precise control over polymer tacticity. Stereoselective anionic vinyl polymerization, where the chain-end carbanion adopts a trigonal pyramidal geometry with the lone pair occupying a sp^3-hybridized orbital, offers a structured stereochemical environment at the chain end and, therefore, has been successfully exploited for a variety of stereoselective polymerization methods. In this case, the stereochemistry of each repeat unit is established upon monomer addition. In contrast, cationic and radical vinyl polymerizations feature planar sp^2-hybridized carbenium (empty p-orbital) and carbon centered radical (singly occupied p-orbital) chain ends, respectively, which are not stereochemically defined. As such, an additional propagation event is required in order to establish their stereochemistry. The prochiral chain end exhibited in cationic and radical propagation mechanisms is responsible, in part, for the difficulty associated with the development of stereoselective polymerizations that utilize these methodologies.

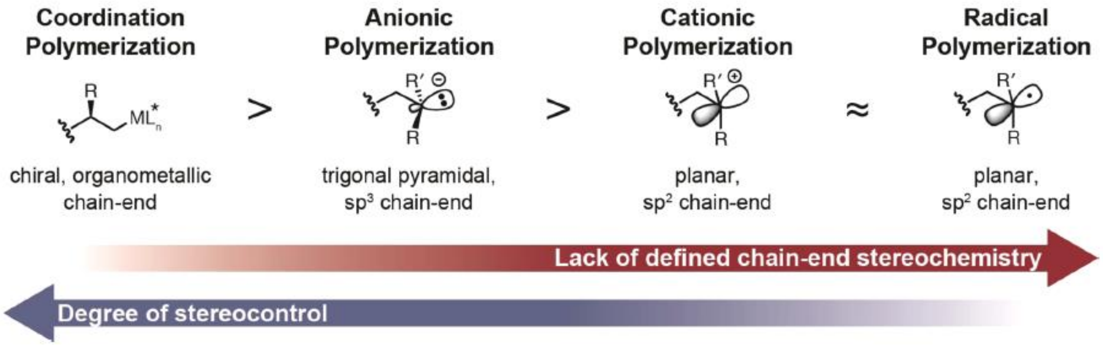

Figure 1.6. Comparison of chain-end stereochemistry between common polymerization mechanisms illustrating the increasing difficulty in controlling tacticity as the chain-end stereochemistry becomes less defined.

Despite these challenges, Schildknecht, who studied the cationic polymerization of vinyl ethers, was one of the first researchers to consider how synthetic polymer stereochemistry could influence material properties. In the late 1940s,[91,92] he discovered that polymerization of isobutyl vinyl ether (iBVE), at cold temperatures (e.g., −78 °C) using $BF_3 \cdot OEt_2$ gave rise to semicrystalline polymers that were substantially harder and tougher than those prepared previously (**Figure 1.7A**). The authors correctly hypothesized at the time that the cis/trans relationship between adjacent pendant alkoxy chains was directly responsible for the differences in polymer crystallinity and, by extension, the observed property differences. Natta and coworkers later utilized X-ray diffraction to confirm that semicrystalline poly(vinyl ether)s were indeed isotactic, while amorphous analogs lacked such stereoregularity.[93–95] Since then, a number of Ziegler-type catalysts,[94–100] non-metallocene and metallocene transition metal catalysts,[101,102] metal-sulfate complexes,[103–105] and others[106–108] have been explored to facilitate semistereoselective polymerization of vinyl ethers.

While the previously mentioned catalytic systems laid a strong initial foundation, stereoselective cationic polymerization to furnish materials with high degrees of tacticity (≥90% *m*) remained challenging. In response, multiple groups continued to design more elaborate catalyst systems. While there is other modern work relating to the stereoregular cationic polymerization of styrenics, N-vinylcarbazole, and oxazolidinone monomers, the bulk of the focus in the literature and in this dissertation will be on vinyl ethers. For example, Sawamoto and coworkers developed a class of phenoxy-bound titanium Lewis acid catalysts (**Figure 1.7B**).[109,110] When used in combination with alkyl chloride initiators in nonpolar solvents, this led to significant improvements in stereoselectivity during the polymerization of iBVE. Specifically, the authors found that the sterically bulky isopropyl groups at the 2,6-positions of the phenoxy ligand were key to achieving highly isotactic (90–92% *m*) poly(iBVE). However, similarly high levels of stereocontrol were not observed when exploring monomers bearing alternate pendant side chains, such as *n*-butyl (76% m), *tert*-butyl (69% m), *iso*-propyl (88% m), *n*-propyl (78% m), and ethyl (64% m) pendant groups.

Sawamoto and coworkers additionally investigated various combinations of protic and Lewis acids for the stereoselective polymerization of vinyl ethers.[111] In the polymerization of iBVE, modest levels of isotacticity (68–86% m) were achieved using $SnCl_4$ combined with a bulky phosphoric acid ligand (**Figure 1.7C**). While typical environmental factors such as solvent dielectric and reaction temperature influenced the degree of stereoinduction, phosphoric acids bearing long alkyl chains (i.e., *n*-decyl) outperformed phenyl, benzyl, and shorter alkyl chains. Despite being outperformed by the previously described Ti–phenoxy complex, this example was a demonstration that counterion structure can have a substantial effect on stereoselectivity during cationic polymerization.

Building upon this precedent, our group recently sought to apply the principles of asymmetric ion-pairing catalysis to cationic polymerization through the design of chiral counterions to induce enantiofacial monomer addition (**Figure 1.7D**).[112] Counterions derived from the combination of enantiopure 1,1-bi-2-naphthol (BINOL)-based phosphoric acids with a Ti-based Lewis acid enabled the synthesis of highly isotactic poly(vinyl ether)s in a catalyst-controlled manner. This chiral Lewis acid system was able to override the conventional chain-end stereochemical control seen in all previous methods of stereoselective cationic polymerization. Further, this general method led to highly isotactic (88–95% *m*) materials from a wide variety of vinyl ether monomers. A series of experiments showed that the obtained materials display the tensile properties of commercial polyolefins, but adhere more strongly to polar substrates by an order of magnitude, indicating their promise for next-generation polar thermoplastics.

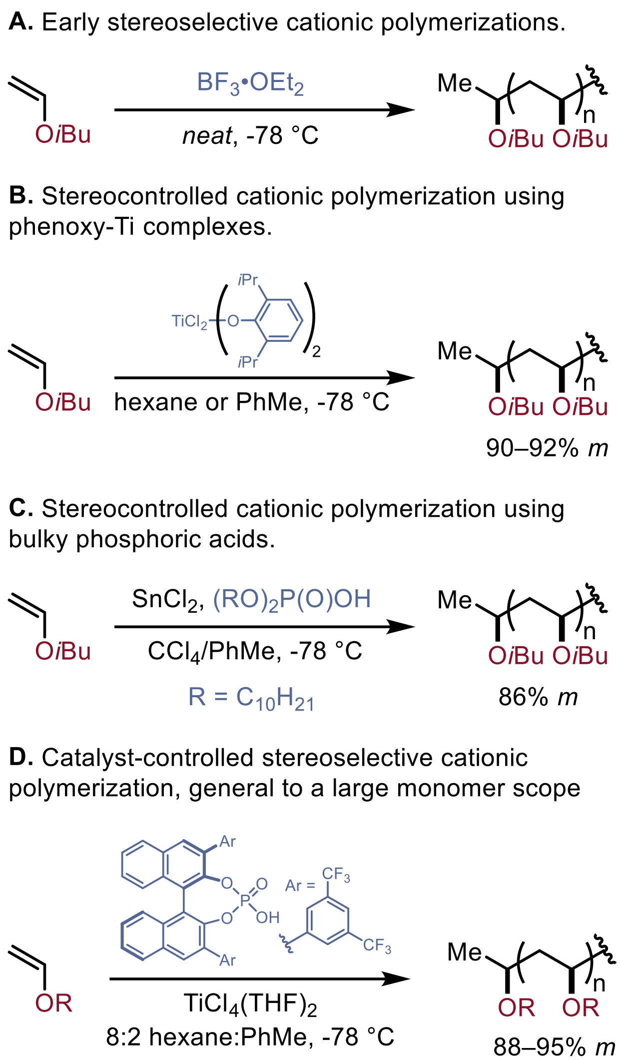

Figure 1.7. Selected examples of stereoselective cationic polymerization.

1.6 Outlook

In order to obtain more complete control over polymer structure and properties, ongoing research in stereoselective polymerization will continue. Additional methods for stereoregular polymer synthesis for a variety of monomers and polymerization mechanisms must be pursued. Likewise, the properties of the stereodefined polymers must also be thoroughly studied in order to enable the application of these materials. In this dissertation, three new synthetic strategies towards the stereoselective cationic polymerization of vinyl ethers are discussed: a chiral Lewis acid, a chiral Bronsted acid, and a chiral hydrogen bond donor. Chapter 2 focuses on the mechanistic probing of the chiral Lewis acid system, while Chapter 3 expands the same method for the stereoselective homo- and copolymerization of a wide variety of vinyl ether monomers. Chapter 4 discusses the role of catalyst and monomer chirality in both the chiral Lewis acid system, as well as the chiral Bronsted acid system. Finally, Chapter 5 reports the use a of chiral hydrogen bond donor to enable the first example of anion binding catalysis applied to stereoselective cationic polymerization.

REFERENCES

(1) Teator, A. J.; Varner, T. P.; Knutson, P. C.; Sorensen, C. C.; Leibfarth, F. A. 100th Anniversary of Macromolecular Science Viewpoint: The Past, Present, and Future of Stereocontrolled Vinyl Polymerization. *ACS Macro Lett.* **2020**, 1638–1654.

(2) Busico, V. Giulio Natta and the Development of Stereoselective Propene Polymerization. *Adv. Polym. Sci.* **2013**, *257*, 37–58.

(3) Worch, J. C.; Prydderch, H.; Jimaja, S.; Bexis, P.; Becker, M. L.; Dove, A. P. Stereochemical Enhancement of Polymer Properties. *Nat. Rev. Chem.* **2019**, *3* (9), 514–535.

(4) Busico, V. Giulio Natta and the Development of Stereoselective Propene Polymerization. *Adv. Polym. Sci.* **2013**, *257*, 37–58.

(5) Brintzinger, H. H.; Fischer, D.; Mülhaupt, R.; Rieger, B.; Waymouth, R. M. Stereospecific Olefin Polymerization with Chiral Metallocene Catalysts. *Angew. Chemie Int. Ed.* **1995**, *34* (11), 1143–1170.

(6) Resconi, L.; Cavallo, L.; Fait, A.; Piemontesi, F. Selectivity in Propene Polymerization with Metallocene Catalysts. *Chem. Rev.* **2000**, *100* (4), 1253–1346.

(7) W. Coates, G. Precise Control of Polyolefin Stereochemistry Using Single-Site Metal Catalysts. *Chem. Rev.* **2000**, *100* (4), 1223–1252.

(8) Tabba, H. D.; Hijji, Y. M.; Abu- Surrah, A. S. *Polyolefin Compounds and Materials: Fundamentals and Industrial Applications*; Al-Ali AlMa'adeed, M., Krupa, I., Eds.; Springer International Publishing: Switzerland, 2016.

(9) Worch, J. C.; Prydderch, H.; Jimaja, S.; Bexis, P.; Becker, M. L.; Dove, A. P. Stereochemical Enhancement of Polymer Properties. *Nat. Rev. Chem.* **2019**, *3*, 514–535.

(10) Domski, G. J.; Rose, J. M.; Coates, G. W.; Bolig, A. D.; Brookhart, M. Living Alkene Polymerization: New Methods for the Precision Synthesis of Polyolefins. *Prog. Polym. Sci.* **2007**, *32*, 30–92.

(11) De Rosa, C.; Auriemma, F.; Di Capua, A.; Resconi, L.; Guidotti, S.; Camurati, I.; E. Nifant'ev, I.; P. Laishevtsev, I. Structure−Property Correlations in Polypropylene from Metallocene Catalysts: Stereodefective, Regioregular Isotactic Polypropylene. *J. Am. Chem. Soc.* **2004**, *126* (51), 17040–17049.

(12) Coates, G. W. Precise Control of Polyolefin Stereochemistry Using Single-Site Metal

Catalysts. *Chem. Rev.* **2000**, *100* (4), 1223–1252.

(13) Miller, S. A.; Bercaw, J. E. Mechanism of Isotactic Polypropylene Formation with C 1-Symmetric Metallocene Catalysts. *Organometallics* **2006**, *25* (15), 3576–3592.

(14) Franssen, N. M. G.; Reek, J. N. H.; de Bruin, B. Synthesis of Functional 'Polyolefins': State of the Art and Remaining Challenges. *Chem. Soc. Rev.* **2013**, *42* (13), 5809–5832.

(15) Keyes, A.; Basbug Alhan, H. E.; Ordonez, E.; Ha, U.; Beezer, D. B.; Dau, H.; Liu, Y. S.; Tsogtgerel, E.; Jones, G. R.; Harth, E. Olefins and Vinyl Polar Monomers: Bridging the Gap for Next Generation Materials. *Angew. Chemie* **-** *Int. Ed.* **2019**, *58* (36), 12370–12391.

(16) Chen, J.; Gao, Y.; Marks, T. J. Early Transition Metal Catalysis for Olefin-Polar Monomer Copolymerization. *Angew. Chemie - Int. Ed.* **2020**, *59*, 2–12.

(17) Camacho, D. H.; Guan, Z. Designing Late-Transition Metal Catalysts for Olefin Insertion Polymerization and Copolymerization. *Chem. Commun.* **2010**, *46* (42), 7879–7893.

(18) Carrow, B. P.; Nozaki, K. Transition-Metal-Catalyzed Functional Polyolefin Synthesis: Effecting Control through Chelating Ancillary Ligand Design and Mechanistic Insights. *Macromolecules* **2014**, *47* (8), 2541–2555.

(19) Guo, L.; Liu, W.; Chen, C. Late Transition Metal Catalyzed α-Olefin Polymerization and Copolymerization with Polar Monomers. *Mater. Chem. Front.* **2017**, *1* (12), 2487–2494.

(20) Rodriguez-Delgado, A.; Y.-X. Chen, E. Mechanistic Studies of Stereospecific Polymerization of Methacrylates Using a Cationic, Chiral Ansa-Zirconocene Ester Enolate. *Macromolecules* **2005**, *38* (7), 2587–2594.

(21) Chen, E. Y. X. Coordination Polymerization of Polar Vinyl Monomers by Single-Site Metal Catalysts. *Chem. Rev.* **2009**, *109* (11), 5157–5214.

(22) Coates, G. W. Precise Control of Polyolefin Stereochemistry Using Single-Site Metal Catalysts. *Chem. Rev.* **2000**, *100* (4), 1223–1252.

(23) Caporaso, L.; Gracia-Budrìa, J.; Cavallo, L. Stereospecificity in Metallocene Catalyzed Acrylate Polymerizations: The Chiral Orientation of the Growing Chain Selects Its Own Chain End Enantioface. *J. Am. Chem. Soc.* **2006**, *128* (51), 16649–16654.

(24) Caporaso, L.; Cavallo, L. Mechanism of Stereocontrol in Methyl Methacrylate Polymerization Promoted by C1-Symmetric Metallocenes. *Macromolecules* **2008**, *41* (10), 3439–3445.

(25) Hong, E.; Kim, Y.; Do, Y. A Neutral Group 4 Poly(Methyl Methacrylate) Catalyst Derived from o-Carborane. *Organometallics* **1998**, *17* (14), 2933–2935.

(26) Hyung Lee, M.; Hwang, J.-W.; Kim, Y.; Kim, J.; Han, Y.; Do, Y. The First Fluorenyl Ansa-Yttrocene Complexes: Synthesis, Structures, and Polymerization of Methyl Methacrylate. *Organometallics* **1999**, *18* (24), 5124–5129.

(27) Qian, C.; Zou, G.; Chen, Y.; Sun, J. Synthesis, Structure, and Catalytic Behavior of Rac-1,1‘-(3-Oxapentamethylene)-Bridged Bis(Indenyl) Ansa-Lanthanidocenes. *Organometallics* **2001**, *20* (14), 3106–3112.

(28) A. Giardello, M.; Yamamoto, Y.; Brard, L.; J. Marks, T. Stereocontrol in the Polymerization of Methyl Methacrylate Mediated by Chiral Organolanthanide Metallocenes. *J. Am. Chem. Soc.* **2002**, *117* (11), 3276–3277.

(29) Jin, J.; Mariott, W. R.; Chen, E. Y. X. Polymerization of Methyl Methacrylate by Metallocene Imido Complexes and Tris(Pentafluorophenyl)Alane. *J. Polym. Sci. Part A Polym. Chem.* **2003**, *41* (20), 3132–3142.

(30) Collins, S.; G. Ward, D.; H. Suddaby, K. Group-Transfer Polymerization Using Metallocene Catalysts: Propagation Mechanisms and Control of Polymer Stereochemistry. *Macromolecules* **1994**, *27* (24), 7222–7224.

(31) Soga, K.; Deng, H.; Yano, T.; Shiono, T. Stereospecific Polymerization of Methyl Methacrylate Initiated by Dimethylzirconocene/B(C6F5)3 (or Ph3CB(C6F5)4)/Zn(C2H5)2. *Macromolecules* **1994**, *27* (26), 7938–7940.

(32) Deng, H.; Shiono, T.; Soga, K. Isospecific Polymerization of Methyl Methacrylate Initiated by Chiral Zirconocenedimethyl/Ph3CB(C6F5)4 in the Presence of Lewis Acid. *Macromolecules* **1995**, *28* (9), 3067–3073.

(33) Cameron, P. A.; Gibson, V. C.; Graham, A. J. On the Polymerization of Methyl Methacrylate by Group 4 Metallocenes. *Macromolecules* **2000**, *33* (12), 4329–4335.

(34) D. Bolig, A.; Y.-X. Chen, E. Reversal of Polymerization Stereoregulation in Anionic Polymerization of MMA by Chiral Metallocene and Non-Metallocene Initiators: A New Reaction Pathway for Metallocene-Initiated MMA Polymerization. *J. Am. Chem. Soc.* **2001**, *123* (32), 7943–7944.

(35) Bolig, A. D.; Chen, E. Y. X. Ansa-Zirconocene Ester Enolates: Synthesis, Structure, Reaction with Organo-Lewis Acids, and Application to Polymerization of Methacrylates. *J. Am. Chem. Soc.* **2004**, *126* (15), 4897–4906.

(36) R. Mariott, W.; Y.-X. Chen, E. Mechanism and Scope of Stereospecific, Coordinative-Anionic Polymerization of Acrylamides by Chiral Zirconocenium Ester and Amide Enolates. *Macromolecules* **2005**, *38* (16), 6822–6832.

(37) Frauenrath, H.; Keul, H.; Höcker, H. Stereospecific Polymerization of Methyl Methacrylate with Single-Component Zirconocene Complexes: Control of Stereospecificity via Catalyst Symmetry. *Macromolecules* **2001**, *34* (1), 14–19.

(38) Stuhldreier, T.; Keul, H.; Höcker, H. A Cationic Bridged Zirconocene Complex as the Catalyst for the Stereospecific Polymerization of Methyl Methacrylate. *Macromol. Rapid Commun.* **2000**, *21* (15), 1093–1098.

(39) Hölscher, M.; Keul, H.; Höcker, H. Postulation of the Mechanism of the Selective Synthesis of Isotactic Poly(Methyl Methacrylate) Catalysed by [Zr{(Cp)(Ind)CMe2}(Me)(Thf)](BPh4): A Hartree - Fock, MP2 and Density Functional Study. *Chem. Eur. J.* **2001**, *7* (24), 5419–5426.

(40) W. Strauch, J.; Fauré, J.-L.; Bredeau, S.; Wang, C.; Kehr, G.; Fröhlich, R.; Luftmann, H.; Erker, G. (Butadiene)Metallocene/B(C6F5)3 Pathway to Catalyst Systems for Stereoselective Methyl Methacrylate Polymerization: Evidence for an Anion Dependent Metallocene Catalyzed Polymerization Process. *J. Am. Chem. Soc.* **2004**, *126* (7), 2089–2104.

(41) Razavi, A.; Ferrara, J. Preparation and Crystal Structures of the Complexes (H5-C5H4CMe2-H5-C13H8) MCl2 (M=Zr, Hf) and Their Role in the Catalytic Formation of Syndiotactic Polypropylene. *J. Organomet. Chem.* **1992**, *435* (3), 299–310.

(42) Razavi, A.; Thewalt, U. Stabilization of a Catalytically Syndiotactic-Specific Metallocene Cation by Trimethylphosphine. The Crystal Structure of [(H5-C5H4)CMe2-H5-(C13H8)ZrMePME3]+ [B(C6F5)4]-. *J. Organomet. Chem.* **1993**, *445* (1–2), 111–114.

(43) Qian, C.; Nie, W.; Sun, J. Cs-Symmetric Ansa-Lanthanocenes Designed for Stereospecific Polymerization of Methyl Methacrylate. Synthesis and Structural Characterization of Silylene-Bridged Fluorenyl Cyclopentadienyl Lanthanide Halides, Amides, and Hydrocarbyls. *Organometallics* **2000**, *19* (20), 4134–4140.

(44) A. Ewen, J.; L. Jones, R.; Razavi, A.; D. Ferrara, J. Syndiospecific Propylene Polymerizations with Group IVB Metallocenes. *J. Am. Chem. Soc.* **2002**, *110* (18), 6255–6256.

(45) Qian, C.; Nie, W.; Chen, Y.; Sun, J. Synthesis and Crystal Structure of One Carbon-Atom Bridged Lutetium Complex [Ph2C(Flu)(Cp)]LuN(TMS)2 and Catalytic Activity for Polymerization of Polar Monomers. *J. Organomet. Chem.* **2002**, *645* (1–2), 82–86.

(46) Nie, W.; Qian, C.; Chen, Y.; Jie, S. Synthesis, Structural Characterization and Catalytic Behavior of One-Atom Bridged Fluorenyl Cyclopentadienyl Lanthanocene Complexes with

CS- or C1-Symmetry. *J. Organomet. Chem.* **2002**, *647* (1–2), 114–122.

(47) Rodriguez-Delgado, A.; R. Mariott, W.; Y.-X. Chen, E. Living and Syndioselective Polymerization of Methacrylates by Constrained Geometry Titanium Alkyl and Enolate Complexes. *Macromolecules* **2004**, *37* (9), 3092–3100.

(48) Kirillov, E.; W. Lehmann, C.; Razavi, A.; Carpentier, J.-F. Synthesis, Structure, and Polymerization Activity of Neutral Halide, Alkyl, and Hydrido Yttrium Complexes of Isopropylidene-Bridged Cyclopentadienyl-Fluorenyl Ligands. *Organometallics* **2004**, *23* (11), 2768–2777.

(49) Rodriguez-Delgado, A.; Mariott, W. R.; Chen, E. Y. X. Synthesis and MMA Polymerization of Chiral Ansa-Zirconocene Ester Enolate Complexes with C2- and Cs-Ligation. *J. Organomet. Chem.* **2006**, *691* (16), 3490–3497.

(50) Ning, Y.; Y.-X. Chen, E. Metallocene-Catalyzed Polymerization of Methacrylates to Highly Syndiotactic Polymers at High Temperatures. *J. Am. Chem. Soc.* **2008**, *130* (8), 2463–2465.

(51) Zhang, Y.; Ning, Y.; Caporaso, L.; Cavallo, L.; Y.-X. Chen, E. Catalyst-Site-Controlled Coordination Polymerization of Polar Vinyl Monomers to Highly Syndiotactic Polymers. *J. Am. Chem. Soc.* **2010**, *132* (8), 2695–2709.

(52) Zhang, Y.; Caporaso, L.; Cavallo, L.; Y.-X. Chen, E. Hydride-Shuttling Chain-Transfer Polymerization of Methacrylates Catalyzed by Metallocenium Enolate Metallacycle−Hydridoborate Ion Pairs. *J. Am. Chem. Soc.* **2011**, *133* (5), 1572–1588.

(53) Hölscher, M.; Keul, H.; Höcker, H. Explanation of the Different Reaction Behaviors of Bridged and Unbridged Cationic Single Component Zirconocene Catalysts in MMA Polymerizations: A Density Functional Study. *Macromolecules* **2002**, *35* (21), 8194–8202.

(54) Tomasi, S.; Weiss, H.; Ziegler, T. Group Transfer Polymerizations of Acrylates Catalyzed by Mononuclear Early D-Block and f-Block Metallocenes: A DFT Study. *Organometallics* **2006**, *25* (15), 3619–3630.

(55) Ning, Y.; Caporaso, L.; Correa, A.; O. Gustafson, L.; Cavallo, L.; Y.-X. Chen, E. Syndioselective MMA Polymerization by Group 4 Constrained Geometry Catalysts: A Combined Experimental and Theoretical Study. *Macromolecules* **2008**, *41* (19), 6910–6919.

(56) Miyake, G.; Caporaso, L.; Cavallo, L.; Y.-X. Chen, E. Coordination−Addition Polymerization and Kinetic Resolution of Methacrylamides by Chiral Metallocene Catalysts. *Macromolecules* **2009**, *42* (5), 1462–1471.

(57) Chen, X.; Caporaso, L.; Cavallo, L.; Y.-X. Chen, E. Stereoselectivity in Metallocene-

Catalyzed Coordination Polymerization of Renewable Methylene Butyrolactones: From Stereo-Random to Stereo-Perfect Polymers. *J. Am. Chem. Soc.* **2012**, *134* (17), 7278–7281.

(58) Hu, Y.; Wang, X.; Chen, Y.; Caporaso, L.; Cavallo, L.; Y.-X. Chen, E. Rare-Earth Half-Sandwich Dialkyl and Homoleptic Trialkyl Complexes for Rapid and Stereoselective Polymerization of a Conjugated Polar Olefin. *Organometallics* **2013**, *32* (5), 1459–1465.

(59) Vidal, F.; Falivene, L.; Caporaso, L.; Cavallo, L.; Y.-X. Chen, E. Robust Cross-Linked Stereocomplexes and C60 Inclusion Complexes of Vinyl-Functionalized Stereoregular Polymers Derived from Chemo/Stereoselective Coordination Polymerization. *J. Am. Chem. Soc.* **2016**, *138* (30), 9533–9547.

(60) Escude, Nicole C.; Ning, Yalan; and Chen, E. Y.-X. In Situ Stereocomplexing Polymerization of Methyl Methacrylate by Diastereospecific Metallocene Catalyst Pairs. *Polym. Chem.* **2012**, *3*, 3247–3255.

(61) Vidal, F.; R. Gowda, R.; Y.-X. Chen, E. Chemoselective, Stereospecific, and Living Polymerization of Polar Divinyl Monomers by Chiral Zirconocenium Catalysts. *J. Am. Chem. Soc.* **2015**, *137* (29), 9469–9480.

(62) Vidal, F.; M. Watson, E.; Y.-X. Chen, E. All-Methacrylic Stereoregular Triblock Co-Polymer Thermoplastic Elastomers Toughened by Supramolecular Stereocomplexation. *Macromolecules* **2019**, *52* (19), 7313–7323.

(63) R. Mariott, W.; Y.-X. Chen, E. Stereospecific, Coordination Polymerization of Acrylamides by Chiral Ansa-Metallocenium Alkyl and Ester Enolate Cations. *Macromolecules* **2004**, *37* (13), 4741–4743.

(64) M. Miyake, G.; R. Mariott, W.; Y.-X. Chen, E. Asymmetric Coordination Polymerization of Acrylamides by Enantiomeric Metallocenium Ester Enolate Catalysts. *J. Am. Chem. Soc.* **2007**, *129* (21), 6724–6725.

(65) Xu, T.; Liu, J.; Lu, X.-B. Highly Active Half-Metallocene Yttrium Catalysts for Living and Chemoselective Polymerization of Allyl Methacrylate. *Macromolecules* **2015**, *48* (20), 7428–7434.

(66) Vidal, F.; Chen, E. Y. X. Precision Polymer Synthesis via Chemoselective, Stereoselective, and Living/Controlled Polymerization of Polar Divinyl Monomers. *Synlett* **2017**, *28* (9), 1028–1039.

(67) te Nijenhuis, K. Poly(Vinyl Methacrylate). *Adv. Polym. Sci.* **1997**, *130*, 67–81.

(68) Hatada, K.; Kitayama, T. Structurally Controlled Polymerizations of Methacrylates and

Acrylates. *Polym. Int.* **2000**, *49* (1), 11–47.

(69) Kumaki, J.; Kawauchi, T.; Okoshi, K.; Kusanagi, H.; Yashima, E. Supramolecular Helical Structure of the Stereocomplex Composed of Complementary Isotactic and Syndiotactic Poly(Methyl Methacrylate)s as Revealed by Atomic Force Microscopy. *Angew. Chem., Int. Ed.* **2007**, *46* (28), 5348–5351.

(70) Kumaki, J.; Kawauchi, T.; Ute, K.; Kitayama, T.; Yashima, E. Molecular Weight Recognition in the Multiple-Stranded Helix of a Synthetic Polymer without Specific Monomer–Monomer Interaction. *J. Am. Chem. Soc.* **2008**, *130* (20), 6373–6380.

(71) Christofferson, A. J.; Yiapanis, G.; Ren, J. M.; Qiao, G. G.; Satoh, K.; Kamigaito, M.; Yarovsky, I. Molecular Mapping of Poly(Methyl Methacrylate) Super-Helix Stereocomplexes. *Chem. Sci.* **2015**, *6* (2), 1370–1378.

(72) Vidal, F.; Y.-X. Chen, E. Reactivity of Bridged and Nonbridged Zirconocenes toward Biorenewable Itaconic Esters and Anhydride. *Organometallics* **2017**, *36* (15), 2922–2933.

(73) Hu, Y.; Miyake, G. M.; Wang, B.; Cui, D.; Chen, E. Y. X. Ansa-Rare-Earth-Metal Catalysts for Rapid and Stereoselective Polymerization of Renewable Methylene Methylbutyrolactones. *Chem. Eur. J.* **2012**, *18* (11), 3345–3354.

(74) Gowda, R. R.; Caporaso, L.; Cavallo, L.; Chen, E. Y. X. Unusual C-C Bond Cleavage in the Formation of Amine-Bis(Phenoxy) Group 4 Benzyl Complexes: Mechanism of Formation and Application to Stereospecific Polymerization. *Organometallics* **2014**, *33* (15), 4118–4130.

(75) Hatada, K.; Ute, K.; Tanaka, K.; Kitayama, T.; Okamoto, Y. Preparation of Highly Isotactic Poly(Methyl Methacrylate) of Low Polydispersity. *Polym. J.* **1985**, *17* (8), 977–980.

(76) Hatada, K.; Ute, K.; Katsuji, K.; Okamoto, Y.; Kitayama, T. Living and Highly Isotactic Polymerization of Methyl Methacrylate by T-C4h9MgBr in Toluene. *Polym. J.* **1986**, *18* (12), 1037–1047.

(77) Kitayama, T.; Shinozaki, T.; Masuda, E.; Yamamoto, M.; Hatada, K. Highly Syndiotactic Poly(Methyl Methacrylate) with Narrow Molecular Weight Distribution Formed by Tert-Butyllithium-Trialkylaluminium in Toluene. *Polym. Bull.* **1988**, *20* (6), 505–510.

(78) Kitayama, T.; Shinozaki, T.; Sakamoto, T.; Yamamoto, M.; Hatada, K. Living and Highly Syndiotactic Polymerization of Methyl Methacrylate and Other Methacrylates by Tert-Butyllithiumtrialkylaluminium in Toluene. *Die Makromol. Chemie Suppl.* **1989**, *15* (S19891), 167–185.

(79) Hatada, K.; Kitayama, T.; Ute, K.; Nishiura, T. Polymers of α- and β-Substituted Acrylates

with Controlled Structures. *Macromol. Symp.* **1995**, *89* (1), 465–478.

(80) Kitayama, T.; Hirano, T.; Zhang, Y.; Hatada, K. Highly Heterotactic Polymerization of Methacrylates - Higher Order Stereoregulation and Stereochemical Significance. *Macromol. Symp.* **1996**, *107* (1), 297–306.

(81) Schlaad, H.; Müller, A. H. E. Effect of Bulkiness and Lewis Acidity of Aluminium Compounds on the Anionic Polymerization of Methyl Methacrylate in Toluene. *Macromol. Symp.* **1996**, *107* (1), 163–176.

(82) Kitayama, T.; Hirano, T.; Hatada, K. Remarkable Effect of Structure of Bulky Aluminum Phenoxides on Stereospecificity of Methacrylate Polymerization. *Tetrahedron* **1997**, *53* (45), 15263–15279.

(83) Bolig, A. D.; Chen, E. Y. X. Reversal of Polymerization Stereoregulation in Anionic Polymerization of MMA by Chiral Metallocene and Non-Metallocene Initiators: A New Reaction Pathway for Metallocene-Initiated MMA Polymerization. *J. Am. Chem. Soc.* **2001**, *123* (32), 7943–7944.

(84) Kitayama, T.; Kitaura, T. Anionic Polymerization of Methyl Methacrylate with Lithium N-Benzyltrimethylsilylamide. *Polym. J.* **2003**, *35* (6), 539–543.

(85) Rodriguez-Delgado, A.; Chen, E. Y. X. Single-Site Anionic Polymerization. Monomeric Ester Enolaluminate Propagator Synthesis, Molecular Structure, and Polymerization Mechanism. *J. Am. Chem. Soc.* **2005**, *127* (3), 961–974.

(86) Vogt, B.; Wulff, G. Optically Active Living Dimers As Initiators For The Asymmetric Polymerization Of Tritylmethacrylate . *Polym. Prepr. (American Chem. Soc. Div. Polym. Chem.* **1989**, *30* (2), 406–407.

(87) Nakano, T.; Okamoto, Y.; Hatada1, K. Asymmetric Polymerization of Triphenylmethyl Methacrylate Leading to a One-Handed Helical Polymer: Mechanism of Polymerization. *J. Am. Chem. Soc.* **1992**, *114*, 1318–1329.

(88) Nagai, D.; Sudo, A.; Endo, T. Stereocontrolled Anionic Alternating Copolymerization of Ethylphenylketene with Benzaldehyde by a Bisoxazoline Ligand. *J. Polym. Sci. Part A Polym. Chem.* **2004**, *42* (21), 5384–5388.

(89) Iizuka, S.; Nakagaki, N.; Uno, T.; Kubo, M.; Itoh, T. Stereocontrol of Optically Active Polymer by Asymmetric Anionic Polymerization of 7-Cyano-7-Ethoxycarbonyl-1,4-Benzoquinone Methide. *Macromolecules* **2010**, *43* (17), 6962–6967.

(90) Hu, W.; Cao, J.; Huang, Y. ling; Liang, S. Asymmetric Polymerization of N-Vinylcarbazole

with Optically Active Anionic Initiators. *Chinese J. Polym. Sci.* **2015**, *33* (11), 1618–1624.

(91) Schildknecht, C. E.; Zoss, A. O.; McKinley, C. Vinyl Alkyl Ethers. *Ind. Eng. Chem.* **1947**, *39* (2), 180–186.

(92) Schildknecht, C. E.; Gross, S. T.; Davidson, H. R.; Lambert, J. M.; Zoss, A. O. Polyvinyl Isobutyl Ethers. *Ind. Eng. Chem.* **1948**, *40* (11), 2104–2115.

(93) Natta, G.; Pino, P.; Corradini, P.; Danusso, F.; Moraglio, G.; Mantica, E.; Mazzanti, G. Crystalline High Polymers of α-Olefins. *J. Am. Chem. Soc.* **1955**, *77* (6), 1708–1710.

(94) Natta, V. G.; Bassi, I.; Corradini, P. Über Die Kettenstruktur Des Kristallinen Polyvinylisobutyläthers. *Die Makromol. Chemie* **1956**, *18* (1), 455–462.

(95) Natta, G. Stereospecific Polymerizations. *J. Polym. Sci.* **1960**, *48*, 219–239.

(96) Natta, G.; Pino, P.; Corradini, P.; Danusso, F.; Moraglio, G.; Mantica, E.; Mazzanti, G. Crystalline High Polymers of α-Olefins. *J. Am. Chem. Soc.* **1955**, *77* (6), 1708–1710.

(97) Lal, J. Polymerization of Vinyl Ethers by Ziegler Catalysts. *J. Polym. Sci.* **1958**, *31* (122), 179–181.

(98) Vandenberg, E. J.; Heck, R. F.; Breslow, D. S. Crystalline Vinyl Ether Polymers. *J. Polym. Sci.* **1959**, *41* (138), 519–520.

(99) Vandenberg, E. J. The Stereoregular Polymerization of Vinyl Ethers with Transition Metal Catalysts. *J. Polym. Sci. Part C Polym. Symp.* **1963**, *1* (1), 207–236.

(100) Ohgi, H.; Sato, T. Highly Isotactic Poly(Vinyl Alcohol). III: Heterogeneous Cationic Polymerization of Tert-Butyl Vinyl Ether. *Polymer (Guildf).* **2002**, *43* (13), 3829–3836.

(101) Roch, K. M.; Saunders, J. Crystalline Polyisobutyl Vinyl Ether. *J. Polym. Sci.* **1959**, *38* (134), 554–555.

(102) Kawaguchi, T.; Sanda, F.; Masuda, T. Polymerization of Vinyl Ethers with Transition-Metal Catalysts: An Examination of the Stereoregularity of the Formed Polymers. *J. Polym. Sci. Part A Polym. Chem.* **2002**, *40* (22), 3938–3943.

(103) Lal, J.; Mcgrath, J. E. Stereoregular Polymerization of Vinyl Alkyl Ethers with Metal Sulfate-Sulfuric Acid Complex Catalysts Reaction of Ferric Sulfate with Sulfuric Acid. *J. Polym. Sci. Part A Polym. Chem.* **1964**, *2*, 3369–3386.

(104) Hirokawa, Y.; Higashimura, T. Stereochemistry in Cationic Polymerization of Alkenyl Ethers. II. Formation of Poly(Β-Substituted Vinyl Ether)s with Erythro-Meso Structures. *J. Polym. Sci. Polym. Chem.* **1979**, *17* (5), 1473–1481.

(105) Kanazawa, A.; Kanaoka, S.; Aoshima, S. A Stepping Stone to Stereospecific Living Cationic Polymerization: Cationic Polymerization of Vinyl Ethers Using Iron(II) Sulfate. *J. Polym. Sci. Part A Polym. Chem.* **2010**, *48* (16), 3702–3708.

(106) Kamigaito, M.; Maeda, Y.; Sawamoto, M.; Higashimura, T. Living Cationic Polymerization of Isobutyl Vinyl Ether by Hydrogen Chloride/Lewis Acid Initiating Systems in the Presence of Salts: In-Situ Direct NMR Analysis of the Growing Species1. *Macromolecules* **1993**, *26*, 1643–1649.

(107) Aoshima, S.; Ito, Y.; Kobayashi, E. Stereoregularity of Poly(Vinyl Ether)s with a Narrow Molecular Weight Distribution Obtained by the Living Cationic Polymerization. *Polym. J.* **1993**, *25*, 1161–1168.

(108) Terada, Y.; Kanaoka, S.; Higashimura, T. Living Cationic Polymerization of N-Butyl Propenyl Ether. *J. Polym. Sci. Part A Polym. Chem.* **2000**, *38*, 229–236.

(109) Ouchi, M.; Kamigaito, M.; Sawamoto, M. Stereoregulation in Cationic Polymerization by Designed Lewis Acids. 1. Highly Isotactic Poly(Isobutyl Vinyl Ether) with Titanium-Based Lewis Acids. *Macromolecules* **1999**, *32* (20), 6407–6411.

(110) Ouchi, M.; Kamigaito, M.; Sawamoto, M. Stereoregulation in Cationic Polymerization by Designed Lewis Acids. II. Effects of Alkyl Vinyl Ether Structure. *J. Polym. Sci. Part A Polym. Chem.* **2001**, *39*, 1060–1066.

(111) Ouchi, M.; Sueoka, M.; Kamigaito, M.; Sawamoto, M. Stereoregulation in Cationic Polymerization. III. High Isospecificity with the Bulky Phosphoric Acid [(RO) 2 PO 2 H]/ SnCl 4 Initiating Systems: Design of Counteranions via Initiators. *J. Polym. Sci. Part A Polym. Chem.* **2001**, *39*, 1067–1074.

(112) Teator, A. J.; Leibfarth, F. A. Catalyst-Controlled Stereoselective Cationic Polymerization of Vinyl Ethers. *Science.* **2019**, *363*, 1439–1443.

CHAPTER 2: MECHANISTIC INSIGHT INTO USING A CHIRAL LEWIS ACID

2.1 Introduction

This chapter was adapted in part with permission from *J. Am. Chem. Soc.* **2020,** *142*, 17175–17186.[1]

Due to the limitations of coordination—insertion and coordination—addition polymerization, the polymerization of polar vinyl monomers is typically conducted by radical or ionic mechanisms, where the propagating chain-end is a prochiral reactive intermediate with no obvious mode for biasing facial addition of monomer. Stereoselective polymerization in the context of these methods has traditionally been accomplished by chain-end control, whereby the stereochemistry of the last enchained monomer influences the facial addition of the next monomer (**Figure 2.1A**).[2–6] While this approach provides stereoregular polymers in a number of cases, the level of stereoselectivity achieved

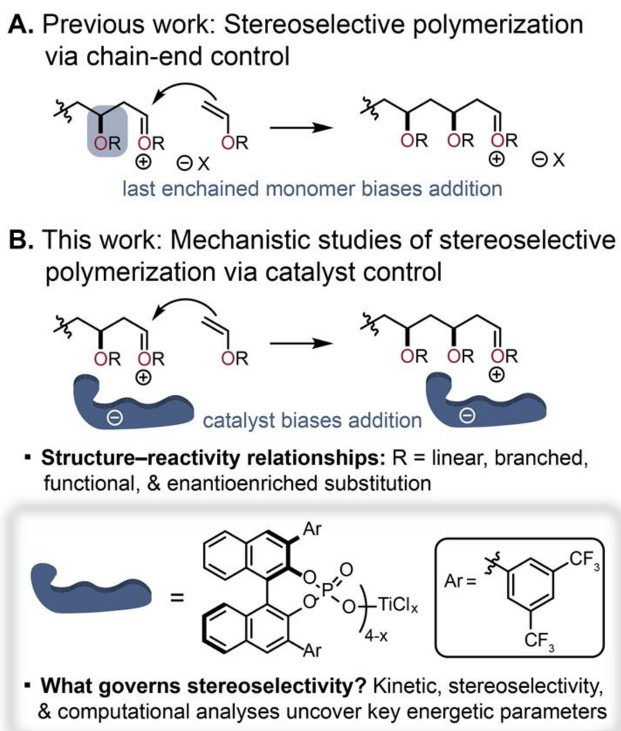

Figure 2.1. Approaches for the stereoselective polymerization of vinyl ether monomers.

is intrinsically linked to the steric demands of each individual substrate and therefore not broadly applicable, even within a monomer class.

Drawing inspiration from many synthetic pathways that involve asymmetric additions into oxocarbenium ions,[7–11] we recently reported a general approach for the stereoselective cationic polymerization of vinyl ethers (**Figure 2.1B**). In this system, stereoselectivity arises as a result of a chiral Lewis acid counterion derived from $TiCl_4(THF)_2$ and 3,3'-bis(3,5-bis(trifluoromethyl)phenyl)-1,1'-binaphthyl phosphate.[12] In the polymerization of isobutyl vinyl ether (iBVE), the integration of the backbone methylene resonances via ^{13}CNMR (39 to 42 ppm, $CDCl_3$) revealed a polymer with 91% *m* (**Figure 2.2**), a dramatic improvement over the analogous control polymerization absent of the chiral phosphate ligand (73% *m*). Further analysis of triad tacticity using Markovian statistics suggested an overwhelming preference for catalyst-controlled stereoselectivity, otherwise known as enantiomorphic site control.[2,13–16] In contrast to alternative methods for stereoselective vinyl ether polymerization,[4,17–25] our catalyst-controlled approach was broadly applicable to a variety of alkyl vinyl ether monomers, whose polymerization resulted in diverse thermomechanical properties.

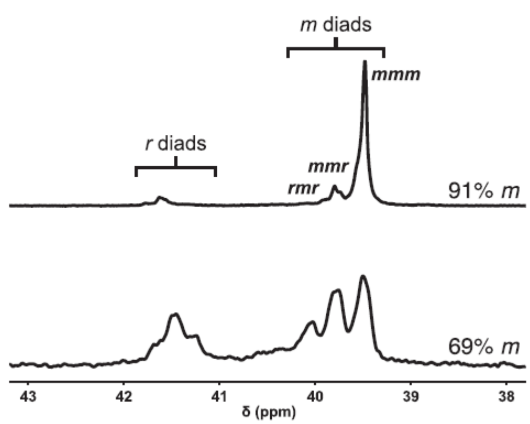

Figure 2.2. Differences in salient ^{13}C NMR resonances observed in atactic (69% *m*) and isotactic (91% *m*) poly(iBVE) samples.

Expanding the scope and utility of this method necessitates deeper mechanistic investigations, similar to those which have enabled the recent advancements in photocontrolled cationic polymerization.[26–32] As such, our current mechanistic hypothesis is depicted in **Figure 2.3**. Addition of chiral BINOL-based phosphoric acid (*R*)-**2.1** to a solution of $TiCl_4$ in toluene results in ligand exchange to generate a chiral Lewis acid (*R*)-**2.2** concomitant with the release of HCl (Step I). Upon addition of vinyl ether monomer to this reaction solution, Markovnikov addition of HCl to the vinyl ether yields alkyl chloride **2.3**, which has been previously validated as an initiating species (Step II).[12] Chloride abstraction from **2.3** generates an anionic titanium species (*R*)-**2.4** along with oxocarbenium ion **2.5** (Step III), which serves as the active species for propagation. A low dielectric solvent facilitates a tight ion pair between (*R*)-**2.4** and **2.5**, enabling selective facial addition of each incoming monomer to the prochiral chain end (Step IV). Finally, chloride transfer from the anionic titanium species (*R*)-**2.4** caps the polymer chain end and regenerates the active catalyst (Step V).

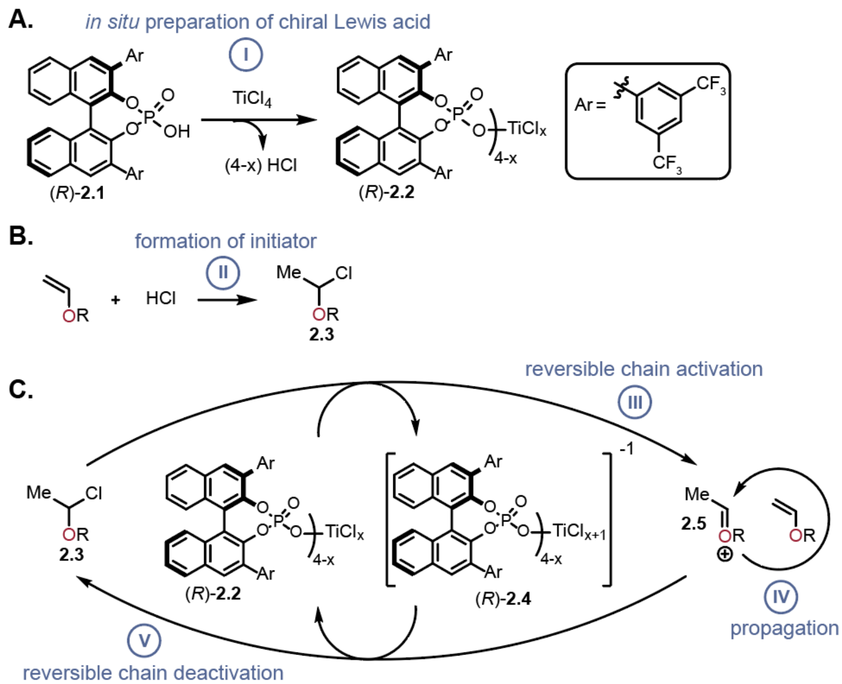

Figure 2.3. Proposed mechanism for the stereoselective polymerization of vinyl ethers.

While our initial work established ion-pairing catalysis as a successful conceptual approach for stereoselective cationic polymerization, a deeper understanding of polymerization mechanism and catalyst identity is required to design improved systems and expand ion-pairing catalysis to a broader range of building blocks. Herein, we use a combination of kinetic investigations, temperature dependent stereoselectivity analyses, and computational studies to probe the elementary steps of the polymerization and to gain insight into catalyst solution structure. The culmination of data reveals key criteria for stereoselectivity in vinyl ether polymerization and ultimately informs an expansion of the monomer scope of this method.

2.2 Kinetic Analysis

Comparative analysis of vinyl ether polymerization kinetics identified key mechanistic insight that informed the selection of optimal stereoselective reaction conditions. Isobutyl vinyl ether (iBVE) was selected as a representative vinyl ether substrate for comparative analysis, and kinetic studies were conducted using *in situ* infrared (IR) spectroscopy to monitor the disappearance of the olefin signal at 1610 cm^{-1} throughout the course of the reaction. The stereoselective polymerization of iBVE using chiral Lewis acid (*R*)-**2.2** ([iBVE] = 0.38 M, [(*R*)-**2.1**] = 5.0 mM, [$TiCl_4$] = 1.0 mM) was compared to a control polymerization catalyzed by achiral $TiCl_4$ in the absence of Brønsted acid *(R)*-**2.1**. Our mechanistic hypothesis includes the endogenous formation of HCl, and thus initiating species **2.3**, under the stereoselective polymerization conditions. Since this does not happen in the polymerization catalyzed by $TiCl_4$ alone, **2.3** was synthesized separately and added to the polymerization ([iBVE] = 0.38 M, [**2.3**] = 5.0 mM, [$TiCl_4$] = 1.0 mM).

Initial rates of the two polymerizations displayed pseudo-first order reaction kinetics in both cases, consistent with previous observations for cationic polymerization.[33–35] The rate constant of conditions that result in stereoselective polymerization, $k_{obs} = 1.0 \times 10^{-3}$ s^{-1}, was eight times slower than that of the control polymerization, $k_{obs} = 8.0 \times 10^{-3}$ s^{-1} (**Figure 2.4A**). This significant decrease in rate observed with the addition of (*R*)-**2.1** represents a case of ligand decelerated catalysis.[36–39] The observed ligand deceleration fits with two notable previously reported empirical observations. First, the addition of $TiCl_4$ to a solution of iBVE and (*R*)-**2.1** resulted in diminished stereoselectivity (82% *m*), compared to an analogous reaction where $TiCl_4$ and (*R*)-**2.1** were pre-mixed and iBVE was subsequently introduced (87% *m*). Second, the addition of excess ligand (*R*)-**2.1** resulted in increased stereoselectivity, with at least five equivalents of (*R*)-**2.1** compared to $TiCl_4$ required to obtain the highest selectivity. In both of these observations, the quantity of free $TiCl_4$ is minimized, thus suppressing the faster, undesired non-stereoselective background reaction.

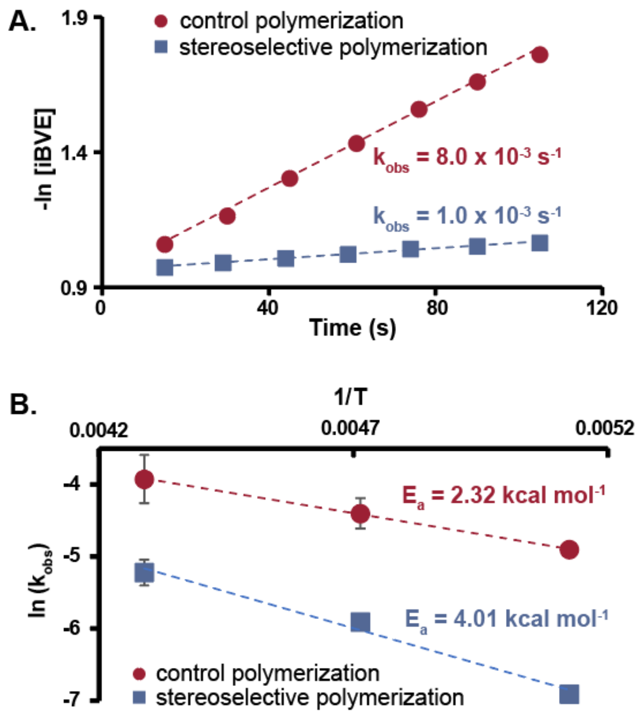

Figure 2.4. A) Kinetic analysis of iBVE polymerization (2.25 mmol scale) at -78 °C under stereoselective conditions (blue squares; [iBVE] = 0.38 M, [(*R*)-**2.1**] = 5.0 mM, [$TiCl_4$] = 1.0 mM) and control conditions (red circles; [iBVE] = 0.38 M, [**2.3**] = 5.0 mM, [$TiCl_4$] = 1.0 mM). Data reported is the median k_{obs} achieved for each set of conditions. B) Arrhenius analysis of stereoselective polymerization conditions (blue squares; [iBVE] = 0.38 M, [(*R*)-**2.1**] = 5.0 mM, [$TiCl_4$] = 1.0 mM) and control polymerization conditions (red circles; [iBVE] = 0.38 M, [**2.3**] = 5.0 mM, [$TiCl_4$] = 1.0 mM) performed on a 2.25 mmol scale. Data reported at each temperature is the average of three individual polymerizations.

Quantitative comparisons of the energy required for monomer addition were obtained by monitoring the kinetics of polymerization by *in situ* IR at different temperatures. An Arrhenius plot of the natural log of k_{obs} as a function of reciprocal temperature yielded a straight line and allowed the derivation of the activation energy (E_a) for polymerization (**Figure 2.4B**). A significant increase in E_a was observed for the stereoselective polymerization (E_a = 4.01 kcal/mol) relative to the control reaction (E_a = 2.32 kcal/mol). This quantitative data fits our hypothesis of ligand decelerated catalysis upon addition of (*R*)-**2.1** to $TiCl_4$. Additionally, the low values for E_a in both polymerizations corroborate the rapid kinetics observed in cationic vinyl ether polymerization.

2.3 Stereoselectivity Analysis

Our previous optimization studies demonstrated a temperature effect on stereoselective polymerization, wherein lower temperatures resulted in enhanced stereoselectivity. In order to gain a quantitative understanding of the influence of temperature on stereoselectivity, an Eyring analysis[40–44] was performed according to a modification of the Eyring equation (Equation 2.1) by plotting the natural log of the ratio of *meso*:*racemo* diads vs. the reciprocal temperature at which the polymerizations were conducted (**Figure 2.5A**).

$$\ln\left(\frac{\%\, m}{\%\, r}\right) = \frac{-\Delta\Delta \mathrm{H}^{\ddagger}}{\mathrm{RT}} + \frac{\Delta\Delta S^{\ddagger}}{\mathrm{R}} \qquad (2.1)$$

From the Eyring analysis, the difference in the energy between diastereomeric transition states ($\Delta\Delta G^{\ddagger}$) can be extracted. We chose to use (*R*)-**2.2** as the chiral Lewis acid for these studies, which achieves 87% *m* at –78 °C. While the use of a chiral Lewis acid derived from (*R*)-**2.1** and $TiCl_4(THF)_2$ achieves higher tacticity (91% *m* at –78 °C), this system is more temperature sensitive and did not result in high molecular weight polymers over a broad temperature range, which made temperature dependent analysis impractical. Polymerizations were not evaluated above –40 °C because the reaction results in only oligomeric products, presumably due to a high degree of chain transfer events commonly observed in cationic polymerizations.[45]

The linear relationship observed for both the stereoselective and control polymerizations demonstrate that neither the overall mechanism nor the rate determining step changes between –78 °C and –40 °C. The control polymerization catalyzed by $TiCl_4$ achieves 71% *m* at –78 °C, which results in a $\Delta\Delta G^{\ddagger}$ of –0.43 kcal/mol; the significant stereoinduction is attributed to a chain-end control effect, which is commonly observed for Lewis acid catalyzed polymerizations of vinyl ethers.[45,46] The polymerization facilitated by chiral Lewis acid (*R*)-**2.2** at -78 °C was found to have a $\Delta\Delta G^{\ddagger}$ of –0.73 kcal/mol and a corresponding stereoselectivity of 87% *m*, confirming a preference towards *meso* diad formation. Therefore, addition of (*R*)-**2.1** to $TiCl_4$ increases the kinetic barrier differentiating *meso* vs. *racemo* addition by 0.30 kcal/mol, resulting in an increase of 16% *m* (**Figure 2.5B**).

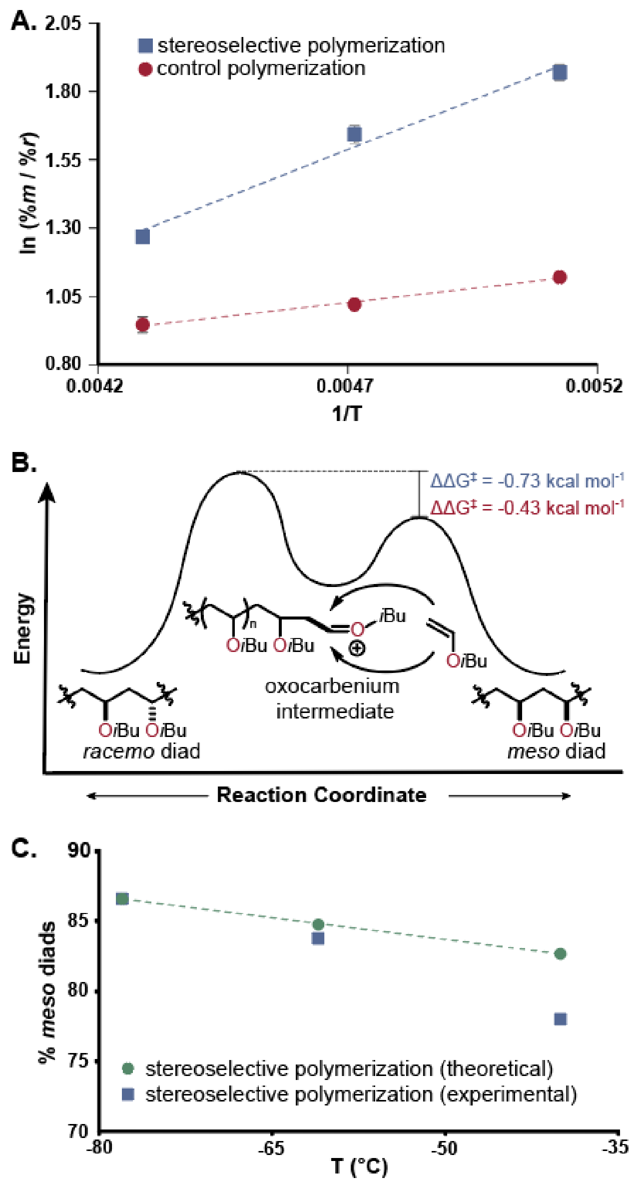

Figure 2.5. A) Eyring analysis of both the stereoselective polymerization (blue squares; [iBVE] = 0.38 M, [(*R*)-**2.1**] = 5.0 mM, [$TiCl_4$] = 1.0 mM) and the control polymerization (red circles; [iBVE] = 0.38 M, [**2.3**] = 5.0 mM, [$TiCl_4$] = 1.0 mM) performed on a 2.25 mmol scale. Each data point represents the average of three polymerizations. **B**) Representative reaction coordinate diagram illustrating the greater energetic preference for *meso* diad formation during stereoselective polymerization. **C**) Theoretical model of stereoselectivity assuming only two diastereomeric reaction pathways and experimental data demonstrating the deviation from theory via other less stereoselective pathways.

Accurate determination of $\Delta\Delta G^{\ddagger}$ in this context assumes that only two diastereomeric reaction pathways contribute to the outcome of the reaction (*i.e.* the addition of a monomer to the polymer chain end to achieve either a *meso* or *racemo* diad).[40,47,48] To probe the magnitude of contributions from alternative reaction pathways, the experimental tacticity observed at –78 °C was used to calculate $\Delta\Delta G^{\ddagger}$ according to Equation 2.2. Using this energetic value, a theoretical % *m versus* temperature line was graphed assuming a purely two-state model.

$$\Delta\Delta G^{\ddagger} = -RT\ln\left(\frac{\%\,m}{\%\,r}\right) \qquad (2.2)$$

As shown in **Figure 2.5C**, the agreement between the experimental and theoretical data is strong at colder temperatures, indicating that a majority of monomer addition is influenced by chiral counterion *(R)*-**2.4**. As temperature increases, the deviation from theory grows, suggesting that an increasing portion of monomer addition is the result of a Ti species that is not the preferred catalyst. The contributions of these less-stereoselective catalytic pathways are presumably exaggerated due to the ligand-deceleration effect of (*R*)-**2.1** (*vide supra*).

The small energetic difference that favors stereoselectivity and the known oxophilicity of titanium Lewis acid complexes motivated us to investigate whether dynamic non-linear effects, resulting from catalyst–product or catalyst–substrate interactions, cause stereoselectivity to vary during the course of the polymerization.[49] The experimental approach involved quenching aliquots of a polymerization at various time points and measuring reaction conversion and tacticity by ^{1}H and ^{13}C NMR, respectively. As shown in **Figure 2.6**, the tacticity remained constant at 87% *m* throughout the reaction, indicating that the growing isotactic poly(vinyl ether) (PVE) does not influence the ability of the catalyst to impart stereoselectivity. Furthermore, measurement of the molar mass (M_n) and dispersity ($Đ$) by gel permeation chromatography (GPC) at the different time points demonstrated that this polymerization proceeds by an uncontrolled chain-growth mechanism with high molecular weights even at low conversion. We hypothesize this phenomenon is due to fast propagation compared to initiation.

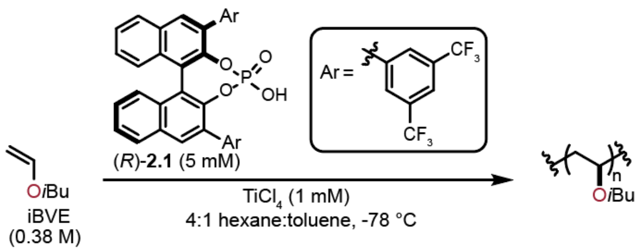

Time (min)	% conv[a]	M_n[b] (kg mol^{-1})	$Đ$[b]	*m* (%)[c]
3	8	31	2.6	87
6	22	38	3.5	87
10	37	47	2.9	87
18	71	101	2.3	87

Figure 2.6. Monitoring the stereoselectivity of the polymerization as a function of conversion. Polymerizations performed on a 0.76 mmol scale. [a] monomer conversion as determined by ^{1}H NMR integration relative to 1,4-dimethoxybenzene as an internal standard. [b] Number average molecular weight and dispersity as characterized via GPC. [c] % *m* characterized via ^{13}C NMR integration.

2.4 Computational Analysis of Catalyst Structure

An understanding of the solution state structure of (*R*)-**2.2** would inform the future optimization of stereoselective cationic polymerization methodology. In an initial attempt to probe the ligand sphere of (*R*)-**2.2**, we performed a series of iBVE polymerizations with varying ratios of (*R*)-**2.1**:$TiCl_4$ (**Figure 2.7**). A molar excess of (*R*)-**2.1** relative to $TiCl_4$ was found to be required for effective stereoinduction during monomer addition. While equimolar amounts of (*R*)-**2.1** and $TiCl_4$ resulted in poly(iBVE) with 76% *m*, an increase to 84% *m* was observed upon using a two-fold excess of (*R*)-**2.1** relative to $TiCl_4$. Further increasing this ratio enabled the preparation of poly(iBVE) materials with increasing levels of isotacticity up to 87% *m.* This data, in combination with our previously reported experimental observations and ^{31}P NMR data,[50] contribute to a hypothesis where the complex responsible for the observed stereoselectivity is ligated by multiple phosphate ligands. In addition, the degree to which this desired complex exists in equilibrium is aided by super-stoichiometric (*R*)-**2.1** relative to $TiCl_4$.

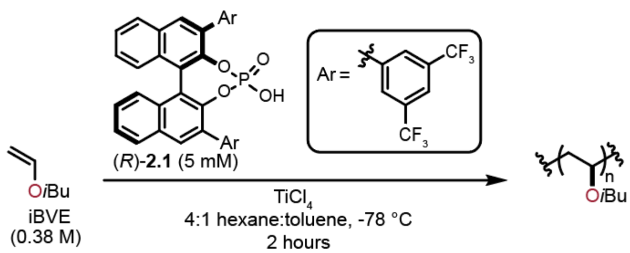

(*R*)-**2.1** : $TiCl_4$	[$TiCl_4$] (mM)	M_n [a] (kg mol^{-1})	*Đ* [a]	*m* (%) [b]
1 : 1	5.0	17	1.5	76
2 : 1	2.5	21	1.8	84
3 : 1	1.7	22	1.6	86
5 : 1	1.0	86	1.9	87

Figure 2.7. Tacticity analysis of poly(iBVE) obtained using varying ratios of (*R*)-**2.1**:$TiCl_4$. Polymerizations performed on a 0.76 mmol scale. [a] Number average molecular weight and dispersity as characterized via Gel Permeation Chromatography (GPC). [b] Percent *meso* diads as characterized via ^{13}C NMR integration.

Given the dynamic nature of the proposed equilibrium process, it remains difficult to directly probe the solution-state structure of the chiral catalyst responsible for achieving highly isotactic PVEs. Indeed, attempts to crystallize any (*R*)-**2.1**-ligated Ti species were unsuccessful, and low-temperature NMR studies provided only qualitative observations of catalyst structure. Thus, we sought to utilize density functional theory (DFT) to investigate the structure computationally. Geometry optimizations using SMD(n-hexane)/MN15/6-311+G(d,p) def2-TZVP and SDD(Ti)//M06/def2-SVP, LANL2DZ(Ti) basis sets were performed on titanium tetrachloride in the presence of one, two, or three equivalents of (*R*)-**2.1**. Analysis of the relative free energies of these structures revealed the most optimal ligand geometry. The lowest energy conformation computed was a conformer of $TiCl_3$((*R*)-**2.1**)$_3$, where one equivalent of HCl has been released, and the (*R*)-**2.1** ligands all exist on the same plane of an overall octahedral geometry (**Figure 2.8**). This structure bearing multiple phosphate ligands is consistent with our previous data whereby multiple equivalents of the (*R*)-**2.1** ligand were necessary to achieve highly isotactic PVEs. Additionally, we previously hypothesized that HCl released upon (*R*)-**2.1** ligation to $TiCl_4$ acts as an endogenous initiating species, again agreeing with this computationally derived structure.

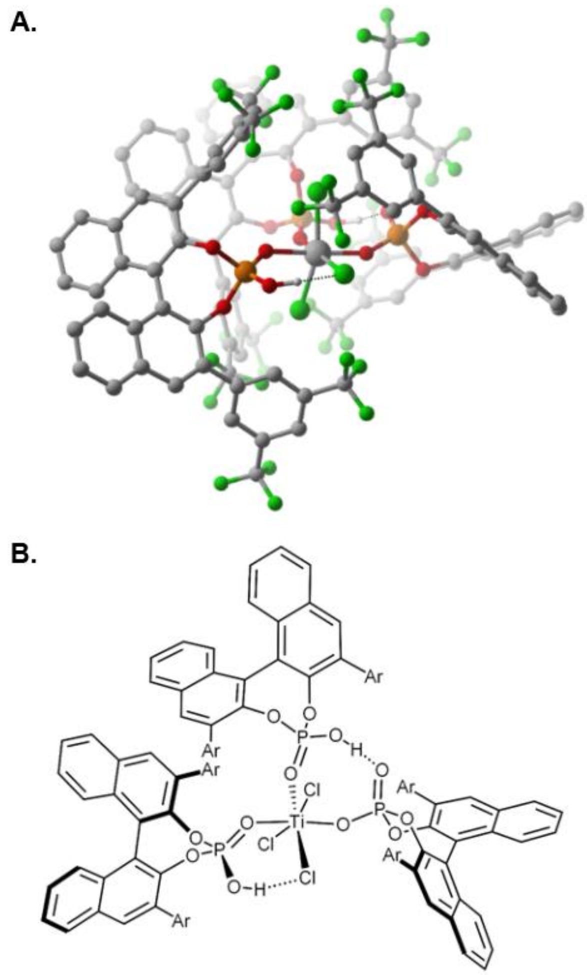

Figure 2.8. A) Three-dimensional ball and stick model of the lowest energy conformation of (*R*)-**2.1** ligand interacting with $TiCl_4$, upon release of 1 eq. of HCl. B) Bond-line representation of the same complex.

2.5 Conclusion

Comprehensive kinetic, experimental, and computational studies have provided valuable knowledge regarding the stereoselective cationic polymerization of vinyl ethers facilitated by catalyst **2.2**. Comparative kinetic studies revealed the importance of ligand deceleration effects in the design of reaction conditions and catalysts to achieve highly stereoselective polymerizations. Evaluation of the temperature dependence on stereoselectivity showed that the preferred catalyst structure resulted in a 0.73 kcal/mol preference for *meso* diad formation at –78 °C, while at increased temperatures the presence of alternative titanium complexes resulted in diminished isotacticity. A computational investigation of the solution-state structure of (*R*)-**2.2** revealed the likely preferred catalyst structure that consists of three chiral phosphoric acids ligated to titanium, which was supported by experimental observations. This comprehensive study enabled both a significantly deeper understanding of the stereoselective cationic polymerization of vinyl ethers and established a broader platform for accessing advanced polar polymeric materials. We envision this work informing future catalyst and materials design related to stereoselective polymerization.

REFERENCES

(1) Varner, T. P.; Teator, A. J.; Reddi, Y.; Jacky, P. E.; Cramer, C. J.; Leibfarth, F. A. Mechanistic Insight into the Stereoselective Cationic Polymerization of Vinyl Ethers. *J. Am. Chem. Soc.* **2020**, *142* (40), 17175–17186.

(2) W. Coates, G. Precise Control of Polyolefin Stereochemistry Using Single-Site Metal Catalysts. *Chem. Rev.* **2000**, *100* (4), 1223–1252.

(3) Okamoto, Y.; Nakano, T. Asymmetric Polymerization. *Chem. Rev.* **1994**, *94* (2), 349–372.

(4) Ouchi, M.; Kamigaito, M.; Sawamoto, M. Stereoregulation in Cationic Polymerization by Designed Lewis Acids. II. Effects of Alkyl Vinyl Ether Structure. *J. Polym. Sci. Part A Polym. Chem.* **2001**, *39* (7), 1060–1066.

(5) Nomura, N.; Ishii, R.; Akakura, M.; Aoi, K. Stereoselective Ring-Opening Polymerization of Racemic Lactide Using Aluminum-Achiral Ligand Complexes: Exploration of a Chain-End Control Mechanism. *J. Am. Chem. Soc.* **2002**, *124* (21), 5938–5939.

(6) Weger, M.; Pahl, P.; Schmidt, F.; Soller, B. S.; Altmann, P. J.; Pöthig, A.; Gemmecker, G.; Eisenreich, W.; Rieger, B. Isospecific Group-Transfer Polymerization of Diethyl Vinylphosphonate and Multidimensional NMR Analysis of the Polymer Microstructure. *Macromolecules* **2019**, *52* (18), 7073–7080.

(7) Sabini, E.; Sulzenbacher, G.; Dauter, M.; Dauter, Z.; Jorgensen, P. L.; Shulein, M.; Dupont, C.; Davies, G. J.; Wilson, K. S. Catalysis and Specificity in Enzymatic Glycoside Hydrolysis: A 2,5B Conformation for the Glycosyl-Enzyme Intermediate Revealed by the Structure of the Bacillus Agaradhaerens Family 11 Xylanase. *Chem. Biol.* **1999**, *6* (7), 483–492.

(8) Unrau, P. J.; Bartel, D. P. An Oxocarbenium-Ion Intermediate of a Ribozyme Reaction Indicated by Kinetic Isotope Effects. *Proc. Natl. Acad. Sci. U. S. A.* **2003**, *100* (26), 15393–15397.

(9) Crich, D. Mechanism of a Chemical Glycosylation Reaction. *Acc. Chem. Res.* **2010**, *43* (8), 1144–1153.

(10) Gómez, H.; Polyak, I.; Thiel, W.; M. Lluch, J.; Masgrau, L. Retaining Glycosyltransferase Mechanism Studied by QM/MM Methods: Lipopolysaccharyl-α-1,4-Galactosyltransferase C Transfers α-Galactose via an Oxocarbenium Ion-like Transition State. *J. Am. Chem. Soc.* **2012**, *134* (10), 4743–4752.

(11) Adero, P. O.; Amarasekara, H.; Wen, P.; Bohé, L.; Crich, D. The Experimental Evidence in Support of Glycosylation Mechanisms at the SN1–SN2 Interface. *Chem. Rev.* **2018**, *118* (17),

8242–8284.

(12) Teator, A. J.; Leibfarth, F. A. Catalyst-Controlled Stereoselective Cationic Polymerization of Vinyl Ethers. *Science.* **2019**, *363*, 1439–1443.

(13) Bovey, F. A.; Tiers, G. V. D. Polymer NSR Spectroscopy. II. The High Resolution Spectra of Methyl Methacrylate Polymers Prepared with Free Radical and Anionic Initiators. *J. Polym. Sci.* **1960**, *44* (143), 173–182.

(14) Fueno, T.; Shelden, R. A.; Furukawa, J. Probabilistic Considerations of the Tacticity of Optically Active Polymers. *J. Polym. Sci. Part A* **1965**, *3*, 1279–1288.

(15) Doi, Y.; Asakura, T. Catalytic Regulation for Isotactic Orientation in Propylene Polymerization with Ziegler-Natta Catalyst. *Die Makromol. Chemie* **1975**, *176* (2), 507–509.

(16) Byers, J. A.; Bercaw, J. E. Kinetic Resolution of Racemic α-Olefins with Ansa-Zirconocene Polymerization Catalysts: Enantiomorphic Site vs. Chain End Control. *Proc. Natl. Acad. Sci. U. S. A.* **2006**, *103* (42), 15303–15308.

(17) Fishbein, L.; Crowe, B. F. The Relation of Structure to Some Physical and Mechanical Properties of Poly(Vinyl Alkyl Ethers). *Die Makromol. Chemie* **1961**, *48* (1), 221–228.

(18) Schildknecht, C. E.; Lee, C. H.; Long, K. P.; Rinehart, L. C. Some Aspects of Polymer Morphology: Time Dependence in Moephology of Polyvinyl Ethers and Polypropylenes. *Polym. Eng. Sci.* **1967**, *7* (4), 257–263.

(19) Natta, G.; Allegra, G.; Bassi, I. W.; Carlini, C.; Chiellini, E.; Montagnoli, G. Isomorphism Phenomena in Isotactic Poly (4-Methyl-Substituted α-Olefins) and in Isotactic Poly(Alkyl Vinyl Ethers). *Macromolecules* **1969**, *2* (4), 311–315.

(20) Aoshima, S.; Ito, Y.; Kobayashi, E. Stereoregularity of Poly(Vinyl Ether)s with a Narrow Molecular Weight Distribution Obtained by the Living Cationic Polymerization. *Polym. J.* **1993**, *25*, 161–1168.

(21) Ouchi, M.; Kamigaito, M.; Sawamoto, M. Stereoregulation in Cationic Polymerization by Designed Lewis Acids. 1. Highly Isotactic Poly(Isobutyl Vinyl Ether) with Titanium-Based Lewis Acids. *Macromolecules* **1999**, *32* (20), 6407–6411.

(22) Ouchi, M.; Sueoka, M.; Kamigaito, M.; Sawamoto, M. Stereoregulation in Cationic Polymerization. III. High Isospecificity with the Bulky Phosphoric Acid [(RO)2PO2H]/SnCl4 Initiating Systems: Design of Counteranions via Initiators. *J. Polym. Sci. Part A Polym. Chem.* **2001**, *39* (7), 1067–1074.

(23) Ohgi, H.; Sato, T. Highly Isotactic Poly(Vinyl Alcohol). III: Heterogeneous Cationic Polymerization of Tert-Butyl Vinyl Ether. *Polymer.* **2002**, *43* (13), 3829–3836.

(24) Kawaguchi, T.; Sanda, F.; Masuda, T. Polymerization of Vinyl Ethers with Transition-Metal Catalysts: An Examination of the Stereoregularity of the Formed Polymers. *J. Polym. Sci. Part A Polym. Chem.* **2002**, *40* (22), 3938–3943.

(25) Watanabe, H.; Yamamoto, T.; Kanazawa, A.; Aoshima, S. Stereoselective Cationic Polymerization of Vinyl Ethers by Easily and Finely Tunable Titanium Complexes Prepared from Tartrate-Derived Diols: Isospecific Polymerization and Recognition of Chiral Side Chains. *Polym. Chem.* **2020**, *11*, 3398–3403.

(26) Kottisch, V.; Michaudel, Q.; P. Fors, B. Cationic Polymerization of Vinyl Ethers Controlled by Visible Light. *J. Am. Chem. Soc.* **2016**, *138* (48), 15535–15538.

(27) Michaudel, Q.; Kottisch, V.; Fors, B. P. Cationic Polymerization: From Photoinitiation to Photocontrol. *Angew. Chemie - Int. Ed.* **2017**, *56* (33), 9670–9679.

(28) Kottisch, V.; Michaudel, Q.; P. Fors, B. Photocontrolled Interconversion of Cationic and Radical Polymerizations. *J. Am. Chem. Soc.* **2017**, *139* (31), 10665–10668.

(29) Michaudel, Q.; Chauviré, T.; Kottisch, V.; J. Supej, M.; J. Stawiasz, K.; Shen, L.; R. Zipfel, W.; D. Abruña, H.; H. Freed, J.; P. Fors, B. Mechanistic Insight into the Photocontrolled Cationic Polymerization of Vinyl Ethers. *J. Am. Chem. Soc.* **2017**, *139* (43), 15530–15538.

(30) Kottisch, V.; Supej, M. J.; Fors, B. P. Enhancing Temporal Control and Enabling Chain-End Modification in Photoregulated Cationic Polymerizations by Using Iridium-Based Catalysts. *Angew. Chemie - Int. Ed.* **2018**, *57* (27), 8260–8264.

(31) Peterson, B. M.; Kottisch, V.; J. Supej, M.; P. Fors, B. On Demand Switching of Polymerization Mechanism and Monomer Selectivity with Orthogonal Stimuli. *ACS Cent. Sci.* **2018**, *4* (9), 1228–1234.

(32) Supej, M. J.; Peterson, B. M.; Fors, B. P. Dual Stimuli Switching: Interconverting Cationic and Radical Polymerizations with Electricity and Light. *Chem* **2020**, *6* (7), 1794–1803.

(33) Kojima, K.; Sawamoto, M.; Higashimura, T. Living Cationic Polymerization of Isobutyl Vinyl Ether by Hydrogen Iodide/Lewis Acid Initiating Systems: Effects of Lewis Acid Activators and Polymerization Kinetics. *Macromolecules* **2002**, *22* (4), 1552–1557.

(34) Gi Cho, C.; Ami Feit, B.; W. Webster, O. Cationic Polymerization of Isobutyl Vinyl Ether: Livingness Enhancement by Dialkyl Sulfides. *Macromolecules* **2002**, *23* (7), 1918–1923.

(35) Hadjikyriacou, S.; Faust, R. Living Cationic Homopolymerization of Isobutyl Vinyl Ether and Sequential Block Copolymerization of Isobutylene with Isobutyl Vinyl Ether. Synthesis and Mechanistic Studies. *Macromolecules* **2002**, *28* (23), 7893–7900.

(36) Sharpless, K. B. Coelacanths and Catalysis. *Tetrahedron* **1994**, *50* (15), 4235–4258.

(37) Evans, D. A.; Murry, J. A.; Von, P. M.; Norcross, R. D.; Miller, S. J.; A Evans, I. D.; Murry, J. A.; von Matt, P.; Norcross R D; Miller S J. C2-Symmetric Cationic Copper(II) Complexes as Chiral Lewis Acids: Counterion Effects in the Enantioselective Diels–Alder Reaction. *Angew. Chem. Int. Ed* **1995**, *34*, 798–800.

(38) Berrisford, D. J.; Bolm, C.; Sharpless, K. B. Ligand-Accelerated Catalysis. *Angew. Chem. Int. Ed* **1995**, *34*, 1059–1070.

(39) A. Evans, D.; M. Barnes, D.; S. Johnson, J.; Lectka, T.; von Matt, P.; J. Miller, S.; A. Murry, J.; D. Norcross, R.; A. Shaughnessy, E.; R. Campos, K. Bis(Oxazoline) and Bis(Oxazolinyl)Pyridine Copper Complexes as Enantioselective Diels−Alder Catalysts: Reaction Scope and Synthetic Applications. *J. Am. Chem. Soc.* **1999**, *121* (33), 7582–7594.

(40) A. Evans, D.; S. Burgey, C.; C. Kozlowski, M.; W. Tregay, S. C2-Symmetric Copper(II) Complexes as Chiral Lewis Acids. Scope and Mechanism of the Catalytic Enantioselective Aldol Additions of Enolsilanes to Pyruvate Esters. *J. Am. Chem. Soc.* **1999**, *121* (4), 686–699.

(41) Ouchi, M.; Sueoka, M.; Kamigaito, M.; Sawamoto, M. Stereoregulation in Cationic Polymerization. III. High Isospecificity with the Bulky Phosphoric Acid [(RO)2PO2H]/SnCl4 Initiating Systems: Design of Counteranions via Initiators. *J. Polym. Sci. Part A Polym. Chem.* **2001**, *39* (7), 1067–1074.

(42) R. Knowles, R.; Lin, S.; N. Jacobsen, E. Enantioselective Thiourea-Catalyzed Cationic Polycyclizations. *J. Am. Chem. Soc.* **2010**, *132* (14), 5030–5032.

(43) Ford, D. D.; Lehnherr, D.; Kennedy, C. R.; Jacobsen, E. N. Anion-Abstraction Catalysis: The Cooperative Mechanism of α-Chloroether Activation by Dual Hydrogen-Bond Donors. *ACS Catal.* **2016**, *6* (7), 4616–4620.

(44) Wang, X.-Y.; Sun, X.-L.; Wang, F.; Tang, Y. SaBOX/Copper Catalysts for Highly Syndio-Specific Atom Transfer Radical Polymerization of Methyl Methacrylate. *ACS Catal.* **2017**, *7* (7), 4692–4696.

(45) Kanazawa, A.; Kanaoka, S.; Aoshima, S. Major Progress in Catalysts for Living Cationic Polymerization of Isobutyl Vinyl Ether: Effectiveness of a Variety of Conventional Metal Halides. *Macromolecules* **2009**, *42* (12), 3965–3972.

(46) Aoshima, S.; Kanaoka, S. A Renaissance in Living Cationic Polymerization. *Chem. Rev.* **2009**, *109* (11), 5245–5287.

(47) Annamalai, V.; F. DiMauro, E.; J. Carroll, P.; C. Kozlowski, M. Catalysis of the Michael Addition Reaction by Late Transition Metal Complexes of BINOL-Derived Salens. *J. Org. Chem.* **2003**, *68* (5), 1973–1981.

(48) Walsh, P. L.; C. Kozlowski, M. *Fundamentals of Asymmetric Catalysis*; University Science Books: Sausalito, CA, 2009.

(49) Bryliakov, K. P. Dynamic Nonlinear Effects in Asymmetric Catalysis. *ACS Catal.* **2019**, *9* (6), 5418–5438.

(50) Shuai, L.; Amiri, M. T.; Questell-Santiago, Y. M.; Héroguel, F.; Li, Y.; Kim, H.; Meilan, R.; Chapple, C.; Ralph, J.; Luterbacher, J. S. Formaldehyde Stabilization Facilitates Lignin Monomer Production during Biomass Depolymerization. *Science.* **2016**, *354* (6310), 329–333.

CHAPTER 3: SUBSTSRATE SCOPE AND COPOLYMERIZATION USING A CHIRAL LEWIS ACID

3.1 Hompolymerization of Alkyl Vinyl Ethers

This chapter was adapted in part with permission from the following two manuscripts: *ACS Macro Lett.* **2019,** *8*, 1559−1563[1] and *J. Am. Chem. Soc.* **2020,** *142*, 17175–17186.[2]

Understanding the scope of catalyst *(R)***-2.2** with a diversity of monomers connects the kinetic and computational studies to the performance of the method. To compare substrates against one another under conditions that achieve high stereoselectivity, we conducted all polymerizations at –78 °C and used $TiCl_4(THF)_2$ as a Lewis acid. The ratio of (*R*)**-2.1** to $TiCl_4(THF)_2$ was fixed at 5:1 and the reactions were conducted at a monomer concentration of 0.38 M on a 0.76 mmol scale. Initially, commercially available alkyl vinyl ether monomers with linear side chains were explored and found to be well-tolerated in the stereoselective polymerization. In addition to ethyl vinyl ether (EVE), *n*-propyl vinyl ether (nPrVE), and *n*-butyl vinyl ether (nBVE), which were shown in our previous work to engender isotactic PVEs,[3] the polymerization of octyl vinyl ether (OcVE) also yielded an isotactic material (94% *m*). Despite demonstrating a slightly higher level of isotacticity as chain length increased, a corresponding decrease in the melting temperature (T_m) of the materials was observed (**Figure 3.1**). This observation suggests that the conformational flexibility of the side chains has an impact on polymer crystallization within this series.[4]

The steric properties of branched alkyl vinyl ether monomers demonstrated a pronounced influence on the stereoselectivity achieved with catalyst (*R*)**-2.2** (**Figure 3.1**). In order to probe these effects systematically, the site of branching was placed progressively closer to the ether through the evaluation of isoamyl vinyl ether (iAVE), iBVE, and isopropyl vinyl ether (iPVE). While iAVE and iBVE demonstrated similar stereoselectivity (90 and 91% *m*, respectively), a decrease in isotacticity

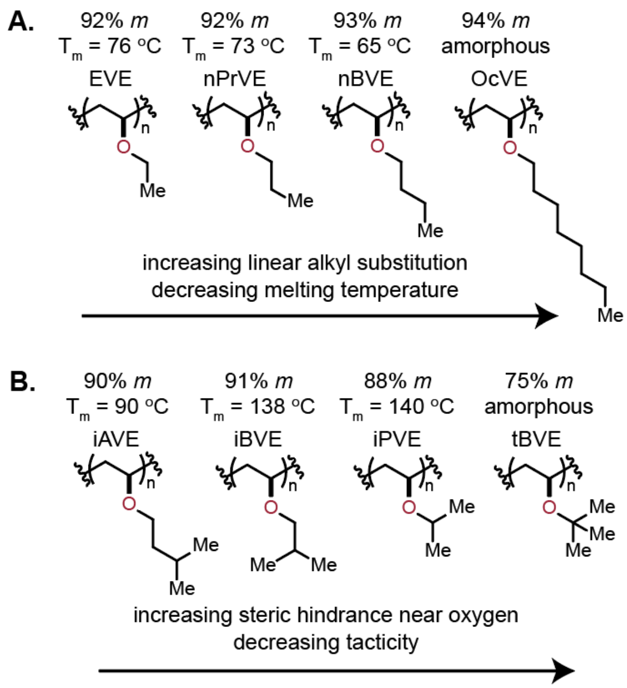

Figure 3.1. Representative structure-property and structure-reactivity profiles for a variety of vinyl ethers. Polymers prepared using optimized reaction conditions ([VE] = 0.38 M, [(*R*)-**2.1**] = 5.0 mM, $[TiCl_4(THF)_2]$ = 1.0 mM) at –78 °C in 4:1 hexane:toluene on a 0.76 mmol scale.

was observed when the branch point was placed *alpha* to the vinyl ether in iPVE (88% *m*). Within this series, the T_m of the isotactic PVEs increased as the branch point was placed progressively closer to the ether, indicating that compact side chains lead to higher melting isotactic PVEs. In contrast, the presence of a quaternary center *alpha* to the vinyl ether, such as in *tert*-butyl vinyl ether (tBVE), proved to be detrimental to stereoselectivity, resulting in poly(tBVE) with 75% *m* and no discernable melting temperature. This systematic screen of monomer steric parameters implies that increasing steric hindrance close to the ether oxygen results in a diminished stereoselectivity during polymerization. Our proposed mechanism indicates that facial addition in these polymerizations is biased by the close association of the cationic chain-end with anionic counterion *(R)*-**2.4** (Step IV in **Figure 2.2**). Therefore, we hypothesize that an increase in steric bulk close to the oxocarbenium ion disrupts the tight ion pair and causes a decrease in the stereoselectivity of monomer addition.[5–7]

3.2 Copolymerization of Alkyl Vinyl Ethers

The identity of the alkyl side chain functionality had a distinct impact on the thermal properties of the obtained polymers. PVEs bearing linear alkyl substitution maintained a lower T_m of 65-76 °C, while those with branched alkyl substitution possessed a higher T_m up to 140 °C (**Figure 3.2**). We envisioned leveraging this disparity of thermal properties between vinyl ether substituents to prepare semicrystalline thermoplastics with tunable thermomechanical properties. Herein, the generality of catalyst (*R*)-**2.2** is demonstrated through systematic evaluation of the stereoselective copolymerization of alkyl vinyl ether monomers. The introduction of comonomers does not influence the stereoselectivity of catalyst (*R*)-**2.2**; rather, it enables the realization of semicrystalline thermoplastics derived from polar vinyl monomers with tunable thermal properties. Considering the disparate thermal properties exhibited by isotactic PVEs bearing linear and branched alkyl substituents, we chose to first explore the copolymerization of nBVE with iBVE (**Figure 3.3**). The optimized reaction conditions produced high molecular weight materials ($M_n > 70$ kg mol^{-1}) via an uncontrolled chain-growth polymerization. In order to tune the ultimate incorporation of nBVE in the resulting copolymers, reactions were performed using a variety of molar feed ratios of nBVE (f_{Bu}) relative to iBVE. As shown in **Figure 3.4A**, distinct ^{1}H NMR resonances were observed for iBVE (δ

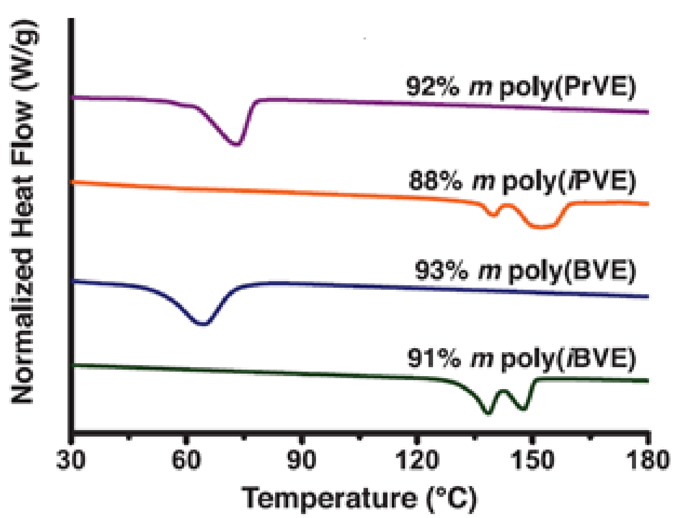

Figure 3.2. Differential scanning calorimetry second-heating-scan curves (10 °C/min) for select isotactic PVEs.

3.25–2.05 ppm, $CDCl_3$) and nBVE (δ 1.40–1.30 ppm, $CDCl_3$) repeat units, which were integrated relative to each other in order to determine the mole fraction of nBVE (F_{Bu}). Analysis of the ^{13}CNMR enabled the determination of stereoselectivity by comparing the integration of the region corresponding to the *racemo* diads (δ 42.0–41.0 ppm, $CDCl_3$) to the region corresponding to the *meso* diads (δ 40.4–39.2 ppm, $CDCl_3$) (**Figure 3.4B**). Catalyst (*R*)-**2.2** enabled the preparation of poly(iBVE-co-nBVE) with high degrees of isotacticity (91–94% *m*) for all copolymer compositions, demonstrating the generality of (*R*)-**2.2** for stereoselective copolymerization of multiple alkyl vinyl ethers. This substrate tolerance represents an improvement over previous work where stereoselectivity was sensitive to even slight changes in monomer structure.[8,9]

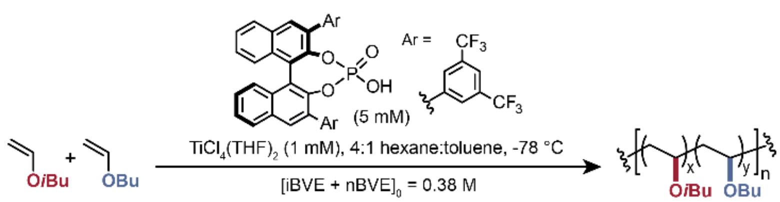

f_{Bu}[a]	F_{Bu}[b]	M_n[c] (kg mol^{-1})	*Đ*[c]	*m* (%)	T_g (°C)[d]	T_m(°C)[d]
0.05	0.11	72	1.7	92	-28	131
0.10	0.20	88	2.0	93	-22	122
0.20	0.30	121	2.0	94	-31	105
0.30	0.43	113	2.1	94	-37	89
0.40	0.54	157	2.4	94	-42	74
0.50	0.63	241	2.5	91	-45	63
0.60	0.74	238	2.4	94	-49	56
0.70	0.82	211	2.7	93	-55	57
0.80	0.87	211	2.7	92	-51	51
0.90	0.93	182	2.5	93	-56	53

Figure 3.3. Reaction scheme depicting the stereoselective copolymerization of iBVE and nBVE using (*R*)-**2.2** and a summary of copolymerization experiments. [a] Mole fraction of nBVE in the monomer feed. [b] Mole fraction of nBVE in copolymer determined by ^{1}H NMR integration. [c] M_n indicates the number average molecular weight of the polymer. Dispersity was calculated according to $Đ = M_w/M_n$ where M_w is weight average molecular weight. [d] T_g and T_m obtained from a second heating scan (10 °C/min) after the thermal history was removed.

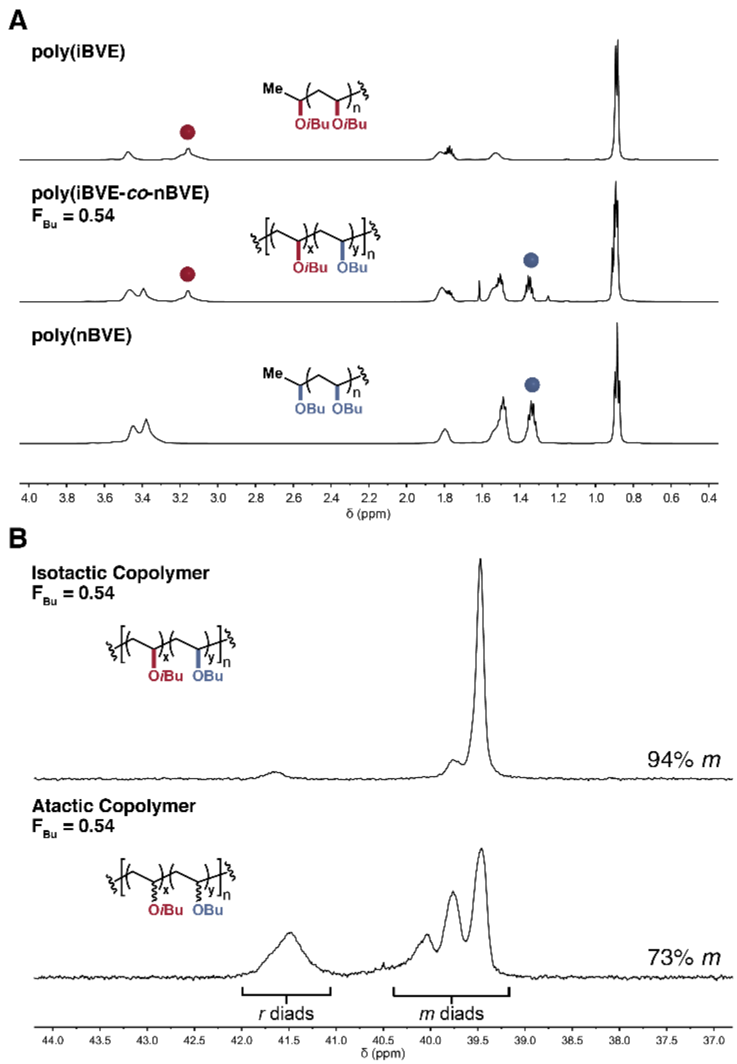

Figure 3.4. (A) ^{1}H NMR ($CDCl_3$) spectra of poly(iBVE) (top), poly(iBVE-co-nBVE) (middle), and poly(nBVE) (bottom) highlighting the distinct resonances observed for iBVE (red sphere) and nBVE (blue sphere) repeat units. (B) Observed differences of the backbone methylene ^{13}C NMR ($CDCl_3$) resonances in an isotactic poly(iBVE-co-nBVE) made using (*R*)-**2.2** and an atactic poly(iBVE-co-nBVE) made using trifluoromethanesulfonic acid.

Next, we sought to investigate the relationship between f_{Bu} and F_{Bu} through kinetic analysis. Although values of F_{Bu} did not scale proportionally to f_{Bu}, increasing f_{Bu} resulted in increased F_{Bu} which enabled the preparation of copolymers with predetermined F_{Bu} values. In order to gain a deeper understanding of the reaction, a series of copolymerizations where $f_{\mathrm{Bu}} = 0.50$ were quenched at various time points to evaluate reaction kinetics. As shown in **Figure 3.5**, iBVE was consumed at a slower rate ($k_{\mathrm{obs}} = 4.4 \times 10^{-4}\ \mathrm{s}^{-1}$) relative to the consumption of nBVE ($k_{\mathrm{obs}} = 7.8 \times 10^{-4}\ \mathrm{s}^{-1}$) throughout the copolymerization. Previous explorations of vinyl ether copolymerization, in particular those initiated by trifluoromethanesulfonic acid or boron trifluoride diethyl etherate, observed the opposite reactivity trend, whereby the more sterically hindered comonomer was consistently incorporated at a faster rate.[10,11] The catalyst-controlled stereoselectivity exhibited in polymerizations mediated by (*R*)-**2.2** suggests a close interaction between the chiral anion and the propagating chain end, which we hypothesize to be interrupted by sterically demanding side chains. The relatively slow rate of iBVE consumption observed during copolymerization with nBVE is thus likely related to an adverse steric interaction between iBVE and (*R*)-**2.2**. Comonomer consumption plateaus at a combined monomer conversion of ~65% after 30 min (see Appendix B) which, combined with the aforementioned rates, is consistent with the observed F_{Bu} values.

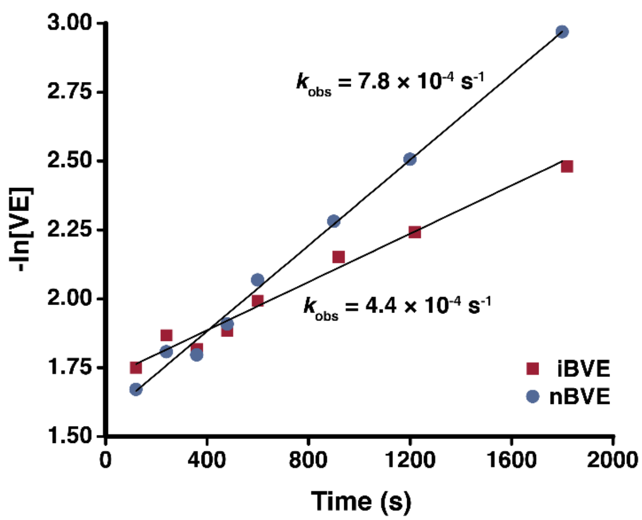

Figure 3.5. Plot of −ln[VE] versus time of the copolymerization of iBVE and nBVE. Conversions of iBVE (■) and nBVE (●) monitored independently by ^{1}H NMR ($CDCl_3$). VE = vinyl ether. $[iBVE]_0$ = 0.19 M. $[nBVE]_0$ = 0.19 M.

Each of the obtained poly(iBVE-co-nBVE) samples were semicrystalline thermoplastics at room temperature. As shown in **Figure 3.6**, differential scanning calorimetry (DSC) analysis at a scan rate of 10 °C/min with data taken from the second heating cycle revealed the copolymers exhibited T_g and T_m values that span the range between those of poly(iBVE) (T_g = −20 °C, T_m = 138 °C) and poly(nBVE) (T_g = −53 °C, T_m =65 °C). The T_g values observed by DSC scale with F_{Bu} as predicted by the Fox equation[12,13] and remain well below room temperature. The apparent T_m values decrease linearly with increasing F_{Bu} as expected but reach an inflection point at approximately F_{Bu} = 0.7, which we hypothesize is due to a switch in the composition of the crystalline regions from iBVE repeat units to nBVE repeat units. Accordingly, as incorporation of nBVE increases from this point (i.e., $F_{Bu} > 0.7$) a slight increase in T_m is observed, likely resulting from decreasing contributions from iBVE "defects" within the nBVE crystalline phase. Regardless, the observed trends afford the ability to rationally tune both T_g and T_m by selecting the appropriate f_{Bu} and highlight the general utility of vinyl ether copolymerizations facilitated by (*R*)-**2.2**.

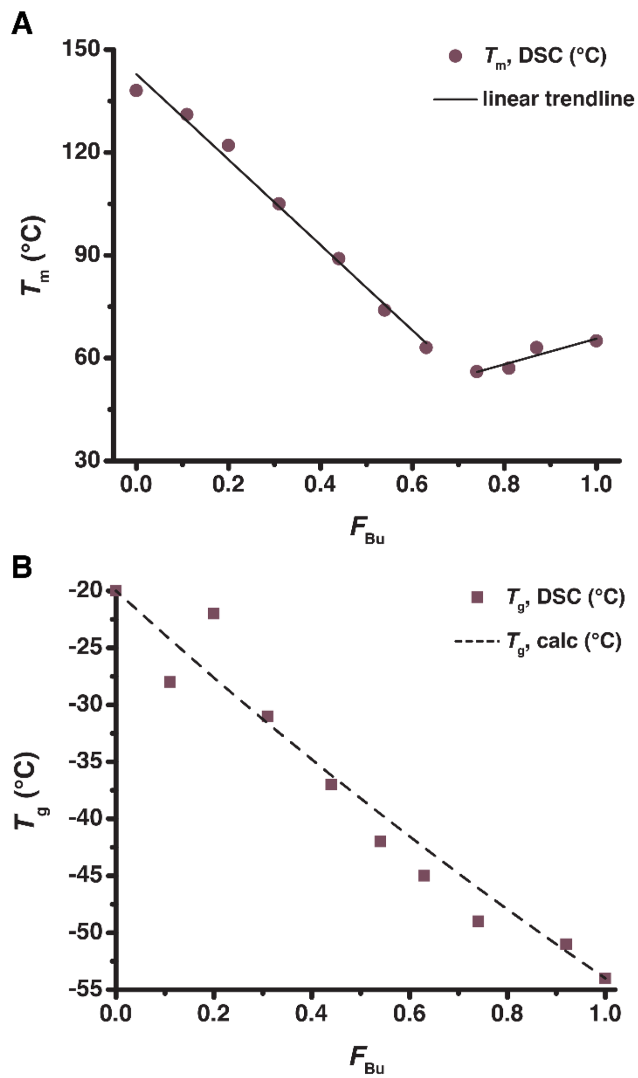

Figure 3.6. (A) Plot of T_m obtained by DSC as a function of molar incorporation of nBVE (F_{Bu}). Solid lines highlight observed trends. (B) Plot of T_g obtained by DSC as a function of F_{Bu}. Dashed line indicates T_g values predicted using the Fox equation.

In an effort to explore the substrate scope of this methodology, we next performed a series of copolymerizations using EVE as a comonomer with iBVE. Similar to the iBVE/nBVE comonomer pair, utilizing a variety of EVE molar feed ratios (f_{Et}) resulted in isotactic copolymers (91−93% *m*) with tunable degrees of EVE incorporation (F_{Et}) (see Appendix B). The obtained F_{Et} values were again consistently higher than f_{Et}, likely due to a kinetic phenomenon similar to that described above. The T_g values exhibited by poly(iBVE-co-EVE) decreased as expected with increasing F_{Et} but appeared to plateau at $T_g = -37$ °C when $F_{Et} \geq 0.5$. Similarly, the observed T_m values decreased linearly with increasing F_{Et} from 138 °C until plateauing at ∼40 °C when $F_{Et} \geq 0.5$. No T_m was reliably observed in the second heating cycle by DSC when $F_{Et} \geq 0.3$, although these materials crystallized slowly at room temperature and exhibited obvious first-order transitions in the first heating cycle.

3.3 Copolymerization of Functional Vinyl Ethers with Isobutyl Vinyl Ether

The polymerization of vinyl ether substrates that contain polar functional groups would expand the potential utility of isotactic PVEs. To interrogate the functional group compatibility of catalyst (*R*)-**2.2**, we identified a series of vinyl ether monomers with functionality connected via an ethylene glycol spacer. This approach provided a systematic comparison of functional groups while remaining isoelectronic at the vinyl ether. Initial trials indicated that none of the monomers in **Figure 3.7** underwent homopolymerization using catalyst (*R*)-**2.2**, presumably due to deleterious interactions of Lewis basic functionality on the substrates with the oxophilic Ti Lewis acid.[14]

The above described previous demonstration of stereoselective copolymerization of vinyl ethers[1] using catalyst (*R*)-**2.2** inspired the exploration of functional group rich vinyl ethers as comonomers in the same catalyst-controlled methodology. For these copolymers, iBVE was used as a representative alkyl vinyl ether comonomer and various substituted oxyethylene vinyl ethers (ROVE, where R is a variable substituent) were included at a specified molar fraction (f_{ROVE}) relative to iBVE. In the isolated copolymer, distinct ^{1}H NMR resonances of iBVE and ROVE repeat units were integrated relative to each other in order to determine the actual molar incorporation of ROVE (F_{ROVE}).

We first investigated the functional comonomer 2-methoxy ethyl vinyl ether (MOVE), which has been shown to chelate with a growing cationic chain end and increase the rate of polymerization under Lewis acid catalyzed conditions.[15,16] When f_{MOVE} = 0.20 or below (**Figure 3.7** entries 1-2, see Appendix B for additional experiments), high monomer conversions (>73%) and isotactic copolymers (89-91% *m*) were observed, with F_{MOVE} remaining similar to f_{MOVE}. Attempts to achieve higher incorporations of MOVE by increasing f_{MOVE}, however, led to significant decreases in overall monomer conversion and tacticity (entries 3-4).

We next investigated phenoxy ethyl vinyl ether (PhOVE), which represents a phenyl ether functionality that is less Lewis basic than the alkyl ether in MOVE. A consistent increase in F_{PhOVE} was observed as f_{PhOVE} increased, albeit concomitant with a decrease in the overall monomer conversion (entries 5-9). Notably, F_{PhOVE} reached a maximum of 0.22 while retaining high isotacticity (90% *m*), demonstrating the promise of incorporating significant amounts of phenyl ether functionality into isotactic PVEs. Since phenyl ethers are prominent in numerous small molecule derivatives of lignin,[17–20] we chose to study a vinyl ether monomer derived from creosol as a representative lignin derivative. The vinyl ether monomer 2-methoxy-4-methyl-phenoxy ethyl vinyl ether (MOPhOVE) was synthesized from creosol and subjected to the stereoselective polymerization conditions (entries 10-13). At $f_{MOPhOVE}$ = 0.05, copolymerization proceeds to 50% conversion and yields a copolymer of $F_{MOPhOVE}$ = 0.04 and 92% *m*. An interesting phenomenon was observed where increasing $f_{MOPhOVE}$ has little influence on $F_{MOPhOVE}$ or isotacticity. Overall, phenyl ether substituents were tolerated better than methyl ether groups and enabled the incorporation of the lignin derived MOPhOVE into isotactic PVE copolymers.

Carbonyl groups represent a functional group class with a rich array of accessible chemistry. Acetoxy ethyl vinyl ether (AcOVE) was investigated as the simplest ester-containing vinyl ether monomer for stereoselective polymerization. AcOVE demonstrated a pronounced poisoning effect on

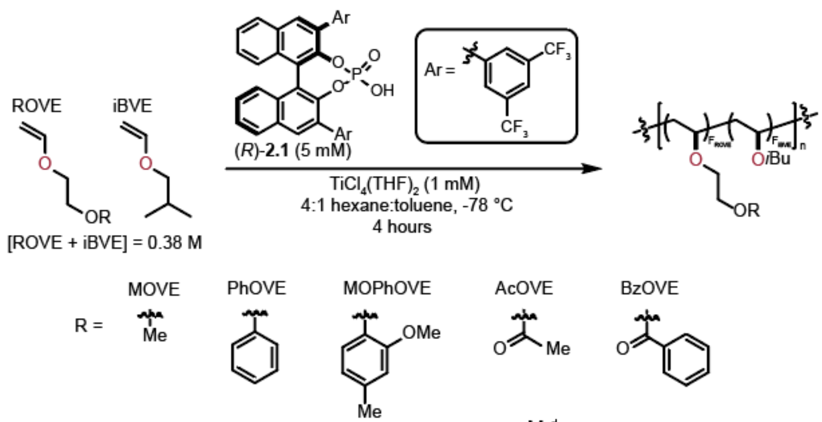

Entry	ROVE	f_{ROVE}[a]	F_{ROVE}[b]	% conv[c]	M_n[d] (kg mol^{-1})	*Đ*[d]	*m* (%)[e]
1	MOVE	0.05	0.06	84	56	2.1	91
2	MOVE	0.15	0.16	85	68	1.4	89
3	MOVE	0.30	0.50	40	49	2.2	81
4	MOVE	0.40	0.70	18	32	1.6	72
5	PhOVE	0.05	0.06	61	74	2.1	89
6	PhOVE	0.15	0.07	60	47	1.9	88
7	PhOVE	0.30	0.09	41	54	1.9	89
8	PhOVE	0.40	0.13	39	42	1.7	90
9	PhOVE	0.50	0.22	29	39	1.6	90
10	MOPhOVE	0.05	0.04	50	69	2.1	92
11	MOPhOVE	0.15	0.05	47	52	1.8	90
12	MOPhOVE	0.30	0.05	48	36	1.7	90
13	MOPhOVE	0.40	0.07	25	30	1.5	91
14	AcOVE	0.01	0.02	70	72	2.1	92
15	AcOVE	0.03	0.09	35	47	1.8	83
16	AcOVE	0.05	0.12	20	35	1.6	85
17	BzOVE	0.01	0.03	38	75	2.0	92
18	BzOVE	0.03	0.09	18	47	1.8	93
19	BzOVE	0.05	0.15	7	50	1.6	87

Figure 3.7. Structure-reactivity analysis of functional comonomers bearing Lewis basic sites. Polymerizations performed on a 1.0 mmol total vinyl ether monomer scale. [a] molar fraction of the functional comonomer (ROVE) relative to iBVE in the initial reaction solution prior to initiation (*i.e.* f_{ROVE} = 0.05 is 5 mol% ROVE and 95 mol% iBVE) [b] mole fraction of ROVE in final copolymer as determined by ^{1}H NMR integration. [c] monomer conversion as determined by ^{1}H NMR integration relative to 1,4-dimethoxybenzene as an internal standard. [d] Number average molecular weight and dispersity as characterized via GPC. [e] Percent *meso* diads as characterized via ^{13}C NMR integration.

catalyst (*R*)-**2.2.** While addition of f_{AcOVE} = 0.01 as a comonomer with iBVE resulted in a material with 2 mol% AcOVE while retaining high levels of isotacticity (92% *m*) and monomer conversion (70 %), the inclusion of higher concentrations of AcOVE had a negative effect on both overall monomer conversion and tacticity (entries 15-16). Benzoyloxy ethyl vinyl ether (BzOVE) represented an ester-containing monomer that performed better in the stereoselective copolymerization. The copolymerization of BzOVE and iBVE resulted in copolymers with moderate conversions (18-38%) and high isotacticities (92-93% *m*) with F_{BzOVE} values up to 0.09. BzOVE incorporation higher than 9 mol% decreased both conversion and tacticity (entry 19). Overall, the culmination of these experiments demonstrates that catalyst (*R*)-**2.2** can successfully incorporate functional vinyl ether monomers through copolymerization. We observed that Lewis basic functionality in comonomers can reduce overall catalyst efficiency and stereoselectivity; however, this can be mitigated to an extent by incorporating phenyl groups that increase the steric environment and decrease the overall Lewis basicity of oxygen-rich vinyl ethers.

To further diversify the scope of materials that can be made through this methodology, we also explored performing a post-polymerization modification reaction with one of these copolymers. Deprotection of the acyl functional group of isotactic poly(iBVE-co-AcOVE) using NaOH efficiently yielded copolymer **3.1** which features repeat units containing free hydroxyl groups (**Figure 3.8A**). As shown in **Figure 3.8B**, the gel permeation chromatography (GPC) traces for the starting copolymer material and **3.1** closely overlap indicating the reaction proceeds without appreciable byproduct formation. Subsequent coupling with 1-pyrenebutyryl chloride yielded pyrene-appended copolymer **3.2**, as evidenced by ^{1}H and ^{13}C NMR, as well as GPC in conjunction with a photodiode array (PDA) detector (**Figure 3.8C**). This material exhibited a slightly increased T_g of −16 °C relative to the starting copolymer material and remained a high-melting thermoplastic with a T_m of 126 °C, but was now fluorescent under UV irradiation (**Figure 3.8D**).

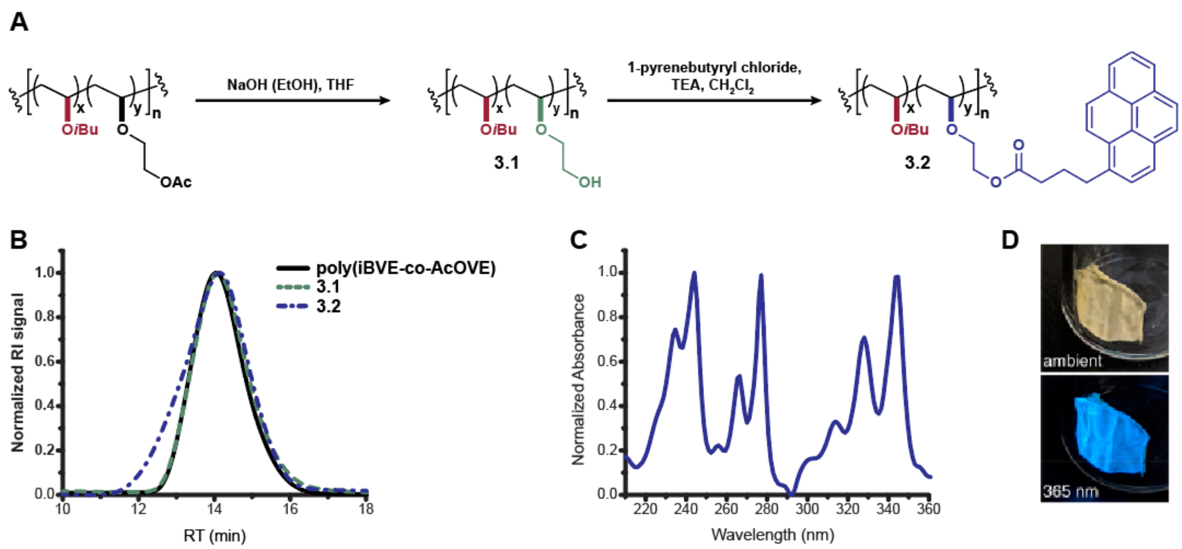

Figure 3.8. (A) Reaction scheme depicting deprotection of isotactic poly(iBVE-co-AcOVE) and postfunctionalization of **3.1** to generate **3.2**. (B) Overlay of GPC traces before and after each step depicted in A. (C) Photodiode array (PDA) trace at 13.9 min retention time (RT) confirming the structure of **3.2**. (D) Visual representation (photo) highlighting the solid-state fluorescence of **3.2** observed under 365 nm irradiation.

3.4 Conclusion

In summary, we have demonstrated catalyst (*R*)-**2.2** to be general to a wide variety of vinyl ether substrates. We first established structure—reactivity and structure—property relationships in simply alkyl vinyl ethers by probing monomers with systematic variations in steric parameters. Increasing the alkyl chain length for linear substituents resulted in increasing isotacticity and decreasing T_m values, while increasing the steric bulk of branched alkyl substituents in proximity to the vinyl ether decreased isotacticity. Second, we leveraged this methodology to prepare a series of isotactic vinyl ether-based copolymers. Through judicious choice of comonomer pairs, the thermal properties of the resulting materials can be rationally tuned by modulating the relative incorporation of each comonomer. Finally, we have shown the tolerance of this method towards aryl, ether, and ester functionality. The ability to copolymerize these monomers without sacrificing the control of tacticity and desirable thermal properties represents a practical approach toward polar, high performance thermoplastics.

REFERENCES

(1) Teator, A. J.; Varner, T. P.; Jacky, P. E.; Sheyko, K. A.; Leibfarth, F. A. Polar Thermoplastics with Tunable Physical Properties Enabled by the Stereoselective Copolymerization of Vinyl Ethers. *ACS Macro Lett.* **2019**, *8* (12), 1559–1563.

(2) Varner, T. P.; Teator, A. J.; Reddi, Y.; Jacky, P. E.; Cramer, C. J.; Leibfarth, F. A. Mechanistic Insight into the Stereoselective Cationic Polymerization of Vinyl Ethers. *J. Am. Chem. Soc.* **2020**, *142* (40), 17175–17186.

(3) Teator, A. J.; Leibfarth, F. A. Catalyst-Controlled Stereoselective Cationic Polymerization of Vinyl Ethers. *Science.* **2019**, *363*, 1439–1443.

(4) Trafara, G. State of Order in Isotactic Polyhexylethylene. *J. Polym. Sci. Polym. Chem. Ed.* **1980**, *18* (1), 321–326.

(5) Knowles, R. R.; Jacobsen, E. N. Attractive Noncovalent Interactions in Asymmetric Catalysis: Links between Enzymes and Small Molecule Catalysts. *Proc. Natl. Acad. Sci. U. S. A.* **2010**, *107* (48), 20678–20685.

(6) Brak, K.; Jacobsen, E. N. Asymmetric Ion-Pairing Catalysis. *Angew. Chemie* **-** *Int. Ed.* **2013**, *52* (2), 534–561.

(7) Yepes, D.; Neese, F.; List, B.; Bistoni, G. Unveiling the Delicate Balance of Steric and Dispersion Interactions in Organocatalysis Using High-Level Computational Methods. *J. Am. Chem. Soc.* **2020**, *142* (7), 3613–3625.

(8) Ouchi, M.; Kamigaito, M.; Sawamoto, M. Stereoregulation in Cationic Polymerization by Designed Lewis Acids. 1. Highly Isotactic Poly(Isobutyl Vinyl Ether) with Titanium-Based Lewis Acids. *Macromolecules* **1999**, *32* (20), 6407–6411.

(9) Gridnev, A. A.; Cotts, P. M.; Roe, C.; Barth, H. Stereoregulation in Cationic Polymerization by Designed Lewis Acids. II. Effects of Alkyl Vinyl Ether Structure. *J. Polym. Sci. Part A Polym. Chem.* **2001**, *39* (7), 1060–1066.

(10) Higashimura, T.; Masamoto, J.; Okamura, S. Cationic Copolymerization of Vinyl Ethers Catalyzed by BF3•(OC2H5)2. *Kibunski Kagaku* **1968**, *25* (282), 702–707.

(11) Yuki, H.; Hatada, K.; Nagata, K.; Emura, T. Reactivities and 13C NMR Spectra of Alkyl Vinyl Ethers. *Polym. J.* **1970**, *1* (2), 269–270.

(12) Fox, T. G.; Flory, P. J. Second-Order Transition Temperatures and Related Properties of

Polystyrene. I. Influence of Molecular Weight. *J. Appl. Phys.* **1950**, *21* (6), 581–591.

(13) Fox, T. G.; Flory, P. J. The Glass Temperature and Related Properties of Polystyrene. Influence of Molecular Weight. *J. Polym. Sci.* **1954**, *14* (75), 315–319.

(14) Oda, Y.; Tsujino, T.; Kanaoka, S.; Aoshima, S. Lewis Acid-Specific Polymerization Behaviors in Living Cationic Polymerization of Vinyl Ether with a Malonate Group. *J. Polym. Sci. Part A Polym. Chem.* **2012**, *50* (15), 2993–2998.

(15) Higashimura, T.; Aoshima, S.; Sawamoto, M. Vinyl Ethers with a Functional Group: Living Cationic Polymerization and Synthesis of Monodisperse Polymers. *Makromol. Chemie. Macromol. Symp.* **1986**, *3* (1), 99–111.

(16) Nakamura, T.; Aoshima, S.; Higashimura, T. Living Cationic Polymerization of Vinyl Ethers with a Functional Group. *Polym. Bull.* **1985**, *14* (6), 515–521.

(17) O'Dea, R. M.; Willie, J. A.; Epps, T. H. 100th Anniversary of Macromolecular Science Viewpoint: Polymers from Lignocellulosic Biomass. Current Challenges and Future Opportunities. *ACS Macro Lett.* **2020**, *9*, 476–493.

(18) Gandini, A. The Irruption of Polymers from Renewable Resources on the Scene of Macromolecular Science and Technology. *Green Chem.* **2011**, *13*, 1061–1083.

(19) Shuai, L.; Amiri, M. T.; Questell-Santiago, Y. M.; Héroguel, F.; Li, Y.; Kim, H.; Meilan, R.; Chapple, C.; Ralph, J.; Luterbacher, J. S. Formaldehyde Stabilization Facilitates Lignin Monomer Production during Biomass Depolymerization. *Science.* **2016**, *354* (6310), 329–333.

(20) Zakzeski, J.; C. A. Bruijnincx, P.; L. Jongerius, A.; M. Weckhuysen, B. The Catalytic Valorization of Lignin for the Production of Renewable Chemicals. *Chem. Rev.* **2010**, *110* (6), 3552–3599.

CHAPTER 4: CATALYST AND MONOMER CHIRALITY

4.1 Using a Chiral Lewis Acid

4.1.1 Investigating Ligand Chirality in Chiral Lewis Acid Mediated Polymerizations

Parts of this chapter were adapted with permission from the following manuscript: *J. Am. Chem. Soc.* **2020,** *142*, 17175–17186.[1]

A key aspect of stereoselective vinyl ether polymerization by (*R*)-**2.2** is that it proceeds by enantiomorphic site control,[2,3] whereby a stereochemical error during monomer enchainment is corrected during subsequent monomer addition. This implies that the catalyst is primarily responsible for achieving facial discrimination during monomer enchainment, and it can override the influence of the stereochemistry of the last enchained monomer unit. While enantiomorphic site control is commonly observed in coordination—insertion polymerization approaches, it is rarely reported in ionic polymerizations[4–11] and thus we endeavored to study this phenomenon in more depth.

We hypothesized that the axial chirality of the (*R*)-**2.1** ligand serves an influential role in stereoselective polymerization. However, the difficulty understanding the exact catalyst solution structure and the dynamic nature of ligands on titanium complicate experimental design and analysis. In an attempt to initially explore the role of ligand chirality in our system, we polymerized iBVE in our optimized reaction conditions with differing enantiomeric ratios of the phosphoric acid ligand **2.1** (**Figure 4.1**), and in all cases, the tacticity of the resultant polymer was not affected. A similar phenomenon was recently observed by Aoshima and coworkers in the cationic polymerization of vinyl ethers using a titanium Lewis acid ligated with α,α,α’,α’-tetraaryl-1,3-dioxolane-4,5-dimethanol (TADDOL),[12] wherein they hypothesized that the catalyst remains with the same polymer chain-end throughout propagation. While this could presumably be occurring herein, the difficulty

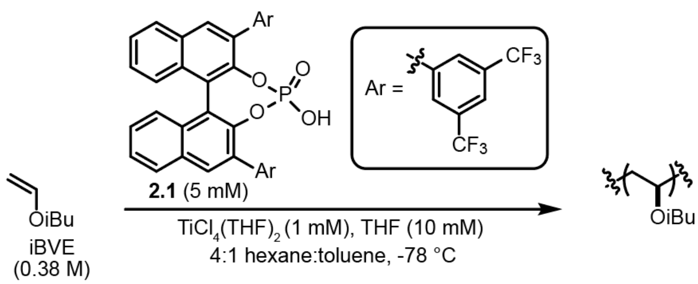

[*R*-**2.1**] : [*S*-**2.1**]	M_n (kg mol^{-1})	Đ	*m* (%)
1 : 0	79	2.0	91
7 : 3	88	1.6	90
1 : 1	52	2.4	90
3 : 7	83	1.7	91
0 : 1	54	2.2	90

Figure 4.1. Nonlinear effects analysis showing no significant change in polymer tacticity when using ligand **2.1** of differing enantiomeric ratios. Polymerizations performed on a 0.75 mmol scale.

understanding the exact catalyst solution structure, the probability that the stereochemistry of a ligand on titanium may influence the binding of subsequent enantiomers, and the dynamic nature of ligands on titanium complicate quantitative correlations. In response to these intriguing results, we sought out a complementary experimental approach (see section 4.1.2) to further probe the influence of ligand stereochemistry on reaction outcome.

4.1.2 Investigating Monomer Chirality in Chiral Lewis Acid Mediated Polymerizations

We hypothesized that the absolute stereochemistry of the phosphoric acid ligands in catalyst **2.2** may play a role in the stereochemical outcome of polymerizations using monomers bearing pendant enantioenriched substitution through a match–mismatch effect. The polymerization of an enantioenriched monomer with a chiral catalyst to yield an isotactic polymer represents a case where a triple diastereoselection model may be operative. Each monomer enchainment event involves two chiral reactants (*i.e.*, the attacking monomer and the chain end bearing a pendant stereocenter) and one chiral catalyst. While double diastereoselection has been probed in detail in small molecule asymmetric catalysis,[13,14] triple diastereoselection represents a case of match–mismatch catalysis that remains underexplored.[15–18] In cases of triple diastereoselection, the interaction of three stereocenters adds the possibility of a partially matched case, in addition to a fully matched and fully mismatched case.[19]

To probe potential match–mismatch effects in the stereoselective polymerization of vinyl ethers, we synthesized two substrates with stereogenic centers placed in differing proximity to the vinyl ether. The first monomer, (*S*)-2-methylbutyl vinyl ether ((*S*)-MBVE), possesses a stereocenter *beta* to the ether oxygen. A control polymerization initiated by triflic acid generated a polymer of 70% *m* (**Figure 4.2**). We reasoned that the non-coordinating triflate counteranion enabled the best assessment of the influence of monomer chirality on the resulting tacticity of the material, absent from counterion effects. This stereoselectivity is analogous to the polymerization of achiral iBVE under the same conditions (71% *m*), which demonstrates that the stereochemistry of this substrate plays no discernable role on the stereoselectivity of polymerization. (*S*)-MBVE was subsequently subjected to reaction conditions using either enantiomer of phosphoric acid ligand **2.1**. In the presence of catalyst (*R*)-**2.2**, a polymer with 89.6 ± 0.1% *m* is produced, while in the presence of catalyst (*S*)-**2.2**, a polymer with 92.5 ± 0.5% *m* is produced. These levels of stereoselectivity are similar to those observed when using (*R*)-**2.2** or (*S*)-**2.2** in the polymerization of iBVE (91% *m* with either enantiomer of **2.1**). Regarding (*S*)-MBVE, the lack of stereoselectivity without the presence of **2.1** and the high stereoselectivity achieved in the presence of either enantiomer of **2.1** indicates a preference for the reaction outcome to be dictated by the catalyst, which supports the enantiomorphic site control we observe using (*R*)-**2.2** with achiral monomers. We hypothesize that these results represent fully matched (92.5 ± 0.5% *m*) and partially matched (89.6 ± 0.1% *m*) examples of stereoselective polymerization. Our thorough analysis of tacticity, calculating standard deviations from 0.1 to 0.5, demonstrates the reproducibility of our synthetic methodology and ^{13}C NMR measurements, justifying the significance of these results.

In a complementary set of experiments, (*S*)-sec-butyl vinyl ether ((*S*)-SBVE) was synthesized to serve as a monomer with a stereocenter *alpha* to the oxygen. Polymerization initiated by triflic acid resulted in a PVE with 88% *m* (**Figure 4.2**). Compared to the polymerization of achiral iPVE under

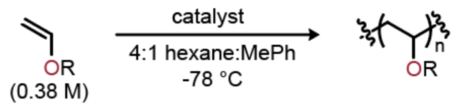

monomer	catalyst	*m* (%)
R = 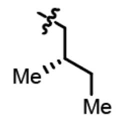 (*S*)-MBVE	CF_3SO_3H	70
	(*R*)-**2.2**	89.6 ± 0.1
	(*S*)-**2.2**	92.5 ± 0.5
R = 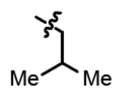 iBVE	CF_3SO_3H	70
	(*R*)-**2.2**	91
	(*S*)-**2.2**	91
R = 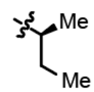 (*S*)-SBVE	CF_3SO_3H	88
	(*R*)-**2.2**	91.8 ± 0.3
	(*S*)-**2.2**	95.1 ± 0.1
R = 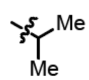 iPVE	CF_3SO_3H	71
	(*R*)-**2.2**	88
	(*S*)-**2.2**	88

Figure 4.2. Match-mismatch effect analysis. Polymerizations performed on a 0.76 mmol scale. The polymerizations of the two chiral monomers with (*R*)-**2.2** and (*S*)-**2.2** were conducted three times. Standard deviation values were calculated from subsequent ^{13}C NMR analysis of the three individual polymer samples.

identical conditions (71% *m*), a pronounced influence of substrate stereochemistry is observed. To probe the influence of catalyst stereochemistry on polymerization outcome, (*S*)-SBVE was subjected to the reaction conditions using either enantiomer of the chiral phosphoric acid (**Figure 4.2**). In the presence of catalyst (*R*)-**2.2**, a polymer with 91.8 ± 0.3% *m* is produced while in the presence of catalyst (*S*)-**2.2**, a polymer with 95.1 ± 0.1% *m* is produced. We hypothesize the use of (*R*)-**2.2** results in a partially matched case. For the polymerization catalyzed by (*S*)-**2.2**, a fully matched system appears to be evident that enables both substrate and catalyst stereocontrol to contribute to the reaction outcome. These synergistic effects result in isotactic poly((*S*)-SBVE) at 95.1 ± 0.1% *m*, the highest stereoselectivity ever reported for a vinyl ether polymerization.

In the analysis of isotactic PVEs derived from enantioenriched monomers, the quantification of % *m* with low standard deviations between 0.1 and 0.5 demonstrates the significance, accuracy, and reproducibility of both our synthetic methodology and ^{13}C NMR measurements. This difference in stereoselectivity is further highlighted when considering the thermal properties of these polymers. Differential Scanning Calorimetry (DSC) analysis at a scan rate of 10 °C/min with data taken from the second heating cycle revealed that poly((*S*)-MBVE) with 89.6 ± 0.1% *m* shows a T_m at 98 °C, while poly((*S*)-MBVE) with 92.5 ± 0.5% *m* shows a T_m at 104 °C. In poly((*S*)-SBVE), a more pronounced relationship between tacticity and thermal properties is observed. Poly((*S*)-SBVE) with 91.8 ± 0.3% *m* lacks a T_m, while poly((*S*)-SBVE) with 95.1 ± 0.1% *m* shows a T_m at 137 °C. This suggests that there exists a critical threshold of isotacticity required to enable this material to undergo reversible crystallization. Altogether, the upshot of this ^{13}C NMR and DSC data is two-fold. First, it allows for more confident differentiation between the partially and fully matched cases. Second, it spurs our efforts to continue pursuing methodologies that enable exceedingly high levels of stereoregularity.

The results presented herein indicate that placing a stereocenter *alpha* to the vinyl ether results in substrate stereocontrol having a larger influence on reaction outcome than if the stereocenter is more remote from the reactive center. This structure–selectivity relationship is commonly observed in asymmetric transformations of small molecules that are governed by double diastereocontrol,[19] providing support to our observations. While more remains to be discovered regarding the influence of ligand chirality on vinyl ether polymerizations, these results indicate that stereochemically matched catalyst–monomer interactions represent a viable approach to push the stereoselectivity of ionic polymerizations to unprecedented levels.

4.2 Using a Chiral Imidodiphosphorimidate (IDPi)

4.2.1 Introduction and Background

Our work using a chiral Lewis acid, as well as previous work by the Sawamoto and Aoshima groups, have all relied exclusively on ligated titanium complexes.[20–22] Subsequently, the polymers made from these approaches can also suffer from the presence of residual metal species, leading to environmental concerns and deterioration of material properties.[23–26] Additionally, in our work, a large excess of equivalents of the BINOL-derived phosphate ligand is needed to form the anionic species responsible for stereoinduction. Therefore, complementary methods that provide access to isotactic poly(vinyl ethers) without the required use of a transition metal or superstoichiometric amounts of chiral ligand could enable expand innovation and application of this class of thermoplastics.

Due to their high acidity, trifluoromethanesulfonic acid[27] and pentacarbomethoxycyclopentadiene acids[28] have already been successfully employed in the cationic polymerization of vinyl ethers, albeit the resulting materials are atactic and amorphous. Thus, we hypothesized the development of a single-component chiral Brønsted acid initiating species with the acidity necessary to initiate polymerization, and a chiral conjugate base capable of directing the stereochemistry of monomer addition. Inspired again by the field of asymmetric small molecule catalysis,[29,30] imidodiphosphormidates (IDPis)[31] were explored as a chiral Brønsted acid scaffold for this purpose. Screening and reaction optimization led to the realization of IDPi **4.1**, suitable for the isotactic polymerization of a variety of alkyl vinyl ethers with high stereoselectivity and high molecular weights (M_n > 100 kg/mol).

To compare substrates against one another under conditions that achieve high stereoselectivity, we conducted all polymerizations at –78 °C in 20:1 methylcyclohexane:toluene with a monomer and **4.1** concentration of 0.2 M and 0.5 mM, respectively. Alkyl vinyl ether monomers with linear side chains were explored first and found to be well-tolerated in the stereoselective polymerization (**Figure 4.3B**). The polymerization of *n*-propyl vinyl ether (nPrVE) engendered a polymer with 85% *m*, while the polymerization of *n*-butyl vinyl ether (nBVE) and *n*-hexyl vinyl ether (nHVE) resulted in polymers with 87% *m*. Further increasing the length of the linear alkyl substitution, as in octyl vinyl ether (OcVE), also resulted in the concomitant increase in stereoselectivity (90% *m*).

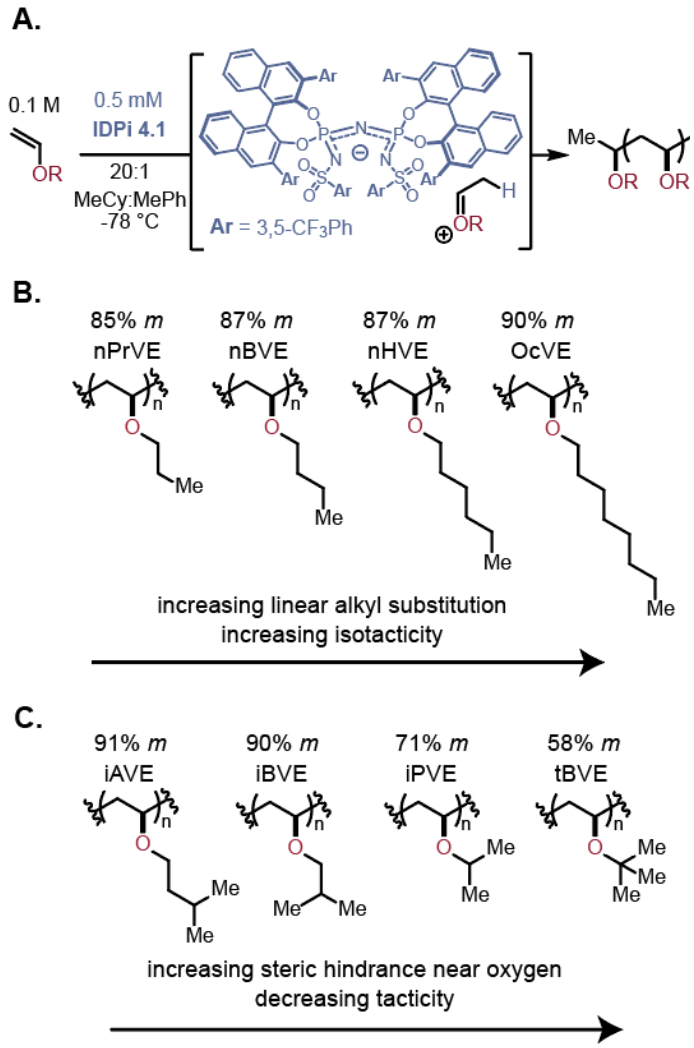

Figure 4.3. A) Reaction scheme showing optimized reaction conditions and IDPi **4.1**. MeCy = methylcyclohexane. MePh = toluene. B) Representative structure-reactivity profiles for a variety of vinyl ethers with linear alkyl substitution. C) Representative structure-reactivity profiles for a variety of vinyl ethers with branched alkyl substitution.

The steric properties of branched alkyl vinyl ether monomers demonstrated a pronounced influence on the stereoselectivity achieved with the optimized IDPi **4.1** (**Figure 4.3C**). In order to probe these effects systematically, the site of branching was placed progressively closer to the ether through the evaluation of isoamyl vinyl ether (iAVE), iBVE, and isopropyl vinyl ether (iPVE). While iAVE and iBVE demonstrated similar stereoselectivity (91 and 90% *m*, respectively), a large decrease in isotacticity was observed when the branch point was placed *alpha* to the vinyl ether in iPVE (71% *m*). Likewise, the presence of a quaternary center *alpha* to the vinyl ether, such as in *tert*-butyl vinyl ether (tBVE), proved to be detrimental to stereoselectivity, resulting in poly(tBVE) with 58% *m*. This systematic screen of monomer steric parameters implies that increasing steric hindrance close to the ether oxygen results in a diminished stereoselectivity during polymerization. Our proposed hypothesis indicates that facial addition in these polymerizations is biased by the close association of the cationic chain-end with conjugate base counterion of the IDPi catalyst. Therefore, we hypothesize that an increase in steric bulk close to the oxocarbenium ion disrupts the tight ion pair and causes a decrease in the stereoselectivity of monomer addition.[30,32,33]

4.2.2 Investigating Counteranion Chirality in IDPi Mediated Polymerizations

We hypothesized that the axial chirality of **4.1** could serve an influential role in stereoselective polymerization. Further, we also posited that the probing of these effects in the single component IDPi catalyst scaffold could be more straightforward than in the case of catalyst **2.2**, whose dynamic ligands complicated experimental design and analysis. Thus, we polymerized iBVE in our optimized reaction conditions with differing enantiomeric ratios of **4.1** (**Figure 4.4**), and in all cases, the tacticity of the resultant polymer was not affected. Because similar results were seen by Aoshima[12] and our work with catalyst **2.2**,[1] we again sought out a complementary experimental approach (see section 4.2.3) to further probe the influence of the anion's axial chirality on tacticity.

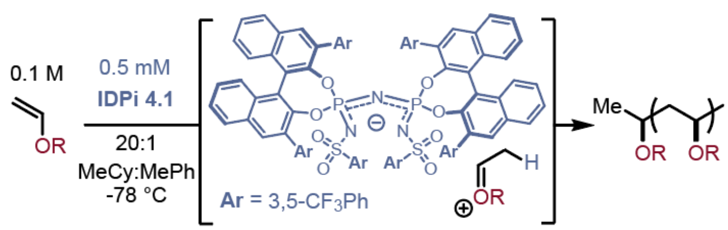

[*R*-**4.1**] : [*S*-**4.1**]	M_n (kg mol^{-1})	Đ	*m* (%)
1 : 0	123	1.4	91
3 : 1	79	2.6	90
1 : 1	103	2.1	90
1 : 3	126	1.9	90
0 : 1	104	2.3	90

Figure 4.4. Nonlinear effects analysis showing no significant change in polymer tacticity when using IDPi **4.1** of differing enantiomeric ratios.

4.2.3 Investigating Monomer Chirality in IDPi Mediated Polymerizations

We hypothesized that the absolute stereochemistry of the imidodiphosphormidate scaffold may play a role in the stereochemical outcome of polymerizations using monomers bearing pendant enantioenriched substitution through a match–mismatch effect. To probe potential match–mismatch effects in the stereoselective polymerization of vinyl ethers, we again investigated two substrates with stereogenic centers placed in differing proximity to the vinyl ether. (*S*)-MBVE, possessing a stereocenter *beta* to the ether oxygen, generated a polymer of 70% *m* when initiated with triflic acid (**Figure 4.5**). In the presence of either (*R*)-**4.1** or (*S*)-**4.1**, a polymer with 90% *m* was produced, identical to the level of stereoselectivity observed when using IDPi **4.1** in the polymerization of iBVE. Unlike the polymerization of (*S*)-MBVE with both enantiomers of catalyst **2.2**, we do not observe fully matched and partially matched cases herein.

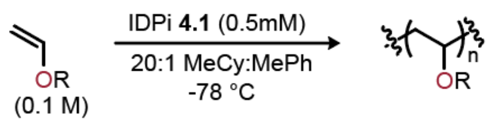

monomer	catalyst	*m* (%)
R = (*S*)-MBVE	CF_3SO_3H	70
	(*R*)-**4.1**	90
	(*S*)-**4.1**	90
R = iBVE	CF_3SO_3H	70
	(*R*)-**4.1**	90
	(*S*)-**4.1**	90
R = (*S*)-SBVE	CF_3SO_3H	88
	(*R*)-**4.1**	86
	(*S*)-**4.1**	85
R = iPVE	CF_3SO_3H	71
	(*R*)-**4.1**	71
	(*S*)-**4.1**	71

Figure 4.5. Match-mismatch effect analysis. IDPi **4.1** catalyzed polymerization of two chiral monomers and their achiral analogs.

In a complementary set of experiments, (*S*)-sec-butyl vinyl ether ((*S*)-SBVE) was used as a monomer with a stereocenter *alpha* to the oxygen. Polymerization initiated by triflic acid resulted in a PVE with 88% *m* (**Figure 4.5**). Compared to the polymerization of achiral iPVE under identical conditions (71% *m*), an effect of internal substrate control is at play in the polymerization of (*S*)-SBVE, engendering high isotacticity without the use of a chiral coutneranion. To probe the influence of counteranion stereochemistry on polymerization outcome, (*S*)-SBVE was subjected to the reaction conditions using either enantiomer of IDPi **4.1** (**Figure 4.5**). In the presence of (*R*)-**4.1** or (*S*)-**4.1**, a significant difference in polymer tacticity (86 and 85% *m*, respectively) is not observed, suggesting that match–mismatch effects were not consequential to the outcome of the polymerization.

4.3 Conclusion

Catalyst and monomer chirality were thoroughly probed in the cationic polymerization of vinyl ethers enabled by both catalyst **2.2** and **4.1**. In turn, these investigations revealed new possibilities in the pursuit of highly isotactic polymers. In the context of investigating the axial chirality of our catalyst scaffolds, we found using that differing enantiomeric ratios of either catalyst did not result in a change to polymer tacticity. However, drawing concrete conclusions from these analyses are often complicated by a myriad of factors, including the fact that we are not setting only a single stereocenter in the product; rather, we are setting hundreds and can only accurately evaluate the product's relative stereochemistry (% *m*). There also exists the likely possibility for polymer chain exchange between catalysts of differing chirality. Specific to the system involving catalyst **2.2**, data evaluation is further problematic as there are likely multiple chiral ligands, possibly of different handedness, coordinated to a single titanium center.

In regards to investigating monomer chirality, we found that match–mismatch effects were not consequential to the outcome of the polymerization when using catalyst **4.1**. However, when using catalyst **2.2**, we synthesized an isotactic poly(vinyl ether) with the highest stereoselectivity (95.1% ± 0.1 *meso* diads) reported to date, which occurred when monomer and catalyst stereochemistry were fully matched under a triple diastereocontrol model. While more remains to be discovered regarding the influence of both catalyst and monomer chirality on vinyl ether polymerizations, these results indicate that stereochemically matched catalyst–monomer interactions represent a viable approach to push the stereoselectivity of ionic polymerizations to unprecedented levels.

REFERENCES

(1) Varner, T. P.; Teator, A. J.; Reddi, Y.; Jacky, P. E.; Cramer, C. J.; Leibfarth, F. A. Mechanistic Insight into the Stereoselective Cationic Polymerization of Vinyl Ethers. *J. Am. Chem. Soc.* **2020**, *142* (40), 17175–17186.

(2) Okamoto, Y.; Nakano, T. Asymmetric Polymerization. *Chem. Rev.* **2002**, *94* (2), 349–372.

(3) W. Coates, G. Precise Control of Polyolefin Stereochemistry Using Single-Site Metal Catalysts. *Chem. Rev.* **2000**, *100* (4), 1223–1252.

(4) Y. Svirkin, Y.; Xu, J.; A. Gross, R.; L. Kaplan, D.; Swift, G. Enzyme-Catalyzed Stereoelective Ring-Opening Polymerization of α-Methyl-β-Propiolactone. *Macromolecules* **1996**, *29* (13), 4591–4597.

(5) Collins, S.; G. Ward, D.; H. Suddaby, K. Group-Transfer Polymerization Using Metallocene Catalysts: Propagation Mechanisms and Control of Polymer Stereochemistry. *Macromolecules* **2002**, *27* (24), 7222–7224.

(6) Chisholm, M. H.; Patmore, N. J.; Zhou, Z. Concerning the Relative Importance of Enantiomorphic Site vs. Chain End Control in the Stereoselective Polymerization of Lactides: Reactions of (R,R-Salen)- and (S,S-Salen)-Aluminium Alkoxides LAlOCH2R Complexes (R = CH3 and S-CHMeCl). *Chem. Commun.* **2005**, No. 1, 127–129.

(7) J. Darensbourg, D.; Karroonnirun, O.; J. Wilson, S. Ring-Opening Polymerization of Cyclic Esters and Trimethylene Carbonate Catalyzed by Aluminum Half-Salen Complexes. *Inorg. Chem.* **2011**, *50* (14), 6775–6787.

(8) Aluthge, D. C.; Patrick, B. O.; Mehrkhodavandi, P. A Highly Active and Site Selective Indium Catalyst for Lactide Polymerization. *Chem. Commun.* **2013**, *49* (39), 4295–4297.

(9) Pilone, A.; Press, K.; Goldberg, I.; Kol, M.; Mazzeo, M.; Lamberti, M. Gradient Isotactic Multiblock Polylactides from Aluminum Complexes of Chiral Salalen Ligands. *J. Am. Chem. Soc.* **2014**, *136* (8), 2940–2943.

(10) Altenbuchner, P. T.; Adams, F.; Kronast, A.; Herdtweck, E.; Pöthig, A.; Rieger, B. Stereospecific Catalytic Precision Polymerization of 2-Vinylpyridine via Rare Earth Metal-Mediated Group Transfer Polymerization with 2-Methoxyethylamino-Bis(Phenolate)-Yttrium Complexes. *Polym. Chem.* **2015**, *6* (38), 6796–6801.

(11) Kronast, A.; Reiter, D.; T. Altenbuchner, P.; I. Vagin, S.; Rieger, B. 2-Methoxyethylamino-Bis(Phenolate)Yttrium Catalysts for the Synthesis of Highly Isotactic Poly(2-Vinylpyridine) by Rare-Earth Metal-Mediated Group Transfer Polymerization. *Macromolecules* **2016**, *49*

(17), 6260–6267.

(12) Watanabe, H.; Yamamoto, T.; Kanazawa, A.; Aoshima, S. Stereoselective Cationic Polymerization of Vinyl Ethers by Easily and Finely Tunable Titanium Complexes Prepared from Tartrate-Derived Diols: Isospecific Polymerization and Recognition of Chiral Side Chains. *Polym. Chem.* **2020**, *11*, 3398–3403.

(13) Masamune, S.; Choy, W.; Petersen, J. S.; Sita, L. R. Double Asymmetric Synthesis—a New Strategy for Stereochemical Control in Organic Synthesis. *Angew. Chem. Int. Ed* **1985**, *24* (1), 1–76.

(14) A. Evans, D.; J. Miller, S.; Lectka, T.; von Matt, P. Chiral Bis(Oxazoline)Copper(II) Complexes as Lewis Acid Catalysts for the Enantioselective Diels−Alder Reaction. *J. Am. Chem. Soc.* **1999**, *121* (33), 7559–7573.

(15) Duplantier, A. J.; Nantz, M. H.; Roberts, J. C.; Short, R. P.; Somfai, P.; Masamune, S. Triple Asymmetric Synthesis for Fragment Assembly: Validity of Approximate Multiplicativity of the Three Diastereofacial Selectivities. *Tetrahedron Lett.* **1989**, *30* (52), 7357–7360.

(16) Crowden, C. J.; Paterson, I. Asymmetric Aldol Reactions Using Boron Enolates. *Org. React.* **1997**, *51*, 1–200.

(17) Wan, Z.-K.; Choi, H.; Kang, F.-A.; Nakajima, K.; Demeke, D.; Kishi, Y. Asymmetric Ni(II)/Cr(II)-Mediated Coupling Reaction: Stoichiometric Process. *Org. Lett.* **2002**, *4* (25), 4431–4434.

(18) Choi, H.; Nakajima, K.; Demeke, D.; Kang, F.-A.; Jun, H.-S.; Wan, Z.-K.; Kishi, Y. Asymmetric Ni(II)/Cr(II)-Mediated Coupling Reaction: Catalytic Process. *Org. Lett.* **2002**, *4* (25), 4435–4438.

(19) Walsh, P. L.; C. Kozlowski, M. *Fundamentals of Asymmetric Catalysis*; University Science Books: Sausalito, CA, 2009.

(20) Ouchi, M.; Kamigaito, M.; Sawamoto, M. Stereoregulation in Cationic Polymerization by Designed Lewis Acids. 1. Highly Isotactic Poly(Isobutyl Vinyl Ether) with Titanium-Based Lewis Acids. *Macromolecules* **1999**, *32* (20), 6407–6411.

(21) Ouchi, M.; Sueoka, M.; Kamigaito, M.; Sawamoto, M. Stereoregulation in Cationic Polymerization. III. High Isospecificity with the Bulky Phosphoric Acid [(RO)2PO2H]/SnCl4 Initiating Systems: Design of Counteranions via Initiators. *J. Polym. Sci. Part A Polym. Chem.* **2001**, *39* (7), 1067–1074.

(22) Watanabe, H.; Yamamoto, T.; Kanazawa, A.; Aoshima, S. Stereoselective Cationic

Polymerization of Vinyl Ethers by Easily and Finely Tunable Titanium Complexes Prepared from Tartrate-Derived Diols: Isospecific Polymerization and Recognition of Chiral Side Chains. *Polym. Chem.* **2020**, *11* (20), 3398–3403.

(23) Cam, D.; Marucci, M. Influence of Residual Monomers and Metals on Poly (L-Lactide) Thermal Stability. *Polymer.* **1997**, *38* (8), 1879–1884.

(24) Kim, K. J.; Doi, Y.; Abe, H. Effects of Residual Metal Compounds and Chain-End Structure on Thermal Degradation of Poly(3-Hydroxybutyric Acid). *Polym. Degrad. Stab.* **2006**, *91* (4), 769–777.

(25) Usluer, Ö.; Abbas, M.; Wantz, G.; Vignau, L.; Hirsch, L.; Grana, E.; Brochon, C.; Cloutet, E.; Hadziioannou, G. Metal Residues in Semiconducting Polymers: Impact on the Performance of Organic Electronic Devices. *ACS Macro Lett.* **2014**, *3* (11), 1134–1138.

(26) Rudenko, A. E.; Thompson, B. C. Optimization of Direct Arylation Polymerization (DArP) through the Identification and Control of Defects in Polymer Structure. *J. Polym. Sci. Part A Polym. Chem.* **2015**, *53* (2), 135–147.

(27) Uchiyama, M.; Satoh, K.; Kamigaito, M. Cationic RAFT Polymerization Using Ppm Concentrations of Organic Acid. *Angew. Chemie - Int. Ed.* **2015**, *54* (6), 1924–1928.

(28) Kottisch, V.; O'Leary, J.; Michaudel, Q.; Stache, E. E.; Lambert, T. H.; Fors, B. P. Controlled Cationic Polymerization: Single-Component Initiation under Ambient Conditions. *J. Am. Chem. Soc.* **2019**, *141* (27), 10605–10609.

(29) Mahlau, M.; List, B. Asymmetric Counteranion-Directed Catalysis: Concept, Definition, and Applications. *Angew. Chemie - Int. Ed.* **2013**, *52* (2), 518–533.

(30) Brak, K.; Jacobsen, E. N. Asymmetric Ion-Pairing Catalysis. *Angew. Chemie - Int. Ed.* **2013**, *52* (2), 534–561.

(31) Schreyer, L.; Properzi, R.; List, B. IDPi Catalysis. *Angew. Chemie - Int. Ed.* **2019**, *58* (37), 12761–12777.

(32) Knowles, R. R.; Jacobsen, E. N. Attractive Noncovalent Interactions in Asymmetric Catalysis: Links between Enzymes and Small Molecule Catalysts. *Proc. Natl. Acad. Sci. U. S. A.* **2010**, *107* (48), 20678–20685.

(33) Yepes, D.; Neese, F.; List, B.; Bistoni, G. Unveiling the Delicate Balance of Steric and Dispersion Interactions in Organocatalysis Using High-Level Computational Methods. *J. Am. Chem. Soc.* **2020**, *142* (7), 3613–3625.

CHAPTER 5: USING CHIRAL HYDROGEN BOND DONORS

5.1 Introduction

Although our previous work using a chiral Lewis acid derived from $TiCl_4(THF)_2$ and 3,3'-bis(3,5-bis(trifluoromethyl)phenyl)-1,1'-binaphthyl phosphate provided substantial advancements,[1–3] there are two notable drawbacks. First, the use of titanium is required; residual metal species present in polymeric products are environmentally unfriendly and can often deteriorate polymer properties.[4–7] Second, a large excess of equivalents of the BINOL-derived phosphate ligand is needed to form the anionic species responsible for stereoinduction. Thus, we wanted to pull inspiration from alternative strategies in asymmetric ion pairing catalysis to both address these limitations and expand the synthetic toolbox used for accessing isotactic polymers.

In the asymmetric synthesis of small molecules, the ability of neutral hydrogen bond donors to bind anions has been recently leveraged to enable enantioselective additions in reactions proceeding through ion-pair intermediates.[8] This specific subset of ion pairing catalysis, termed anion-binding catalysis, relies on the binding of a chiral hydrogen bond donor to the counteranion of a cationic intermediate, forming a chiral complex suitable for facilitating nucleophilic enantiofacial discrimination.[9–19] In one particular early example, Jacobsen employed a chiral thiourea catalyst to facilitate the ionization of 1-chloroisochroman and the subsequent enantioselective addition of a silyl ketene acetal (**Figure 5.1B**).[10] Systematic interrogation of the thiourea scaffold revealed that the identity of the two stereocenters could allow for either a detrimental or complementary influence on the reaction stereoselectivity. In a more recent example, Jacobsen used a chiral squaramide to enhance the Lewis acidity of a silyl triflate, enabling an asymmetric Mukaiyama aldol reaction from a more stable acetal starting material (**Figure 5.1C**).[17] In these two examples, the aryl identity of arylpyrrolidine group was found to exhibit a strong influence on both reactivity and

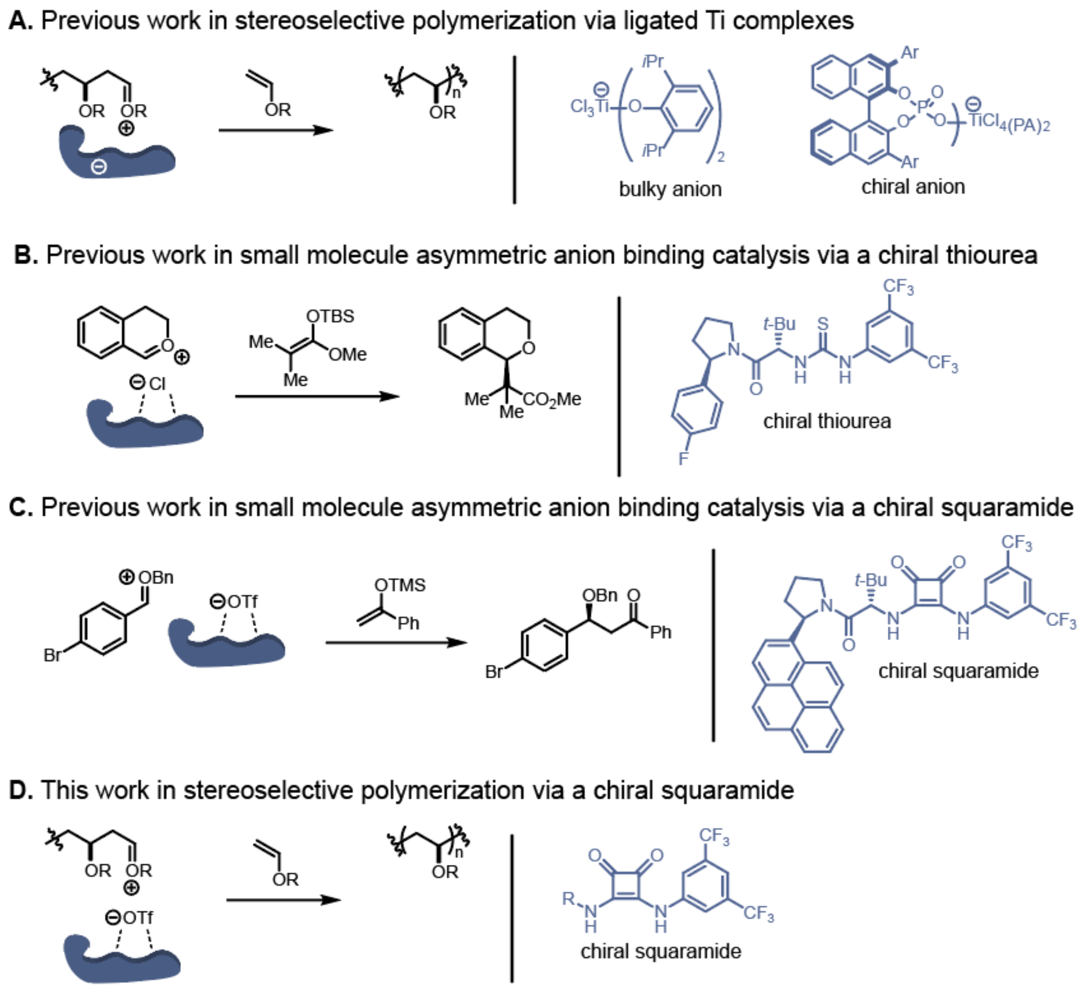

Figure 5.1. A) Previous work towards the stereoselective cationic polymerization of vinyl ethers by Sawamoto (bulky anion) and Leibfarth (chiral anion). Ar=bis(trifluoromethyl)phenyl. PA=(*R*)-3,3'-bis(3,5-bis(trifluoromethyl)phenyl)-1,1'-binaphthyl phosphate. B and C) Selected examples of small molecule asymmetric anion binding catalysis by Jacobsen. D) This work applying the principles of asymmetric anion binding catalysis to stereoselective cationic polymerization.

enantioselectivity, suggesting that this aromatic group may engage in stabilizing interactions with the oxocarbenium ion; therefore, we hypothesized that this foundation in anion binding catalysis could be translated to also enable the stereoselective cationic polymerization of vinyl ethers, which proceeds through the same cationic intermediate. Herein is reported the targeted binding of triflate anions with chiral squaramides for the stereoselective polymerization of vinyl ethers (**Figure 5.1D**).

5.2 Screening of Scaffold and Reaction Conditions

Given the literature precedent for chiral hydrogen bond donors binding strongly to sulfonates,[17,20,21] we first explored interfacing these motifs in the trifluoromethanesulfonic acid-initiated polymerization of vinyl ethers.[22] Rapid kinetics have been previously exhibited with this initiator.[23] Thus, we also thought it important to devise reaction conditions that allowed for binding between the hydrogen bond donor and trifluoromethanesulfonate anion, prior to exposure to monomer for propagation. For this concern and the ease of experimental preparation, we devised a novel initiating system comprising an isochroman acetal and trimethylsilyl thrifluoromethanesulfonate (**Figure 5.2**). Addition of a chiral hydrogen bond donor to a solution of these reagents forms methoxytrimethylsilane, an isochroman-derived cationogen, and a trifluoromethanesulfonate-squaramide complex.[10,17] Subsequent addition of monomer to this solution thereby enables propagation.

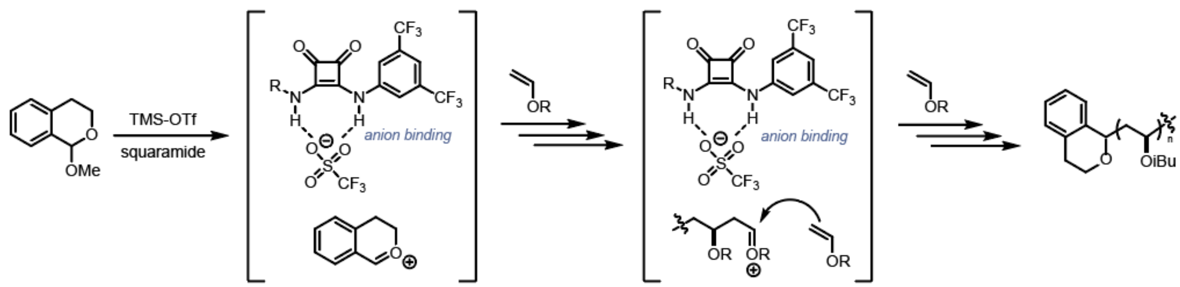

Figure 5.2. Polymerization mechanism for the reaction conditions described herein.

We next began assessing the viability of different classes of hydrogen bond donors within this reaction scheme. No polymerization was observed with thioureas (see Appendix D). Presumably, rapid addition of the Lewis basic thiocarbonyl into the oxocarbenium ion prevents propagation.[24] Fortunately, squaramides did interface well with this strategy and permit polymerization. We next performed an initial reaction condition optimization study (see Appendix D), leading to the use of a 1000:1:1:1 molar ratio of monomer/isochroman acetal/ trimethylsilyl thrifluoromethanesulfonate/squaramide in 1:3 methylcyclohexane/diethyl ether at -78 °C (**Figure 5.3**). Low temperature and low dielectric solvents are used to promote the formation of a tight ion pair between the prochiral oxocarbenium chain end and the trifluoromethanesulfonate-squaramide complex, thereby encouraging selective monomer facial addition.[3,8]

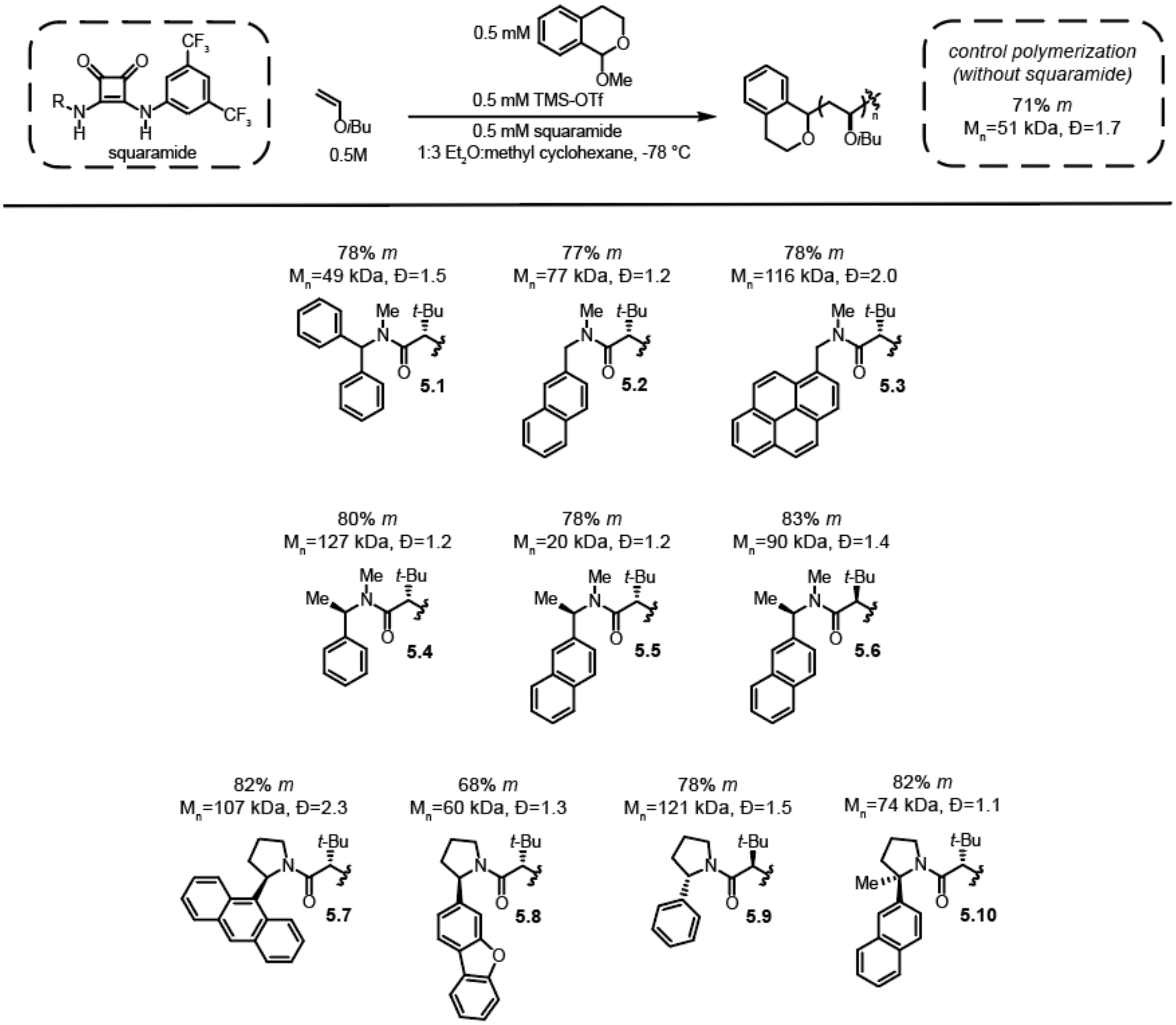

Figure 5.3. Variations in the chiral squaramide scaffold were screened in the polymerization of a model substrate, isobutyl vinyl ether (iBVE). Theoretical M_n=100 kDa.

Using these optimized reaction conditions, we next screened variations in the squaramide scaffold against a model bio-derived[25–29] substrate, isobutyl vinyl ether (iBVE). Aryl-substituted amido squaramides possessing benzyhydryl (**5.1**), 2-naphthalenyl (**5.2**), and 1-pyrenyl substituents (**5.3**) showed moderate stereoselectivities of 77-78% *m*, 6-7% *m* above that seen in an analogous control polymerization absent of chiral hydrogen bond donor (**Figure 5.3**). Placing an additional stereocenter onto the phenyl (**5.4**) and 2-naphthalenyl (**5.5** and **5.6**) amide moieties led to overall improvements in stereoselectivity (76-83% *m*). Within this series, the relative stereochemistry of the squaramide scaffold proved to be important. Diastereomeric squaramides **5.5** and **5.6** produced poly(iBVE) with 78 and 83% *m*, respectively.

Encouraged by these results, we next wanted to explore an arylpyrrolidino squaramide framework. The Jacobsen group has seen success with this scaffold which contains a rigidified aryl component. In the context of cationic polymerization, however, varied results were achieved. Both 9-anthracenyl derivative **5.7** and fully substituted 2-naphthyl derivative **5.10** yielded poly(iBVE) with 82% *m*. Phenyl derivative **5.9** shows only moderate stereoselectivity at 78% *m*. Finally, a dramatic decrease in stereoselectivity (68% *m*) was observed when using heterocyclic 3-dibenzofuranyl derivative **5.8**.

In addition to stereoselectivity, observing trends in reactivity also aids in uncovering the influence that the squaramide has on the polymerization. For instance, the control polymerization absent of squaramide is not living. Deleterious side reactions, such as chain transfer by monomer and chain transfer by counteranion, serve to broaden dispersity and suppress the ability to target polymer molecular weight.[30–35] However, in most cases when a squaramide was present, we observed a decrease in dispersity and obtained polymers closer to the targeted M_n (100 kDa). This suggests that the hydrogen bonding of the squaramide decreases the basicity of trifluoromethanesulfonate, thereby reducing the amount of chain transfer by counteranion. In regard to stereoinduction, analysis is complicated by the fact that we are setting hundreds of stereocenters in a single polymer chain, but we can only accurately evaluate the relative stereochemistry (% *m*) of the product. Despite this constraint, we found that the identity of the pendant aryl group and the relative stereochemistry of the squaramide scaffold were influential components in achieving high stereoselectivity. In order to more thoroughly probe the mechanism and scope of this method, squaramide **5.6** was chosen as the optimal chiral hydrogen bond donor for the ensuing studies.

5.3 Kinetic and Stereoselectivity Analyses

To gain further insight into the influence of the squaramide, we first investigated the rate of two polymerizations: the stereoselective polymerization of iBVE using **5.6** ([iBVE]=0.5 M, [isochroman acetal] = 0.5 mM, [TMS-OTf] = 0.5 mM, [**5.6**] = 0.5 mM) and the atactic control polymerization of iBVE in the absence of **5.6** ([iBVE]=0.5 M, [isochroman acetal] = 0.5 mM, [TMS-OTf] = 0.5 mM). Polymerizations were quenched at five second intervals, and distinct ^{1}H NMR resonances for iBVE and an internal standard were integrated relative to each other in order to determine monomer conversion. Pseudo-first order reaction kinetics were displayed by the initial rates of the two polymerizations.[22,36,37] The rate constant of the stereoselective polymerization, k_{obs} = 9.8 × 10^{-3} s^{-1}, was approximately 1.5 times slower than that of the control polymerization, k_{obs} = 1.5 × 10^{-2} s^{-1} (**Figure 5.4**). This slight decrease in rate observed with the addition of **5.6** is consistent with previous reports of negative catalysis in which a hydrogen bond donor shuts down the background reaction by binding to all of the trifluoromethanesulfonate anion present in solution.[20] As a result, the reaction is then forced through a slower, stereoselective pathway. The decreased rate also agrees with a model of ligand decelerated catalysis, described in our previous reports of stereoselective cationic polymerization.[3] Attempts to fully suppress any amount of the faster, undesired atactic background reaction by utilizing a slight excess of squaramide were unsuccessful, leading to the shutdown of polymerization (see Appendix D).

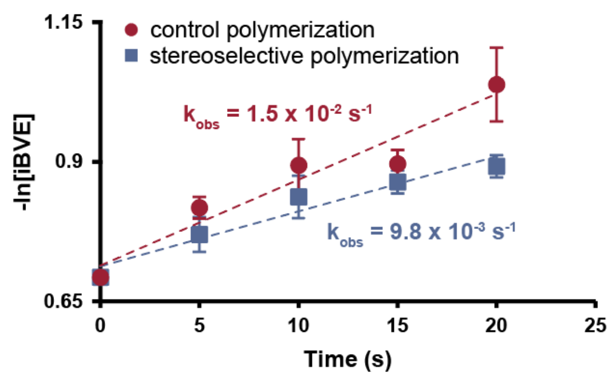

Figure 5.4. Kinetic analysis of iBVE polymerizations under both the stereoselective reaction conditions (blue squares; [iBVE]=0.5 M, [isochroman acetal]=0.5 mM, [TMS-OTf]=0.5 mM, [squaramide **5.6**] =0.5 mM) and the control reaction conditions (red circles; [iBVE]=0.5 M, [isochroman acetal]=0.5 mM, [TMS-OTf]=0.5 mM). Each data point reported shows the average and standard deviation of three individual experiments.

We next performed temperature dependent stereoselectivity analyses on both the stereoselective and control polymerization. In the control polymerization absent of **5.6**, a concomitant linear decrease in stereoinduction was observed as temperature was increased (**Figure 5.5**). This linearity demonstrates that the overall mechanism does not change between −78 °C and −40 °C.[38] However, in the stereoselective polymerization, a dramatic drop from 83% *m* to 75% *m* occurs when the reaction temperature is increased from -78 °C to -61 °C. While this again confirms the need for low temperatures to achieve stereocontrol, it also suggests that there are likely a variety of noncovalent interactions at play giving rise to the observed stereoinduction at -78 °C. Increasing the temperature thereby has a detrimental effect on one or more of the governing interactions, which quickly erodes stereoselectivity.

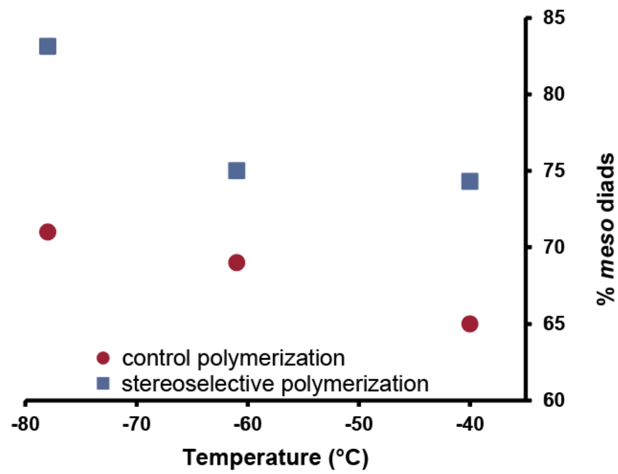

Figure 5.5. Temperature dependence on stereoselectivity of both the stereoselective polymerization (blue squares; [iBVE]=0.5 M, [isochroman acetal]=0.5 mM, [TMS-OTf]=0.5 mM, [squaramide **5.6**] =0.5 mM) and the control polymerization (red circles; [iBVE]=0.5 M, [isochroman acetal]=0.5 mM, [TMS-OTf]=0.5 mM).

5.4 Alkyl Vinyl Ether Substrate Scope

In an effort to explore the substrate scope of this methodology, we applied chiral squaramide **5.6** to the polymerization of several commercially available vinyl ethers with varying alkyl substitution. The preparation of isotactic materials was achieved when the monomeric alkyl substitution was linear, such as in propyl vinyl ether (nPrVE, 80% *m*) and butyl vinyl ether (nBVE, 82% *m*). Introducing a branch point at the position β to the oxygen, for example in iBVE, did not negatively impact the stereoselectivity of the polymerization (83% *m*). However, decreased isotacticity was observed when a branch point was placed α to the oxygen, as in isopropyl vinyl ether (iPVE, 71% *m*) and the fully substituted *tert*-butyl vinyl ether (tBVE, 65% *m*). Because facial addition in these polymerizations is biased by the close association of the cationic chain end with the anionic counterion-squaramide complex,[8] we therefore hypothesize that an increase in steric bulk close to the oxocarbenium ion disrupts this tight ion pair and reduces the stereoselectivity of monomer addition.[3]

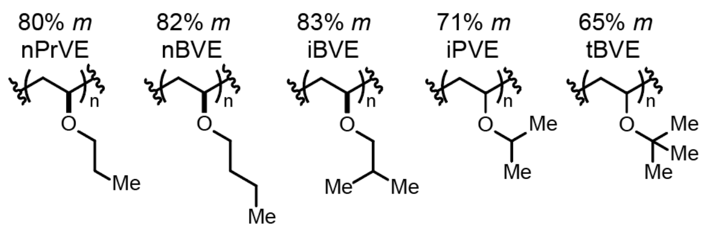

Figure 5.6. Representative structure-reactivity profiles for a variety of alkyl vinyl ethers synthesized with the stereocontrolled reaction conditions using squaramide **5.6**.

5.5 Polymer Thermal Properties

With the substrate scope expanded, we subsequently also wanted to examine the thermal properties of these materials through differential scanning calorimetry (DSC). Overlaid DSC traces of poly(iBVE) samples of 83% *m* (synthesized via the stereoselective polymerization conditions) and 71% m (synthesized via the control polymerization conditions) further highlight the dramatic influence that this increase in stereoselectivity has on material properties (**Figure 5.7**). Poly(iBVE) with 71% *m* is amorphous, but increasing the isotacticity by 12% *m* produces a semicrystalline polymer, exhibiting cold crystallization and a T_m at 89 °C.

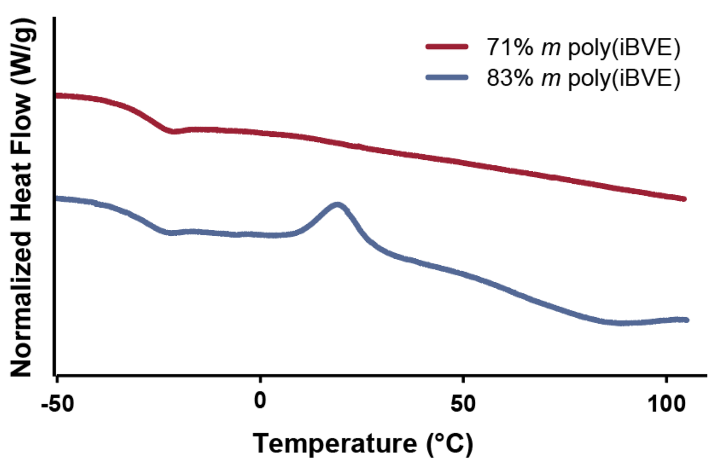

Figure 5.7. Dynamic scanning calorimetry second-heating-scan curves (5 °C/min) of poly(iBVE) with 71% *m* and 83% *m*.

5.6 Conclusion

Using chiral squaramides to target the binding of triflate anion in cationic polymerization affords poly(vinyl ethers) with up to 83% *m*, engendering sufficient stereoregularity to produce a semicrystalline thermoplastic with a melting temperature of 89 °C. Kinetic investigations reveal a ligand deceleration effect, while temperature dependent stereoselectivity analyses confirm the need for low reaction temperatures. Further, this work represents the first example of anion binding catalysis applied to cationic polymerization, thereby introducing a new mechanistic framework for the continued exploration of stereoselective polymerizations as a whole.

REFERENCES

(1) Teator, A. J.; Leibfarth, F. A. Catalyst-Controlled Stereoselective Cationic Polymerization of Vinyl Ethers. *Science.* **2019**, *363*, 1439–1443.

(2) Teator, A. J.; Varner, T. P.; Jacky, P. E.; Sheyko, K. A.; Leibfarth, F. A. Polar Thermoplastics with Tunable Physical Properties Enabled by the Stereoselective Copolymerization of Vinyl Ethers. *ACS Macro Lett.* **2019**, *8* (12), 1559–1563.

(3) Varner, T. P.; Teator, A. J.; Reddi, Y.; Jacky, P. E.; Cramer, C. J.; Leibfarth, F. A. Mechanistic Insight into the Stereoselective Cationic Polymerization of Vinyl Ethers. *J. Am. Chem. Soc.* **2020**, *142* (40), 17175–17186.

(4) Cam, D.; Marucci, M. Influence of Residual Monomers and Metals on Poly (L-Lactide) Thermal Stability. *Polymer.* **1997**, *38* (8), 1879–1884.

(5) Kim, K. J.; Doi, Y.; Abe, H. Effects of Residual Metal Compounds and Chain-End Structure on Thermal Degradation of Poly(3-Hydroxybutyric Acid). *Polym. Degrad. Stab.* **2006**, *91* (4), 769–777.

(6) Usluer, Ö.; Abbas, M.; Wantz, G.; Vignau, L.; Hirsch, L.; Grana, E.; Brochon, C.; Cloutet, E.; Hadziioannou, G. Metal Residues in Semiconducting Polymers: Impact on the Performance of Organic Electronic Devices. *ACS Macro Lett.* **2014**, *3* (11), 1134–1138.

(7) Rudenko, A. E.; Thompson, B. C. Optimization of Direct Arylation Polymerization (DArP) through the Identification and Control of Defects in Polymer Structure. *J. Polym. Sci. Part A Polym. Chem.* **2015**, *53* (2), 135–147.

(8) Brak, K.; Jacobsen, E. N. Asymmetric Ion-Pairing Catalysis. *Angew. Chemie - Int. Ed.* **2013**, *52* (2), 534–561.

(9) Raheem, I. T.; Thiara, P. S.; Peterson, E. A.; Jacobsen, E. N. Enantioselective Pictet-Spengler-Type Cyclizations of Hydroxylactams: H-Bond Donor Catalysis by Anion Binding. *J. Am. Chem. Soc.* **2007**, *129* (44), 13404–13405.

(10) Reisman, S. E.; Doyle, A. G.; Jacobsen, E. N. Enantioselective Thiourea-Catalyzed Additions to Oxocarbenium Ions. *J. Am. Chem. Soc.* **2008**, *130* (23), 7198–7199.

(11) Strassfeld, D. A.; Wickens, Z. K.; Picazo, E.; Jacobsen, E. N. Highly Enantioselective, Hydrogen-Bond-Donor Catalyzed Additions to Oxetanes. *J. Am. Chem. Soc.* **2020**, *142* (20), 9175–9180.

(12) Birrell, J. A.; Desrosiers, J. N.; Jacobsen, E. N. Enantioselective Acylation of Silyl Ketene Acetals through Fluoride Anion-Binding Catalysis. *J. Am. Chem. Soc.* **2011**, *133* (35), 13872–13875.

(13) Bergonzini, G.; Schindler, C. S.; Wallentin, C. J.; Jacobsen, E. N.; Stephenson, C. R. J. Photoredox Activation and Anion Binding Catalysis in the Dual Catalytic Enantioselective Synthesis of β-Amino Esters. *Chem. Sci.* **2014**, *5* (1), 112–116.

(14) Park, Y.; Schindler, C. S.; Jacobsen, E. N. Enantioselective Aza-Sakurai Cyclizations: Dual Role of Thiourea as H-Bond Donor and Lewis Base. *J. Am. Chem. Soc.* **2016**, *138* (45), 14848–14851.

(15) Kennedy, C. R.; Lehnherr, D.; Rajapaksa, N. S.; Ford, D. D.; Park, Y.; Jacobsen, E. N. Mechanism-Guided Development of a Highly Active Bis-Thiourea Catalyst for Anion-Abstraction Catalysis. *J. Am. Chem. Soc.* **2016**, *138* (41), 13525–13528.

(16) Ford, D. D.; Lehnherr, D.; Kennedy, C. R.; Jacobsen, E. N. On- and off-Cycle Catalyst Cooperativity in Anion-Binding Catalysis. *J. Am. Chem. Soc.* **2016**, *138* (25), 7860–7863.

(17) Banik, S. M.; Levina, A.; Hyde, A. M.; Jacobsen, E. N. Lewis Acid Enhancement by Hydrogen-Bond Donors for Asymmetric Catalysis. *Science.* **2017**, *358*, 761–764.

(18) Wang, C.; Chen, Y. H.; Wu, H. C.; Wang, C.; Liu, Y. K. The Quinary Catalyst-Substrate Complex Induced Construction of Spiro-Bridged or Cagelike Polyheterocyclic Compounds via a Substrate-Controlled Cascade Process. *Org. Lett.* **2019**, *21* (17), 6750–6755.

(19) Bendelsmith, A. J.; Kim, S. C.; Wasa, M.; Roche, S. P.; Jacobsen, E. N. Enantioselective Synthesis of α-Allyl Amino Esters via Hydrogen-Bond-Donor Catalysis. *J. Am. Chem. Soc.* **2019**, *141* (29), 11414–11419.

(20) Xu, H.; Zuend, S. J.; Woll, M. G.; Tao, Y.; Jacobsen, E. N. Asymmetric Cooperative Catalysis of Strong Bronsted Acid-Promoted Reactions Using Chiral Ureas. *Science.* **2010**, *327* (5968), 986–990.

(21) Wendlandt, A. E.; Vangal, P.; Jacobsen, E. N. Quaternary Stereocentres via an Enantioconvergent Catalytic SN1 Reaction. *Nature* **2018**, *556* (7702), 447–451.

(22) Cho, C. G.; Feit, B. A.; Webster, O. W. Cationic Polymerization of Isobutyl Vinyl Ether: Livingness Enhancement by Dialkyl Sulfides. *Macromolecules* **1990**, *23* (7), 1918–1923.

(23) Iwasaki, T.; Nagaki, A.; Yoshida, J. I. Microsystem Controlled Cationic Polymerization of Vinyl Ethers Initiated by CF3SO3H. *Chem. Commun.* **2007**, No. 12, 1263–1265.

(24) Uchiyama, M.; Satoh, K.; Kamigaito, M. Cationic RAFT Polymerization Using Ppm Concentrations of Organic Acid. *Angew. Chemie Int. Ed.* **2015**, *54* (6), 1924–1928.

(25) Atsumi, S.; Hanai, T.; Liao, J. C. Non-Fermentative Pathways for Synthesis of Branched-Chain Higher Alcohols as Biofuels. *Nature* **2008**, *451* (7174), 86–89.

(26) Kolodziej, R.; Scheib, J. Bio-Isobutanol: The next-Generation Biofuel. *Hydrocarb. Process.* **2012**, *No. Septem*, 79–85.

(27) Matake, R.; Adachi, Y.; Matsubara, H. Synthesis of Vinyl Ethers of Alcohols Using Calcium Carbide under Superbasic Catalytic Conditions (KOH/DMSO). *Green Chem.* **2016**, *18* (9), 2614–2618.

(28) Lane, S.; Zhang, Y.; Yun, E. J.; Ziolkowski, L.; Zhang, G.; Jin, Y. S.; Avalos, J. L. Xylose Assimilation Enhances the Production of Isobutanol in Engineered Saccharomyces Cerevisiae. *Biotechnol. Bioeng.* **2020**, *117* (2), 372–381.

(29) Claessens, B.; De Staercke, M.; Verstraete, E.; Baron, G. V.; Cousin-Saint-Remi, J.; Denayer, J. F. M. Identifying Selective Adsorbents for the Recovery of Renewable Isobutanol. *ACS Sustain. Chem. Eng.* **2020**, *8* (24), 9115–9124.

(30) Aoshima, S.; Higashimura, T. Vinyl Ether Oligomers with Conjugated-Polyene and Acetal Terminals: A New Chain-Transfer Mechanism for Cationic Polymerization of Vinyl Ethers. *Polym. J.* **1984**, *16* (3), 249–258.

(31) Uchiyama, M.; Satoh, K.; Kamigaito, M. Cationic RAFT Polymerization Using Ppm Concentrations of Organic Acid. *Angew. Chemie* **-** *Int. Ed.* **2015**, *54* (6), 1924–1928.

(32) Uchiyama, M.; Satoh, K.; Kamigaito, M. Thioether-Mediated Degenerative Chain-Transfer Cationic Polymerization: A Simple Metal-Free System for Living Cationic Polymerization. *Macromolecules* **2015**, *48* (16), 5533–5542.

(33) Uchiyama, M.; Satoh, K.; Kamigaito, M. A Phosphonium Intermediate for Cationic RAFT Polymerization. *Polym. Chem.* **2016**, *7* (7), 1387–1396.

(34) Prasher, A.; Hu, H.; Tanaka, J.; Nicewicz, D. A.; You, W. Alcohol Mediated Degenerate Chain Transfer Controlled Cationic Polymerisation of: Para -Alkoxystyrene. *Polym. Chem.* **2019**, *10* (30), 4126–4133.

(35) Boeck, P. T.; Tanaka, J.; Liu, S.; You, W. Importance of Nucleophilicity of Chain-Transfer Agents for Controlled Cationic Degenerative Chain-Transfer Polymerization. *Macromolecules* **2020**, *53* (11), 4303–4311.

(36) Kojima, K.; Sawamoto, M.; Higashimura, T. Living Cationic Polymerization of Isobutyl Vinyl Ether by Hydrogen Iodide/Lewis Acid Initiating Systems: Effects of Lewis Acid Activators and Polymerization Kinetics. *Macromolecules* **1989**, *22* (4), 1552–1557.

(37) Hadjikyriacou, S.; Faust, R. Living Cationic Homopolymerization of Isobutyl Vinyl Ether and Sequential Block Copolymerization of Isobutylene with Isobutyl Vinyl Ether. Synthesis and Mechanistic Studies. *Macromolecules* **1995**, *28* (23), 7893–7900.

(38) Walsh, P. L.; C. Kozlowski, M. *Fundamentals of Asymmetric Catalysis*; University Science Books: Sausalito, CA, 2009.

APPENDIX A: SUPPORTING INFORMATION FOR CHAPTER 2

General Considerations

The following compounds were prepared according to previously reported literature procedures: (*R*)-3,3'-bis(3,5- bis(trifluoromethyl)phenyl)-1,1'-binaphthyl phosphate ((*R*)-**2.2**),[1] and tetrachlorobis(tetrahydrofuran)titanium(IV) ($TiCl_4(THF)_2$).[2] All vinyl ether monomers were dried over CaH_2 and distilled under vacuum prior to storage in a N_2-filled glovebox freezer before further use. Unless otherwise noted, solvents were dried and degassed using a Pure Process Technology solvent purification system and then subsequently stored over molecular sieves (3Å) in a N_2-filled glovebox. Other reagents whose syntheses are not described below were purchased from commercial sources and used without further purification. All syntheses were performed under inert atmosphere (N_2 or Ar) using flame-dried or oven-dried glassware unless specified otherwise. NMR spectra were recorded using a Bruker DRX 400 MHz, Bruker AVANCE III 500 MHz, or Bruker AVANCE III 600 MHz CryoProbe spectrometer. Chemical shifts δ (ppm) are referenced to tetramethylsilane (TMS) using the residual solvent as an internal standard (^{1}H and ^{13}C). For ^{1}H NMR: $CDCl_3$, 7.26 ppm. For ^{13}C NMR: $CDCl_3$, 77.16 ppm. Coupling constants (*J*) are expressed in hertz (Hz). The use of ^{13}C NMR to quantify tacticity of several poly(vinyl ethers) has been established and reported previously.[3,4]

Macromolecular Characterization

Gel permeation chromatography (GPC) was performed on a Waters 2695 separations module liquid chromatograph equipped with either four Waters Styragel HR columns (WAT044225, WAT044231, WAT044237, and WAT054460) arranged in series or two Agilent Resipore columns (PL1113-6300) maintained at 35 °C, and a Waters 2414 refractive index detector at room temperature. GPC was also performed on a Tosoh EcoSEC Elite GPC system equipped with a TSKgel Super HM-M (17392) column maintained at 40 °C with an RI detector. Tetrahydrofuran was used as the mobile phase at a flow rate of 0.5 mL/min (Tosoh GPC) or 1.0 mL/min (Waters GPC). Molecular weight and dispersity data are reported relative to polystyrene standards.

Syntheses and Characterization Data

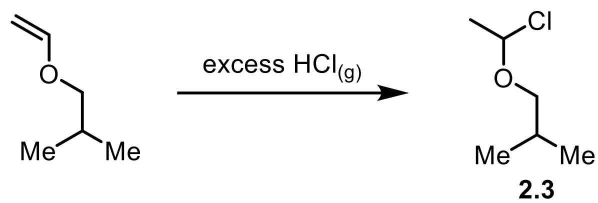

Synthesis of α-chloroethyl isobutyl ether (2.3): This compound was prepared according to a modified literature procedure.[5] A flame-dried 100 mL storage flask equipped with a Teflon screw-cap was charged with 0.2 mL isobutyl vinyl ether (1.53 mmol) and 29.8 mL hexane (0.05 M) under an atmosphere of N_2. The mixture was cooled to 0 °C in an ice bath and bubbled with dry $HCl_{(g)}$. The dry $HCl_{(g)}$ was prepared by drop-wise addition of 15 mL concentrated HCl into concentrated 30 mL H_2SO_4, and adventitious water removed by passing through a glass bubbler filled with concentrated H_2SO_4. After complete generation of $HCl_{(g)}$ (~15 min), the mixture was bubbled with dry N_2 for 15 min to remove any excess HCl from solution. An aliquot was analyzed by ^{1}H NMR to ensure complete conversion of isobutyl vinyl ether.

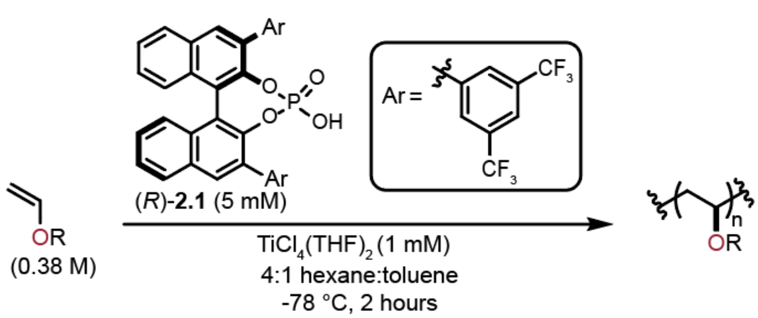

General Homopolymerization Procedure Using (*R*)-2.2 (0.76 mmol scale): Polymerizations were performed in 8 mL septum-capped reaction vials prepared in a N_2-filled glovebox. An oven-dried 8 mL septum-capped vial equipped with a stir bar was charged with vinyl ether monomer (0.76 mmol) and hexane (1.6 mL). A separate 8 mL septum-capped vial equipped with a stir bar was charged with 0.2 mL of a 0.05 M stock solution of **2.1** in MePh (0.01 mmol) and 0.2 mL of a 0.01 M stock solution of $TiCl_4(THF)_2$ in MePh (0.002 mmol). Both vials were removed from the glovebox and cooled to -78 °C in a dry ice/acetone bath. After stirring at -78 °C for 20 min, the entire MePh solution was transferred via dry syringe to the vial containing monomer solution. The reaction was stirred at -78 °C for 2 h, after which 0.33 mL of Et_3N/MeOH solution (10% v/v) was added to quench the polymerization. Upon warming to room temperature, the mixture was washed with 1N HCl, and all volatiles removed in vacuo. The crude polymer was dissolved in minimal (~1 mL) THF and precipitated into 50 mL of cold MeOH, filtered, and washed with cold MeOH. This procedure was repeated two times and the resulting purified polymer was dried under vacuum for at least 12 h to a constant weight.

Kinetics via *In Situ* Infared Spectroscopy

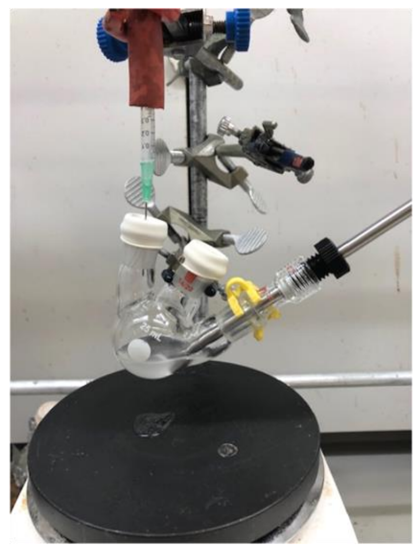

General Instrument Remarks: Reaction monitoring by *in situ* infrared spectroscopy was carried out using a MettlerToledo ReactIR™ 15 instrument with a SiComp™ silicon tip probe, liquid N_2 MCT detector, and the iCIR software 4.3. A MePh reference spectrum was automatically subtracted. The disappearance of the isobutyl vinyl ether alkene stretch at 1610 cm^{-1} was monitored for all kinetics experiments. Fifty scans were averaged together to produce an IR spectrum time point every fifteen seconds. All reactions were run on a 2.25 mmol scale in a three neck 25 mL round bottom flask with a magnetic stir bar at 600 rpm. Two of the three necks were fitted with septa. The SiComp™ silicon tip probe was fitted into the third neck with a greased ground glass joint adaptor to ensure an anhydrous environment (see attached image to the right).

Representative Reaction Set-Up for Stereoselective Polymerization Using (*R*)-2.2: A three neck 25 mL round bottom flask equipped with a magnetic stir bar, two septa, and the SiComp™ silicon tip probe (*vide supra*) was flame-dried, backfilled with inert atmosphere (argon or N_2), and flame-dried again. A sustained vacuum was then pulled on the reaction set-up for at least 30 minutes. Meanwhile, in a N_2 filled glovebox, an 8 mL septum-capped vial equipped with a stir bar was charged with 0.60 mL of a 0.05 M stock solution of (*R*)-**2.1** in MePh (0.030 mmol) and 0.6 mL of a 0.01 M stock solution of $TiCl_4$ in MePh (0.006 mmol). In a separate 8 mL septum-capped vial equipped with a stir bar was added 0.3 mL isobutyl vinyl ether. Both vials were then removed from the glovebox. The reaction vessel set-up was then backfilled with inert atmosphere and charged with 4.2 mL hexane and 1.2 mL of the MePh solution containing (*R*)-1 and $TiCl_4$. Then, both the reaction set-up and the vial containing isobutyl vinyl ether were cooled to -78 °C via a dry ice/acetone bath and allowed to stir for 20 minutes. Then, the recording of IR spectra was started and 0.3 mL (2.3 mmol) of pre-chilled isobutyl vinyl ether was immediately added to the round bottom flask. When the signal from the monomeric alkene had either disappeared or stopped decreasing in intensity, the reaction was quenched via the addition of 1.0 mL of Et_3N/MeOH solution (10% v/v).

Representative Reaction Set-Up for Control Polymerization Absent of (*R*)-2.1: A three neck 25 mL round bottom flask equipped with a magnetic stir bar, two septa, and the attached SiComp™ silicon tip probe (*vide supra*) was flame-dried, backfilled with inert atmosphere (Ar or N_2), and flame-dried again. A sustained vacuum was then pulled on the reaction set-up for at least 30 minutes. Meanwhile, in a N_2 filled glovebox, to an 8 mL septum-capped vial equipped with a stir bar was added 0.6 mL of a 0.050 M stock solution of isobutyl vinyl ether chloride **2.3** (0.030 mmol). In a second separate 8 mL septum-capped vial equipped with a stir bar was added 0.3 mL isobutyl vinyl ether. Both vials were then removed from the glovebox. The three neck reaction vessel set-up was then backfilled with inert atmosphere and charged with 4.2 mL hexane, 0.6 mL MePh, and 0.6 mL of a 0.01 M stock solution of $TiCl_4$ (0.006 mmol) in MePh. Then, the reaction set-up and both vials containing isobutyl vinyl ether and **2.3** were cooled to -78 °C via dry ice/acetone baths and allowed to stir for 20 minutes. Then, the recording of IR spectra was started, immediately followed by the simultaneous addition of pre-chilled 0.3 mL (2.3 mmol) of isobutyl vinyl ether and 0.6 mL of the 0.01 M stock solution of $TiCl_4$. When the signal from the monomeric alkene had either disappeared or stopped decreasing in intensity, the reaction was quenched via the addition of 1.0 mL of Et_3N/MeOH solution (10% v/v).

Pseudo-First Order Kinetics:

The cationic polymerization of vinyl ethers, including isobutyl vinyl ether, facilitated by catalyst **2.2** may be represented as:

$$M + C \longrightarrow P$$

Under the assumption that there are negligible side-reactions taking place in the formation of polymer (P), vinyl ether monomer (M) will always be present in a large excess over the catalyst (C). As such, pseudo-first-order kinetics are valid for rate calculations.[6] In this scenario, the following rate law applies:

$$\frac{d[P]}{dt} = k[M][C]_0 = k[M]$$

The integrated form of the rate equation is represented as:

$$\ln[M] = \ln[M]_0 - kt$$

This equation indicates that plotting -ln[M] versus *t* (s) should give a linear plot where *k* is equal to the slope of the line.

Data Analysis: The isobutyl vinyl ether alkene stretch signal and time point data provided by the ReactIR™ 15 iCIR software was transferred to Excel for further analysis. The first acquired IR spectrum data point was disregarded in the determination of initial rate constants for two reasons: 1) the acquisition of scans was started immediately (~5 seconds) before the final addition of reagents to initiate the polymerization and 2) to account for adequate mixing of the reagents. The magnitude of the alkene stretch at 1610 cm^{-1} present in the second acquired data point was considered to be 0.38 M, the initial monomer concentration.

The monomer concentration present immediately prior to quenching was found through the following protocol. After quenching (*vide supra*) and allowing the reaction set-up to warm to room temperature, an NMR sample was prepared with 0.1 mL of the quenched reaction solution and 0.5

mL of 0.0315 M 1,4-dimethoxybenzene in $CDCl_3$. The unique proton signals from 1,4-dimethoxybenzene allowed this to serve as an internal standard, against which the vinyl protons of isobutyl vinyl ether were integrated to calculate conversion. Knowing the % conversion allowed for the calculation of the monomer concentration present immediately prior to quenching.

A total of seven data points (the second acquired IR spectrum data point through the eighth, spanning 105 seconds) were typically used to calculate a first order rate. Analysis of the stereoselective polymerization using (*R*)-**2.2** ([iBVE] = 0.38 M, [(*R*)-**2.1**] = 5.0 mM, [$TiCl_4$] = 1.0 mM) was conducted three times at each temperature. Analysis of the control polymerization absent of (*R*)-**2.1** ([iBVE] = 0.38 M, [**2.3**] = 5.0 mM, [$TiCl_4$] = 1.0 mM) was also conducted three times at each probed temperature. Initial rate constants for all of these polymerizations can be seen below.

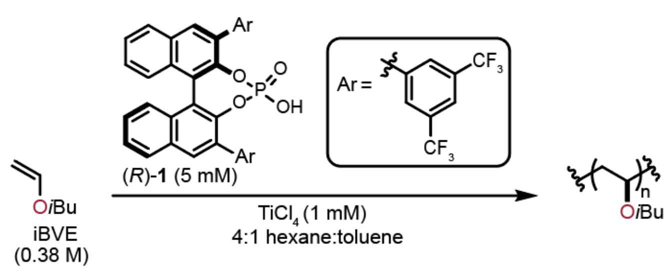

Temp (°C)	1/Temp (x 10^{-3})	k_{obs} (x 10^{-3})	standard error (x 10^{-3})
- 40	4.3	6	1
- 61	4.7	2.7	0.2
-78	5.1	1.01	0.06

Initial rate constants for the stereoselective polymerization conditions.

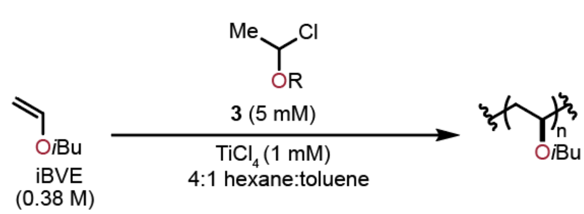

Temp (°C)	1/Temp (x 10^{-3})	k_{obs} (x 10^{-3})	standard error (x 10^{-3})
- 40	4.3	23	6
- 61	4.7	13	2
-78	5.1	7.5	0.7

Initial rate constants for the control polymerization conditions.

Eyring Analysis

Temperature Dependence on Stereoselectivity: The polymers formed from the React-IR experiments (described in Section 2) were isolated and their resulting tacticity was characterized via ^{13}C NMR for the Eyring analysis seen in Figure 2.5A in the main text. Crude polymeric material from the control polymerization was washed with 1N HCl, and all volatiles were removed in vacuo. The resulting polymer was dried under vacuum for at least 12 h to a constant weight. Crude polymeric material formed from the stereoselective polymerization conditions was washed with 1N HCl, and all volatiles were removed in vacuo. The crude polymer was dissolved in 1–2 mL CH_2Cl_2 and filtered through a plug of SiO2 (4-5 cm) in a glass pipette eluting with additional CH_2Cl_2. After removing CH_2Cl_2 via rotary evaporation, the resulting purified polymer was dried under vacuum for at least 12 h to a constant weight. A summary of all data is reported below. The % *m* reported at each temperature is an average of three polymer samples.

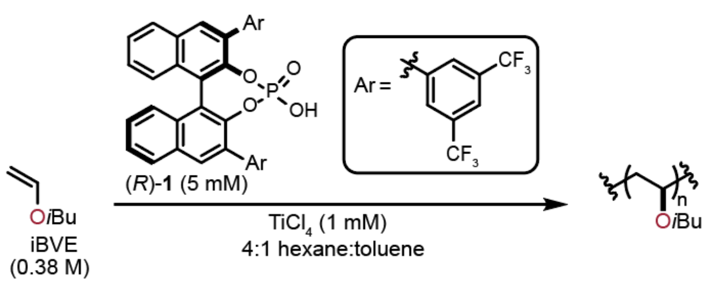

Temp (°C)	1/Temp (K)	*m* (%)	standard error
-40	4.3×10^{-3}	78.0	0.2
-61	4.7×10^{-3}	83.8	0.5
-78	5.1×10^{-3}	86.6	0.3

Tacticity values of the stereocontrolled polymerization performed at different temperatures.

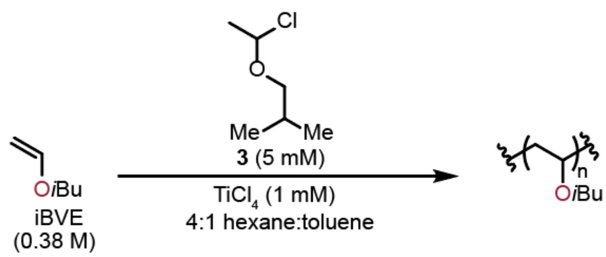

Temp (°C)	1/Temp (K)	*m* (%)	standard error
-40	4.3×10^{-3}	72.0	0.2
-61	4.7×10^{-3}	73.5	0.2
-78	5.1×10^{-3}	75.4	0.1

Tacticity values of the control polymerization performed at different temperatures.

Theoretical Model of Stereoselectivity: Figure 2.5C in the main text compares experimental data to theoretical data of stereoselectivity strictly following a two-state model. In the two-state model based on the Eyring equation, the addition of a monomer to the polymer chain end facilitated by (*R*)-**2.2** assumes the contribution of only two predominating diastereomeric reaction pathways. Other diastereomeric reaction pathways involving (*R*)-2**.2** do not significantly contribute to the stereoselectivity outcome. Additionally, other reaction pathways, in which monomer attack to the polymer chain end is facilitated by a Ti complex that is not the preferred catalyst, also do not significantly contribute to the stereoselectivity outcome. This theoretical data was calculated using both the $\Delta\Delta G^{\ddagger}$ found at -78 °C (-0.724 kcal/mol) and the Eyring equation:

$$\Delta\Delta G^{\ddagger} = -RT\ln\left(\frac{\%\,m}{\%\,r}\right)$$

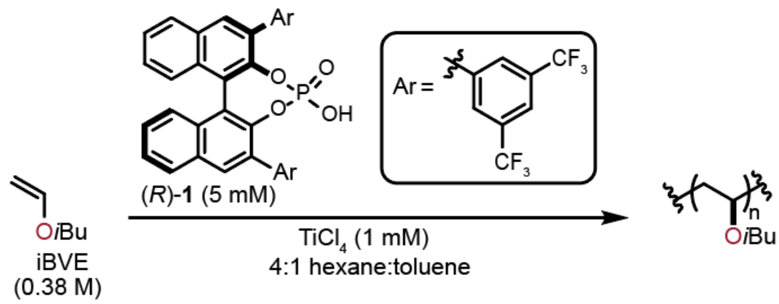

Temp (°C)	(% *m* / % *r*)[a]	% *m*[b]
-78	6.48	86.6
-61	5.58	84.8
-40	4.78	82.7

Theoretical data modeled according to the Eyring equation and a two-state model. [a] calculated via a reorganization of the Eyring equation, $\frac{\%\,m}{\%\,r} = e^{\left(\frac{\Delta\Delta G\ddagger}{-RT}\right)}$. [b] calculated by solving for % *m* via the equation, 100 = % *m* + % *r*

The deviation from theoretical data demonstrates that as temperature increases above -78 °C, other less stereoselective reaction pathways are present. These less stereoselective pathways could be a result of other diastereomeric reaction pathways or a Ti complex that is not the preferred catalyst.

<u>Stereoselectivity as a Function of Conversion</u>

In Figure 2.6 in the main text, polymerizations using the stereoselective reaction conditions ([iBVE] = 0.38 M, [(*R*)-**2.1**] = 5.0 mM, [$TiCl_4$] = 1.0 mM) are quenched at various time points to monitor the resulting molecular weight distribution and stereoselectivity at different % conversion. These polymerizations were performed on a 0.76 mmol scale, with the only difference being the reaction time. After quenching with 0.33 mL of Et_3N/MeOH solution (10% v/v) at the designated time, the reaction vessel was allowed to warm up to room temperature. Then, an NMR sample was prepared with 0.1 mL of the quenched reaction solution and 0.5 mL of 0.0315 M 1,4-dimethoxybenzene in $CDCl_3$. The unique proton signals from 1,4-dimethoxybenzene allowed this to serve as an internal standard, against which the vinyl protons of isobutyl vinyl ether were integrated to calculate conversion. The rest of the crude reaction sample not used for NMR analysis was purified. That purified polymeric material was then used for ^{13}C NMR and GPC analysis.

Computational Analysis

All structures of the interaction of $TiCl_4$ with the ligand x(*R*)-**2.1** (x = 1, 2, and 3 equivalents) were optimized at the M06[7] level of theory using the mixed basis set def2-SVP for C, H, O, P, Cl, and F; and LAN2LDZ for Ti metal. All calculations were carried out using *Gaussian16* program.[8] The vibrational frequency calculations were carried out at the same level of theory in order to verify the nature of these complexes, as well as to compute vibrational partitions functions for use in free energy calculations. Gibbs free energies for all complexes were obtained by adding the zero-point vibrational energy (ZPVE) and thermal energy corrections from standard statistical mechanics approximations at 298.15 K and 1 atm pressure, except that vibrational modes below 50 cm^{-1} were replaced with a value of exactly 50 cm^{-1} in vibrational partition function calculations. Further solvent single point calculations were carried out using the SMD solvation model,[9] where the solvent is n-hexane (ε =1.88) at the M06, MN15,[10] and wB97XD[11] level of theory along with mixed basis set 6-311+G(d,p) for C, H, O, P, Cl, and F; and def2-TZVP and SDD as a pseudopotential for Ti metal. The order of free energies of the conformations of all these complexes is identified as same with all these three methods. The Gibbs free energies (kcal mol^{-1}) are used for discussion in the manuscript at the $SMD_{(n\text{-}hexane)}$/MN15/6-311+G(d,p), def2-TZVP and SDD(Ti)//M06/def2-SVP, LANL2DZ(Ti) level of theory. More detailed computational findings can be found at the following cited reference.[12]

REFERENCES

(1) Akiyama, T.; Morita, H.; Itoh, J.; Fuchibe, K. Chiral Brønsted Acid Catalyzed Enantioselective Hydrophosphonylation of Imines: Asymmetric Synthesis of α-Amino Phosphonates. *Org. Lett.* **2005**, *7* (13), 2583–2585.

(2) Manxzer, L. E.; Deaton, J.; Sharp, P.; Schrock, R. R. *Tetrahydrofuran Complexes of Selected Early Transition Metals.*; Fackler Jr., J. P., Ed.; John Wiley & Sons, Ltd, 1982.

(3) Hatada, K.; Kitayama, T.; Matsuo, N.; Yuki, H. C-13 NMR Spectra and Spin-Lattice Relaxation Times of Poly(Alkyl Vinyl Ether)s. *Polym. J.* **1983**, *15* (10), 715–725.

(4) Teator, A. J.; Leibfarth, F. A. Catalyst-Controlled Stereoselective Cationic Polymerization of Vinyl Ethers. *Science.* **2019**, *363*, 1439–1443.

(5) Higashimura, T.; Kamigaito, M.; Kato, M.; Hasebe, T.; Sawamoto, M. Living Cationic Polymerization of α-Methylstyrene Initiated with a Vinyl Ether-Hydrogen Chloride Adduct in Conjunction with Tin Tetrabromide. *Macromolecules* **1993**, *26* (11), 2670–2673.

(6) Teator, A. J.; Varner, T. P.; Jacky, P. E.; Sheyko, K. A.; Leibfarth, F. A. Polar Thermoplastics with Tunable Physical Properties Enabled by the Stereoselective Copolymerization of Vinyl Ethers. *ACS Macro Lett.* **2019**, *8* (12), 1559–1563.

(7) Zhao, Y.; Truhlar, D. G. The M06 Suite of Density Functionals for Main Group Thermochemistry, Thermochemical Kinetics, Noncovalent Interactions, Excited States, and Transition Elements: Two New Functionals and Systematic Testing of Four M06-Class Functionals and 12 Other Function. *Theor. Chem. Acc.* **2008**, *120* (1–3), 215–241.

(8) Frisch, M. J.; Trucks, G. W.; Schlegel, H. B.; Scuseria, G. E.; Robb, M. A.; Cheeseman, J. R.; Scalmani, G.; Barone, V.; Petersson, G. A.; Nakatsuji, H.; et al. Gaussian 16, Revision C.01, Gaussian, Inc., Wallingford CT, 2016.

(9) V. Marenich, A.; J. Cramer, C.; G. Truhlar, D. Universal Solvation Model Based on Solute Electron Density and on a Continuum Model of the Solvent Defined by the Bulk Dielectric Constant and Atomic Surface Tensions. *J. Phys. Chem. B* **2009**, *113* (18), 6378–6396.

(10) Yu, H. S.; He, X.; Li, S. L.; Truhlar, D. G. MN15: A Kohn-Sham Global-Hybrid Exchange-Correlation Density Functional with Broad Accuracy for Multi-Reference and Single-Reference Systems and Noncovalent Interactions. *Chem. Sci.* **2016**, *7* (8), 5032–5051.

(11) Chai, J. Da; Head-Gordon, M. Long-Range Corrected Hybrid Density Functionals with Damped Atom-Atom Dispersion Corrections. *Phys. Chem. Chem. Phys.* **2008**, *10* (44), 6615–6620.

(12) Varner, T. P.; Teator, A. J.; Reddi, Y.; Jacky, P. E.; Cramer, C. J.; Leibfarth, F. A. Mechanistic Insight into the Stereoselective Cationic Polymerization of Vinyl Ethers. *J. Am. Chem. Soc.* **2020**, *142* (40), 17175–17186.

APPENDIX B: SUPPORTING INFORMATION FOR CHAPTER 3

General Considerations

The following compounds were prepared according to previously reported literature procedures: octyl vinyl ether (OcVE),[1] 2-methoxy ethyl vinyl ether (MOVE),[2] 2-phenoxy ethyl vinyl ether (PhOVE),[1] 2-(vinyloxy)ethyl 4-methylbenzenesulfonate,[3] 2-acetoxy ethyl vinyl ether (AcOVE),[4] 2-benzoyloxy ethyl vinyl ether (BzOVE),[5] (*R*)-3,3'-bis(3,5- bis(trifluoromethyl)phenyl)-1,1'-binaphthyl phosphate ((*R*)-**2.1**),[6] and tetrachlorobis(tetrahydrofuran)titanium(IV) ($TiCl_4(THF)_2$).[7] All vinyl ether monomers were dried over CaH_2 and distilled under vacuum prior to storage in a N_2-filled glovebox freezer before further use. Unless otherwise noted, solvents were dried and degassed using a Pure Process Technology solvent purification system and then subsequently stored over molecular sieves (3Å) in a N_2-filled glovebox. Other reagents whose syntheses are not described below were purchased from commercial sources and used without further purification. All syntheses were performed under inert atmosphere (N_2 or Ar) using flame-dried or oven-dried glassware unless specified otherwise. NMR spectra were recorded using a Bruker DRX 400 MHz, Bruker AVANCE III 500 MHz, or Bruker AVANCE III 600 MHz CryoProbe spectrometer. Chemical shifts δ (ppm) are referenced to tetramethylsilane (TMS) using the residual solvent as an internal standard (^{1}H and ^{13}C). For ^{1}H NMR: $CDCl_3$, 7.26 ppm. For ^{13}C NMR: $CDCl_3$, 77.16 ppm. Coupling constants (*J*) are expressed in hertz (Hz). The use of ^{13}C NMR to quantify tacticity of several poly(vinyl ethers) has been established and reported previously.[8,9] Due to overlapping ^{13}C NMR resonances, the tacticity of poly(isoamyl vinyl ether) was determined using band-selective heteronuclear single quantum coherence (HSQC) spectroscopy.[10]

Macromolecular Characterization

Gel permeation chromatography (GPC) was performed on a Waters 2695 separations module liquid chromatograph equipped with either four Waters Styragel HR columns (WAT044225, WAT044231, WAT044237, and WAT054460) arranged in series or two Agilent Resipore columns (PL1113-6300) maintained at 35 °C, and a Waters 2414 refractive index detector at room temperature. GPC was also performed on a Tosoh EcoSEC Elite GPC system equipped with a TSKgel Super HM-M (17392) column maintained at 40 °C with an RI detector. Tetrahydrofuran was used as the mobile phase at a flow rate of 0.5 mL/min (Tosoh GPC) or 1.0 mL/min (Waters GPC). Molecular weight and dispersity data are reported relative to polystyrene standards.

Melting-transition temperature (T_m) and glass-transition temperature (T_g) of precipitated and dried polymer samples were measured using differential scanning calorimetry (DSC) on a TA Instruments Discovery DSC. Unless specifically noted otherwise, values for T_m and T_g were obtained from a second heating scan after the thermal history was removed. All heating and cooling rates were 10 °C/min.

<u>Syntheses and Characterization Data</u>

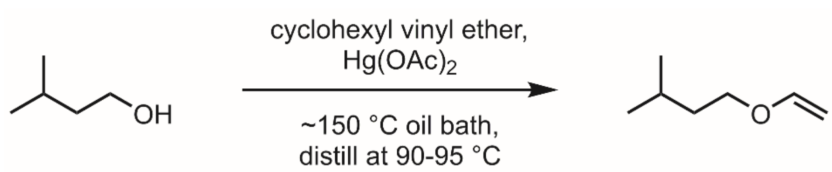

Synthesis of isoamyl vinyl ether (iAVE): A 50 mL oven-dried round-bottom flask equipped with a stir bar was charged with 6.20 mL isoamyl alcohol (56.9 mmol), 7.4 mL cyclohexyl vinyl ether (52.5 mmol), and 258 mg of $Hg(OAc)_2$ (0.810 mmol) under inert atmosphere. The reaction flask was fitted with a glass y-shaped adapter, thermometer, and short-path distillation head leading to a 25 mL round-bottom flask cooled to -78 °C in a dry ice/acetone bath to actively distill forming vinyl ether product. The reaction flask was heated in an oil bath incrementally until colorless liquid began to distill through the short-path (~150 °C oil bath, BP 90–95 °C). Heating continued at this temperature until distillation is complete (20–30 min), at which point reaction flask removed from oil bath and cooled to room temperature. The distilled product contained the desired vinyl ether that was contaminated with cyclohexyl vinyl ether and isoamyl alcohol. The mixture was stirred over CaH_2 for 12 h followed by fractional vacuum distillation to remove cyclohexyl vinyl ether and most of the isoamyl alcohol. The remaining alcohol was removed by passing through a short SiO_2 plug eluting with *n*-pentane. Careful removal of solvent by rotary evaporation yielded the pure product as a colorless oil (620 mg, 10%). BP: ~92 °C (760 torr). ^{1}H NMR (600 MHz, $CDCl_3$): δ 6.46 (dd, *J* = 14.3, 6.8, 1H), 4.16 (dd, *J* = 14.3, 1.9, 1H), 3.96 (dd, *J* = 6.8, 1.9, 1H), 3.70 (t, *J* = 6.7, 2H), 1.73 (septet, *J* = 6.7, 1H), 1.55 (q, *J* = 6.8, 2H), 0.92 (d, *J* = 6.6, 6H) ppm. ^{13}C NMR (151 MHz, $CDCl_3$): δ 152.13, 86.26, 66.56, 37.95, 25.14, 22.67 ppm.

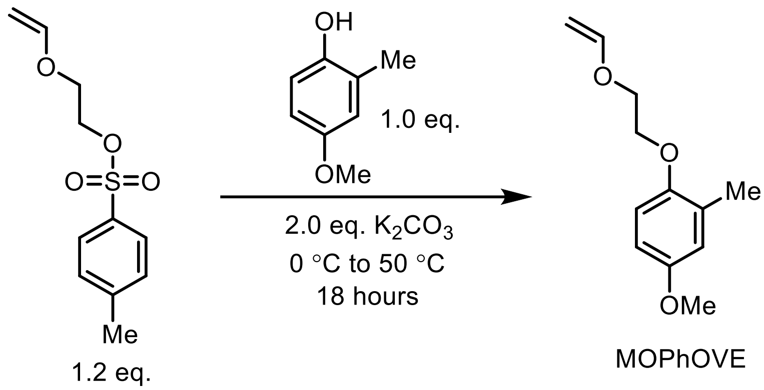

Synthesis of 2-methoxy-4-methyl-phenoxy ethyl vinyl ether (MOPhOVE): To an oven-dried 100 mL round bottom flask equipped with a stir bar was added 2.18 mL (17.2 mmol) creosol, 4.75 g (34.4 mmol) potassium carbonate, and 35 mL acetonitrile under inert atmosphere. The reaction vessel was cooled to 0 °C in an ice water bath, and 2-(vinyloxy)ethyl 4-methylbenzenesulfonate was added dropwise. Once the addition was complete, the ice water bath was removed, and the solution was allowed to warm to room temperature over 30 minutes. The reaction vessel was then heated to 50 °C in an oil bath and allowed to stir for 18 hours. Next, the reaction was removed from the oil bath, allowed to cool to room temperature, and volatiles were removed via rotary evaporation. The crude material was dissolved in dichloromethane and washed with water and brine. The dichloromethane was then removed via rotary evaporation, and the crude material was purified by SiO_2 column chromatography with 9:1 hexane:EtOAc as the mobile phase to afford pure product as a colorless liquid in 21% yield. ^{1}H NMR (400 MHz, $CDCl_3$) δ 6.83 (d, *J* = 8.0, 1H), 6.74 – 6.63 (m, 2H), 6.55 (dd, *J* = 14.3, 6.8, 1H), 4.27 – 4.18 (m, 3H), 4.09 – 4.01 (m, 3H), 3.85 (s, 3H), 2.30 (s, 3H). ^{13}C NMR (151 MHz, $CDCl_3$) δ 151.58, 149.43, 145.68, 131.49, 120.74, 114.40, 112.87, 86.65, 67.76, 66.16, 55.73, 20.98. IR (neat): 2940 (w), 1619 (m, C=C), 1512 (s), 1457 (m), 1414 (w), 1322 (m), 1265 (s, C-O), 1236 (s, C-O), 1199 (s, C-O), 1159 (s), 1142 (s), 1035 (s), 982 (s), 796 (s) cm^{-1}.

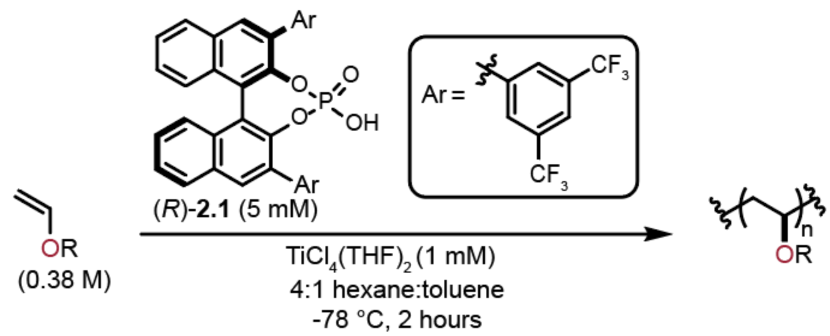

General Homopolymerization Procedure Using (*R*)-2.2 (0.76 mmol scale): Polymerizations were performed in 8 mL septum-capped reaction vials prepared in a N_2-filled glovebox. An oven-dried 8 mL septum-capped vial equipped with a stir bar was charged with vinyl ether monomer (0.76 mmol) and hexane (1.6 mL). A separate 8 mL septum-capped vial equipped with a stir bar was charged with 0.2 mL of a 0.05 M stock solution of **2.1** in MePh (0.01 mmol) and 0.2 mL of a 0.01 M stock solution of $TiCl_4(THF)_2$ in MePh (0.002 mmol). Both vials were removed from the glovebox and cooled to -78 °C in a dry ice/acetone bath. After stirring at -78 °C for 20 min, the entire MePh solution was transferred via dry syringe to the vial containing monomer solution. The reaction was stirred at -78 °C for 2 h, after which 0.33 mL of Et_3N/MeOH solution (10% v/v) was added to quench the polymerization. Upon warming to room temperature, the mixture was washed with 1N HCl, and all volatiles removed in vacuo. The crude polymer was dissolved in minimal (~1 mL) THF and precipitated into 50 mL of cold MeOH, filtered, and washed with cold MeOH. This procedure was repeated two times and the resulting purified polymer was dried under vacuum for at least 12 h to a constant weight.

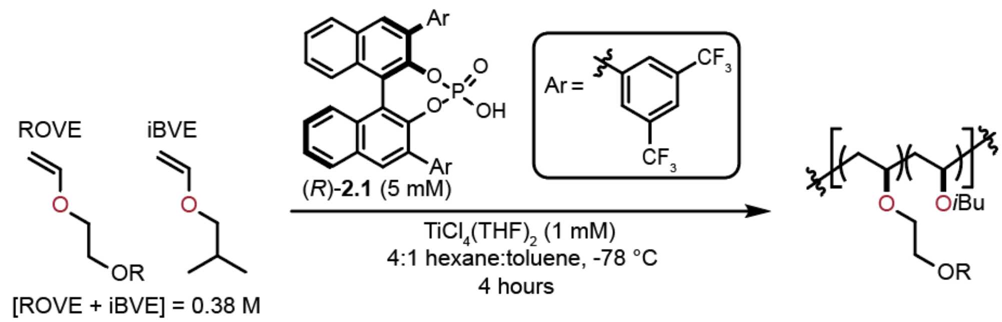

General Copolymerization Procedure using (*R*)-2.2 (1.0 mmol scale): Copolymerizations were performed in 8 mL septum-capped reaction vials prepared in a N_2-filled glovebox. An oven-dried 8 mL septum-capped vial equipped with a stir bar was charged with an appropriate volume of a 1.0 M iBVE stock solution in hexane, an appropriate volume of a 1.0 M ROVE stock solution in hexane, and 1.1 mL hexane such that the total volume was 2.1 mL. A separate 8 mL septum-capped vial equipped with a stir bar was charged with 0.26 mL of a 0.05 M stock solution of (*R*)-**2.1** in MePh (0.013 mmol) and 0.26 mL of a 0.01 M stock solution of $TiCl_4(THF)_2$ in MePh (0.0026 mmol). Both vials were removed from the glove box and cooled to -78 °C in a dry ice/acetone bath. After stirring at -78 °C for 20 min, the entire MePh solution was transferred via dry syringe to the vial containing monomer solution. The reaction was stirred at -78 °C for 4 h, after which 0.38 mL of Et_3N/MeOH solution (10% v/v) was added to quench the polymerization. Upon warming to room temperature, the mixture was washed with 1N HCl, and all volatiles removed in vacuo. The crude polymer was dissolved in 1–2 mL CH_2Cl_2 and filtered through a plug of SiO2 (4-5 cm) in a glass pipette eluting with additional CH_2Cl_2. After removing CH_2Cl_2 via rotary evaporation, the resulting purified polymer was dried under vacuum for at least 12 h to a constant weight.

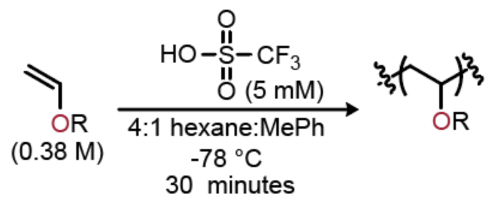

General Homopolymerization Procedure using CF_3SO_3H (0.76 mmol scale): Polymerizations were performed in 8 mL septum-capped reaction vials prepared in a N_2-filled glovebox. An oven-dried 8 mL septum-capped vial equipped with a stir bar was charged with vinyl ether monomer (0.76 mmol), 0.2 mL MePh, and 1.6 mL hexane. The vial was removed from the glovebox and cooled to -78 °C in a dry ice/acetone bath. After stirring at -78 °C for 20 min, 0.2 mL of anhydrous pre-chilled 50 mM trifluoromethanesulfonic acid in MePh was added to initiate the polymerization. The reaction was stirred at -78 °C for 30 minutes, after which 0.33 mL of Et_3N/MeOH solution (10% *v*/*v*) was added to quench the polymerization. Upon warming to room temperature, the mixture was washed with 1N HCl and all volatiles removed in vacuo. The resulting polymer was dried under vacuum for at least 12 h to a constant weight.

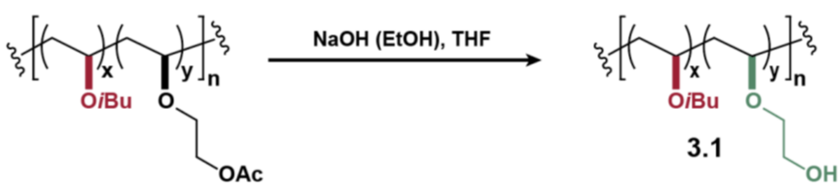

Hydrolysis of poly(iBVE-co-AcOVE): An oven-dried 8 mL septum-capped vial equipped with a stir bar was charged with poly(iBVE-co-AcOVE) (0.215 g, 0.136 mmol AcVE repeat units) and dry THF (2.5 mL). NaOH (55 mg, 1.38 mmol), dissolved in EtOH (0.30 mL), injected into vial containing copolymer solution and mixture heated to 45 °C. After 16 hours, mixture cooled to RT and directly poured into ice-cold H_2O. Pale yellow precipitate collected by filtration and subsequently triturated with excess MeOH by vigorously stirring for 30 min. The resulting material was dissolved in THF (1-2 mL) and precipitated into ice cold H_2O a second time. The pure, white copolymer was collected by filtration and dried under vacuum for at least 12 h to a constant weight. Yield: 140 mg (77%). GPC: M_n = 37 kDa; $Đ$ = 2.1. DSC: T_g = -16 °C, T_m = 131 °C.

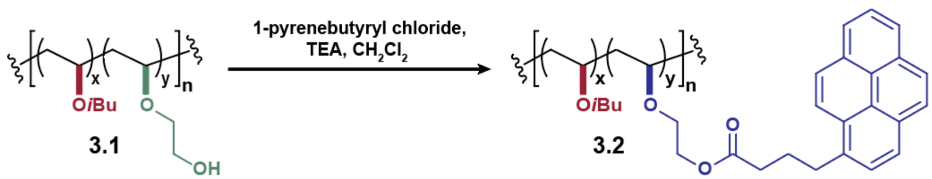

Functionalization of copolymer 3.1 with 1-pyrenebutyryl chloride: An oven-dried 8 mL septum-capped vial equipped with a stir bar was charged with copolymer **3.1** (0.040 g, 0.026 mmol hydroxyl repeat units) and dry CH_2Cl_2 (5.0 mL). Triethylamine (18 µL, 0.130 mmol) added, followed by a solution of 1-pyrenebutyryl chloride (0.040 g, 0.130 mmol) in dry CH_2Cl_2 (1.0 mL). Mixture stirred at room temperature (RT) for 3 hours, at which point it was directly poured into ice-cold MeOH. Pale yellow precipitate collected by filtration, dissolved in THF (1 mL), precipitated into ice cold MeOH a second time. The pure, pale yellow copolymer was collected by filtration and dried under vacuum for at least 12 h to a constant weight. Yield: 33 mg (70%). Note: GPC analysis with photodiode array (PDA) detection (344 nm) confirms the presence of pyrene in copolymer **3.2**. GPC: M_n = 47 kDa; $Đ$ = 2.3. DSC: T_g = -16 °C, T_m = 126 °C.

Substrate Scope

Homopolymerizations Using (*R*)-2.2: In Figure 3.1 in the main text, homopolymerizations using the stereoselective reaction conditions ([VE] = 0.38 M, [(*R*)-**2.1**] = 5.0 mM, [$TiCl_4$] = 1.0 mM) were performed on a 0.76 mmol scale. The M_n, dispersity, tacticity, and T_m characterization of poly(EVE), poly(nPrVE), poly(nBVE), poly(iBVE), poly(iPVE), and poly(tBVE) made via these conditions have been previously reported.[9] Below can be seen more complete characterization of poly(OcVE), poly(iAVE), and poly(tBVE).

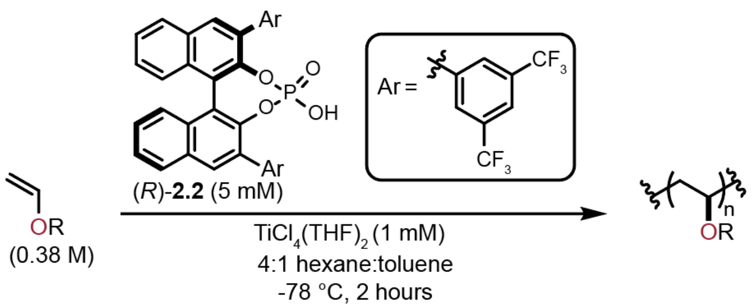

monomer	M_n (kg mol^{-1})	Đ	*m* (%)	T_m
OcVE	131	2.4	94	amorphous
iAVE	114	1.9	90	90 °C
tBVE	14	3.0	75	amorphous

Characterization of poly(OcVE), poly(iAVE), and poly(tBVE).

Copolymerizations Using (R)-2.2: In Figure 3.7 in the main text, copolymerizations using the stereoselective reaction conditions ([iBVE + ROVE] = 0.38 M, [(*R*)-**2.1**] = 5.0 mM, [$TiCl_4$] = 1.0 mM) were performed on a 1.0 mmol scale. These polymerizations were quenched with 0.38 mL of Et_3N/MeOH solution (10% v/v) after 4 hours, and the reaction vessel was subsequently allowed to warm up to room temperature. In order to determine % conversion, an NMR sample was prepared with 0.1 mL of the quenched reaction solution and 0.5 mL of 0.033 M 1,4-dimethoxybenzene in $CDCl_3$. The unique proton signals from 1,4-dimethoxybenzene allowed this to serve as an internal standard, against which the vinyl protons of isobutyl vinyl ether were integrated to calculate conversion. The rest of the crude reaction sample not used for NMR analysis was purified. That purified polymeric material was then used for ^{1}H NMR, ^{13}C NMR, and GPC analysis. Distinct ^{1}H NMR resonances were observed for iBVE and ROVE repeat units, which were integrated relative to each other in order to determine the mole fraction of ROVE (F_{ROVE}) incorporated into the final copolymer. For brevity and clarity, Figure 3.7 in the main text only included selected copolymerization examples of isobutyl vinyl ether with substituted oxyethylene vinyl ethers (ROVE, where R is a variable substituent). Herein, the data from all copolymerizations conducted can be seen below.

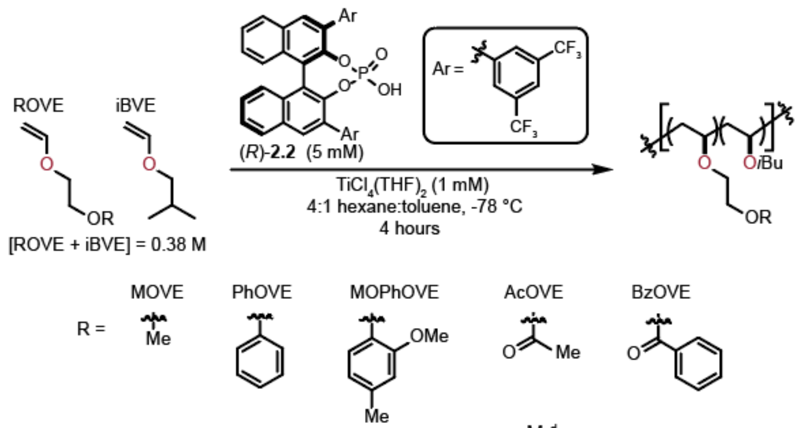

ROVE	f_{ROVE}[a]	F_{ROVE}[b]	% conv[c]	M_n[d] (kg mol^{-1})	Đ[d]	*m* (%)[e]
MOVE	0.01	0.03	61	61	2.5	93
MOVE	0.03	0.04	73	58	2.0	91
MOVE	0.05	0.06	84	56	2.1	91
MOVE	0.10	0.11	79	51	2.0	90
MOVE	0.15	0.16	85	68	1.4	89
MOVE	0.20	0.23	73	68	1.7	91
MOVE	0.30	0.50	40	49	2.2	81
MOVE	0.40	0.70	18	32	1.6	72
PhOVE	0.01	0.02	80	70	2.1	92
PhOVE	0.02	0.04	68	61	2.0	90
PhOVE	0.03	0.05	74	67	1.9	90
PhOVE	0.05	0.06	61	74	2.1	89
PhOVE	0.10	0.06	38	66	2.1	90
PhOVE	0.15	0.07	60	47	1.9	88
PhOVE	0.20	0.07	44	58	1.6	89
PhOVE	0.30	0.09	41	54	1.9	89
PhOVE	0.40	0.13	39	42	1.7	90
PhOVE	0.50	0.22	29	39	1.6	90

All copolymerizations which involved MOVE and PhOVE.

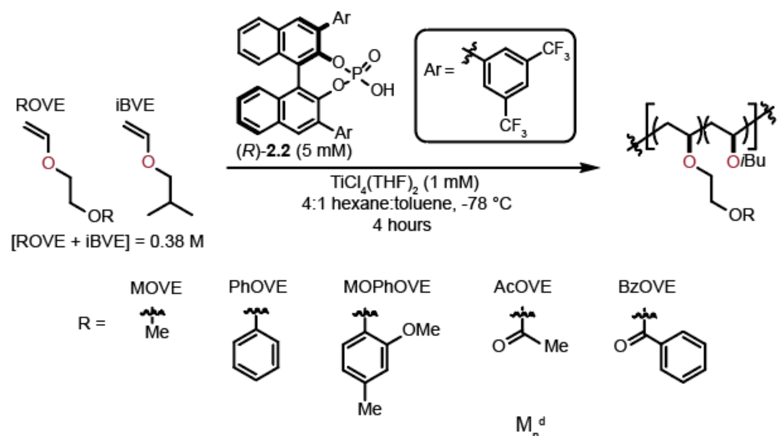

ROVE	f_{ROVE}[a]	F_{ROVE}[b]	% conv[c]	M_n[d] (kg mol^{-1})	Đ[d]	*m* (%)[e]
MOPhOVE	0.05	0.04	50	69	2.1	92
MOPhOVE	0.10	0.05	30	69	2.2	91
MOPhOVE	0.15	0.05	47	52	1.8	90
MOPhOVE	0.20	0.05	55	36	1.7	91
MOPhOVE	0.30	0.05	48	36	1.7	90
MOPhOVE	0.40	0.07	25	30	1.5	91
AcOVE	0.01	0.02	70	72	2.1	92
AcOVE	0.03	0.09	35	47	1.8	83
AcOVE	0.05	0.12	20	35	1.6	85
AcOVE	0.10	0.22	15	47	1.7	83
BzOVE	0.01	0.03	38	75	2.0	92
BzOVE	0.03	0.09	18	47	1.8	93
BzOVE	0.05	0.15	7	50	1.6	87

All copolymerizations which involved MOPhOVE, AcOVE, and BzOVE.

f_{Et}	F_{Et}	M_n (kg mol^{-1})	Đ	T_g (°C)	T_m (°C)
0.05	0.09	58	1.7	-26	132
0.10	0.13	58	1.9	-25	132
0.15	0.22	62	1.9	-29	107
0.20	0.34	83	2.0	-32	66
0.30	0.38	101	2.4	-33	50
0.40	0.52	41	1.7	-37	39
0.50	0.62	90	2.7	-37	40
0.65	0.74	66	2.0	-37	Not observed
0.8	0.83	51	1.8	-38	41
0.9	0.91	82	2.6	-39	42

Copolymerization of EVE with iBVE using (*R*)-**2.2**.

Kinetic Analyses

The cationic polymerization of vinyl ethers, including iBVE, nBVE, EVE, and AcVE, facilitated by catalyst (R)-**2.2** may be represented as:

$$M + C \longrightarrow P$$

Under the assumption that there are negligible side-reactions taking place, any of the above listed monomers (M) will always be present in a large excess over the catalyst (C). As such, pseudo-first-order kinetics are valid for rate calculations. In this scenario, the following rate law applies:

$$\frac{d[P]}{dt} = k[M][C]_0 = k[M]$$

The integrated form of the rate equation is represented as:

$$\ln[M] = \ln[M]_0 - kt$$

This equation indicates that plotting inverse ln[M] versus *t* (s) should give a linear plot where *k* is equal to the slope of the line. Figure 3.5 in the main text illustrates this relationship.

During the copolymerization of iBVE and nBVE, significant overlap occurs in the ^{1}H NMR spectrum that hinders the ability to monitor the relative consumption of each monomer independently. Peak deconvolution of the vinyl region (δ 6.40-6.48 ppm, $CDCl_3$) using OriginPro 8[11] in the presence of an internal standard (*i.e.*, 1,4-dimethoxybenzene), however, enables the accurate determination of individual monomer concentration at various time points (see below). A representative example can be also be seen in the spectra section of this appendix.

Monomer	Peak	Area	Total Area
iBVE	1	9.96E-5	4.26E-4
	2	1.10E-4	
	3	1.12E-4	
	4	1.10E-4	
nBVE	5	7.58E-5	3.00E-4
	6	7.98E-5	
	7	8.10E-5	
	8	7.14E-5	

Summary of peak deconvolution data obtained from a copolymerization of nBVE with iBVE with $f_{Bu} = 0.50$ that was quenched at 20 min (t = 1200 s).

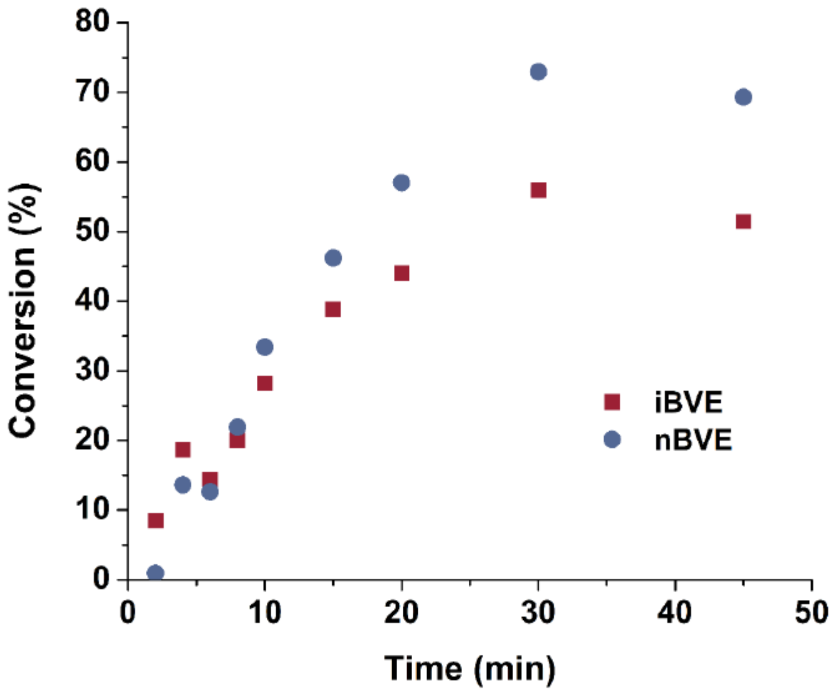

Plot of % conversion versus time of the copolymerization ($f_{Bu} = 0.50$) of iBVE and nBVE. Conversions of iBVE (■) and nBVE (●) monitored independently by ^{1}H NMR ($CDCl_3$). $[iBVE]_0$ = 0.19 M. $[nBVE]_0$ = 0.19 M.

Spectra

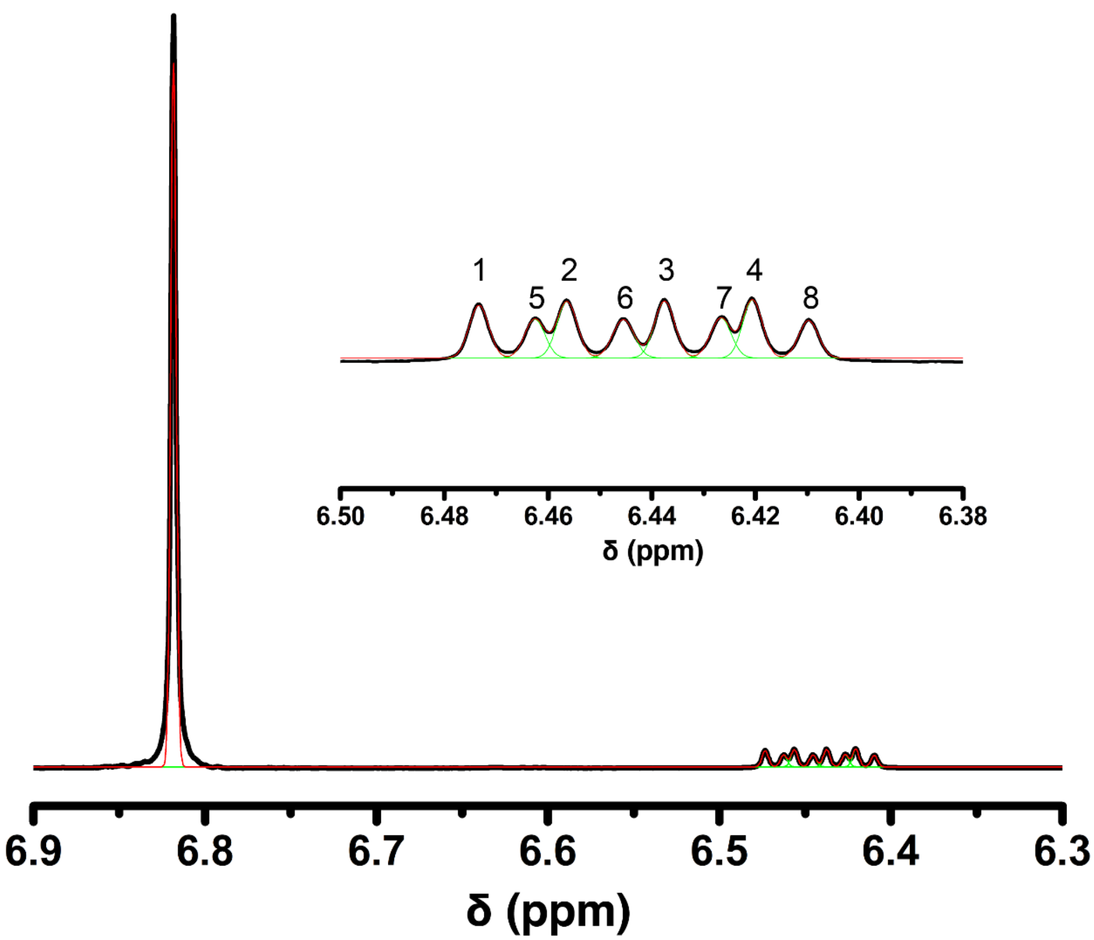

Representative example of peak deconvolution using OriginPro 8 to determine the relative consumption of individual vinyl ether monomers. The aryl resonance of the 1,4-dimethoxybenzene internal standard can be seen at δ 6.8 ppm, while the overlapped vinyl resonances for iBVE and nBVE are between δ 6.40 – 6.48 ppm (expanded in inset). This example represents a copolymerization of nBVE with iBVE with f_{Bu} = 0.50 that was quenched at 20 min (t = 1200 s). Fitted peaks (green) and peak sum (red) are shown overlaid on the original spectrum (black).

REFERENCES

(1) Okimoto, Y.; Sakaguchi, S.; Ishii, Y. Development of a Highly Efficient Catalytic Method for Synthesis of Vinyl Ethers. *J. Am. Chem. Soc.* **2002**, *124* (8), 1590–1591.

(2) Greenland, B. W.; Liu, S.; Cavalli, G.; Alpay, E.; Steinke, J. H. G. Synthesis of Beaded Poly(Vinyl Ether) Solid Supports with Unique Solvent Compatibility. *Polymer.* **2010**, *51* (14), 2984–2992.

(3) Nilsson, P.; Larhed, M.; Hallberg, A. Highly Regioselective, Sequential, and Multiple Palladium-Catalyzed Arylations of Vinyl Ethers Carrying a Coordinating Auxiliary: An Example of a Heck Triarylation Process. *J. Am. Chem. Soc.* **2001**, *123* (34), 8217–8225.

(4) André, M.; Tarrit, S.; Couret, M. J.; Galmier, M. J.; Débiton, E.; Chezal, J. M.; Mounetou, E. Spacer Optimization of New Conjugates for a Melanoma-Selective Delivery Approach. *Org. Biomol. Chem.* **2013**, *11* (37), 6372–6384.

(5) Iengar, H. V. R.; Ritchie, P. D. Studies in Pyrolysis. Part VII. *J. Chem. Soc.* **1956**, 3563–3570.

(6) Akiyama, T.; Morita, H.; Itoh, J.; Fuchibe, K. Chiral Brønsted Acid Catalyzed Enantioselective Hydrophosphonylation of Imines: Asymmetric Synthesis of α-Amino Phosphonates. *Org. Lett.* **2005**, *7* (13), 2583–2585.

(7) Manxzer, L. E.; Deaton, J.; Sharp, P.; Schrock, R. R. *Tetrahydrofuran Complexes of Selected Early Transition Metals.*; Fackler Jr., J. P., Ed.; John Wiley & Sons, Ltd, 1982.

(8) Hatada, K.; Kitayama, T.; Matsuo, N.; Yuki, H. C-13 NMR Spectra and Spin-Lattice Relaxation Times of Poly(Alkyl Vinyl Ether)s. *Polym. J.* **1983**, *15* (10), 715–725.

(9) Teator, A. J.; Leibfarth, F. A. Catalyst-Controlled Stereoselective Cationic Polymerization of Vinyl Ethers. *Science.* **2019**, *363* (6434), 1439–1443.

(10) J. Tiegs, B.; Sarkar, S.; M. Condo, A.; Keresztes, I.; W. Coates, G. Rapid Determination of Polymer Stereoregularity Using Band-Selective 2D HSQC. *ACS Macro Lett.* **2016**, *5* (2), 181–184.

(11) OriginPro, Version 8. OriginLab Corporation, Northampton, MA, USA.

APPENDIX C: SUPPORTING INFORMATION FOR CHAPTER 4

General Considerations

The following compounds were prepared according to previously reported literature procedures: (*R*)-3,3'-bis(3,5- bis(trifluoromethyl)phenyl)-1,1'-binaphthyl phosphate ((*R*)-**2.1**),[1] and tetrachlorobis(tetrahydrofuran)titanium(IV) ($TiCl_4(THF)_2$).[2] All vinyl ether monomers were dried over CaH_2 and distilled under vacuum prior to storage in a N_2-filled glovebox freezer before further use. Unless otherwise noted, solvents were dried and degassed using a Pure Process Technology solvent purification system and then subsequently stored over molecular sieves (3Å) in a N_2-filled glovebox. Other reagents whose syntheses are not described below were purchased from commercial sources and used without further purification. All syntheses were performed under inert atmosphere (N_2 or Ar) using flame-dried or oven-dried glassware unless specified otherwise. NMR spectra were recorded using a Bruker DRX 400 MHz, Bruker AVANCE III 500 MHz, or Bruker AVANCE III 600 MHz CryoProbe spectrometer. Chemical shifts δ (ppm) are referenced to tetramethylsilane (TMS) using the residual solvent as an internal standard (^{1}H and ^{13}C). For ^{1}H NMR: $CDCl_3$, 7.26 ppm. For ^{13}C NMR: $CDCl_3$, 77.16 ppm. Coupling constants (*J*) are expressed in hertz (Hz). The use of ^{13}C NMR to quantify tacticity of several poly(vinyl ethers) has been established and reported previously.[3,4] Due to overlapping ^{13}C NMR resonances, the tacticity of poly(isoamyl vinyl ether) was determined using band-selective heteronuclear single quantum coherence (HSQC) spectroscopy.[5]

Macromolecular Characterization

Gel permeation chromatography (GPC) was performed on a Waters 2695 separations module liquid chromatograph equipped with either four Waters Styragel HR columns (WAT044225, WAT044231, WAT044237, and WAT054460) arranged in series or two Agilent Resipore columns (PL1113-6300) maintained at 35 °C, and a Waters 2414 refractive index detector at room temperature. GPC was also performed on a Tosoh EcoSEC Elite GPC system equipped with a TSKgel Super HM-M (17392) column maintained at 40 °C with an RI detector. Tetrahydrofuran was used as the mobile phase at a flow rate of 0.5 mL/min (Tosoh GPC) or 1.0 mL/min (Waters GPC). Molecular weight and dispersity data are reported relative to polystyrene standards.

Melting-transition temperature (T_m) and glass-transition temperature (T_g) of precipitated and dried polymer samples were measured using differential scanning calorimetry (DSC) on a TA Instruments Discovery DSC. Unless specifically noted otherwise, values for T_m and T_g were obtained from a second heating scan after the thermal history was removed. All heating and cooling rates were 10 °C/min.

Syntheses and Characterization Data

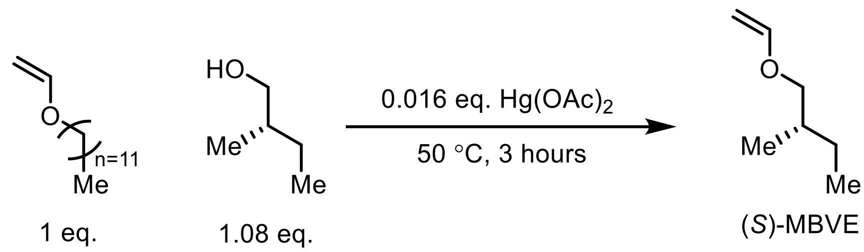

Synthesis of (*S*)-2-methylbutyl vinyl ether ((*S*)-MBVE): Prepared according to a modified literature procedure.[6] In a N_2-filled glovebox, to an oven-dried 100mL round bottom flask equipped with a stir bar was added 548 mg (1.72 mmol) mercury (II) acetate. The septum-capped round bottom flask was then removed from the glovebox and charged with 28.0 mL (107.5 mmol) dodecyl vinyl ether and 12.5 mL (116.1 mmol) (S)-(-)-2-methyl-1-butanol. The reaction was heated to 50 °C via an oil bath and allowed to stir for 3 hours. Then, the product was distilled under vacuum using a distillation short path. To remove small amounts of alcohol impurity, the material was then subjected to SiO_2 column chromatography eluting with pentane. Pentane was then removed via rotary evaporation to afford (S)-MBVE as a colorless liquid in 40% yield. ^{1}H NMR (500 MHz, $CDCl_3$): δ 6.48 (m, 1H), 4.16 (dd, *J* = 14.4, 1.7, 1H), 3.96 (dd, *J* = 6.8, 1.8, 1H), 3.54 (m, 1H), 3.46 (m, 1H), 1.72 (m, 1H), 1.47 (m, 1H), 1.21 (m, 1H) 0.95-0.89 (m, 6H).

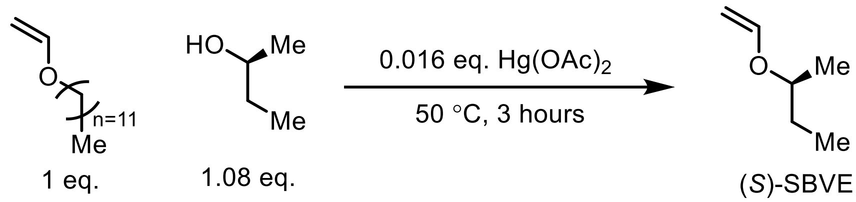

Synthesis of (*S*)-sec-butyl vinyl ether ((*S*)-SBVE): Prepared according to a modified literature procedure.[7] In a N_2-filled glovebox, to an oven-dried 100mL round bottom flask equipped with a stir bar was added 765 mg (2.40 mmol) mercury (II) acetate. The septum-capped round bottom flask was then removed from the glovebox and charged with 39.1 mL (150 mmol) dodecyl vinyl ether and 15.0 mL (163 mmol) (S)-(+)-2-butanol. The reaction was heated to 50 °C via an oil bath and allowed to stir for 3 hours. Then, the product was distilled under vacuum using a distillation short path. To remove small amounts of alcohol impurity, the material was then subjected to column chromatography with silica gel and pentane as the stationary and mobile phase, respectively. Pentane was then removed via rotary evaporation to afford (S)-MBVE as a colorless liquid in 48% yield. ^{1}H NMR (400 MHz, $CDCl_3$) δ 6.32 (dd, *J* = 14.2, 6.6, 1H), 4.26 (dd, *J* = 14.1, 1.6, 1H), 3.97 (dd, *J* = 6.6, 1.5, 1H), 3.80 (sext, *J* = 6.2, 1H), 1.62 (m, 1H), 1.51 (m, 1H), 1.20 (d, *J* = 6.5, 3H), 0.92 (t, *J* = 7.5, 3H).

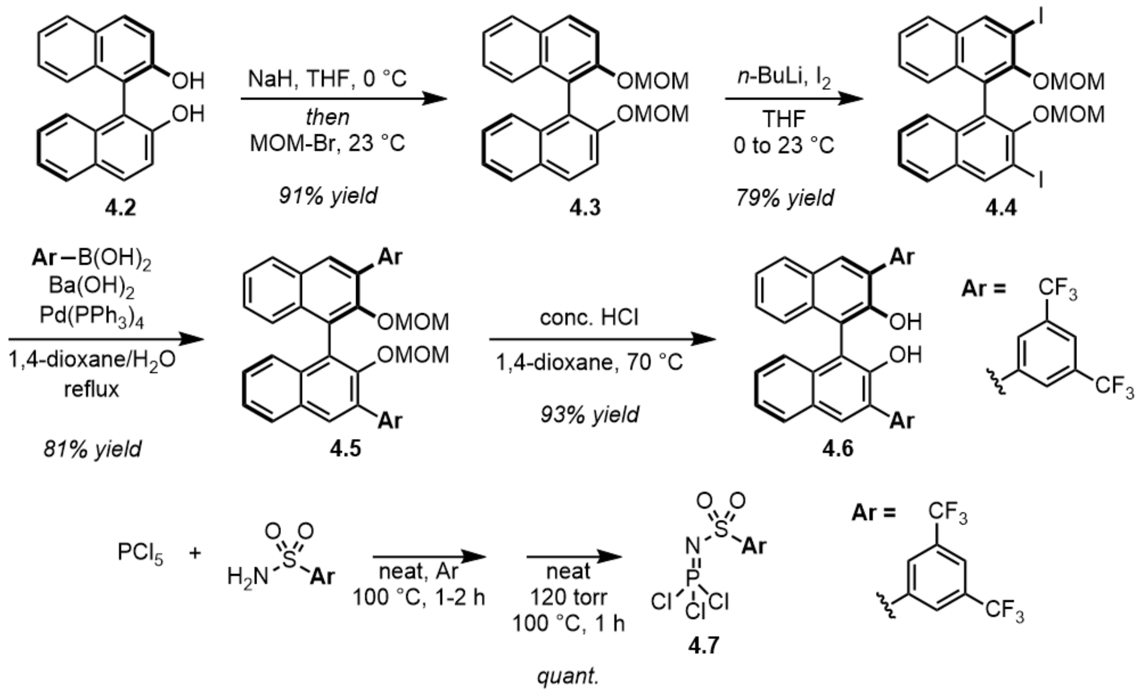

Synthesis route to 3,3'-bis(3,5-bis(trifluoromethyl)phenyl)-[1,1'-binaphthalene]-2,2'-diol and ((3,5-bis(trifluoromethyl)phenyl)sulfonyl)phosphorimidoyl trichloride

The synthesis of intermediates towards IDPi **4.1** is described above. Each intermediate was prepared according to previously reported literature procedures: **4.3**,[8] **4.4**,[8] **4.5**,[9] **4.6**,[9] and **4.7**.[10]

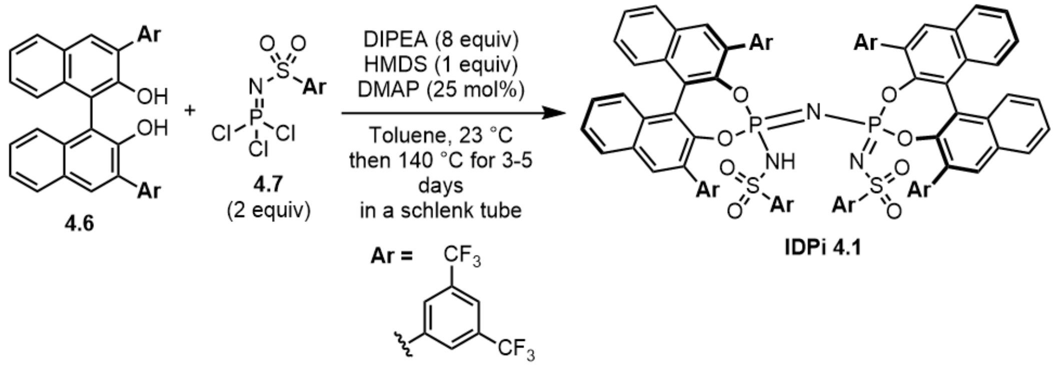

Synthesis of IDPi 4.1: To a 25-mL schlenk tube (a vessel to allow a slight build-up of pressure) equipped with a magnetic stir bar in a glove box under inert atmosphere (N_2) was added the BINOL derivative 3,3'-bis(3,5-bis(trifluoromethyl)phenyl)-[1,1'-binaphthalene]-2,2'-diol (500 mg, 0.704 mmol), ((3,5-bis(trifluoromethyl)phenyl)sulfonyl)phosphorimidoyl trichloride (299 mg, 0.697 mmol) and toluene (7.00 mL). *N*-Ethyl-*N*-isopropylpropan-2-amine (485 µL, 2.79 mmol) was added all at once and the resultant opaque yellow solution was allowed to stir for 30 min at ambient temperature in the glove box. 4-Dimethylaminopyridine (10.6 mg, 0.0871 mmol) followed by hexamethyldisilazane (73.0 µL, 0.349 mmol) were added to the reaction mixture in quick succession and the mixture was allowed to stir for 10 minutes at ambient temperature in the glove box. The Schlenk tube containing the reaction mixture was closed, removed from the glove box, and heated to 140 °C in a silicon oil bath and was stirred for 4 days. After 4 days, the now cloudy yellow reaction was allowed to cool to room temperature and was diluted with EtOAc (10 mL). The diluted reaction mixture was filtered through celite and purified via flash chromatography (9:1 hexanes/EtOAc to 1:1 hexanes EtOAc. After purification, the catalyst was acidified by stirring in a biphasic solution of 6 M $HCl_{(aq)}/CH_2Cl_2$ (20 mL, 20 mL respectively) for two hours. The layers were separated and concentrated in vacuo. To prevent the IDPi from being inactivated, rather than using a drying agent, the residual water was removed by stripping with toluene (5 mL, 3x). The catalyst was stored as a 0.01 M solution in toluene in a glove box freezer (-35 °C) under inert atmosphere (N_2).

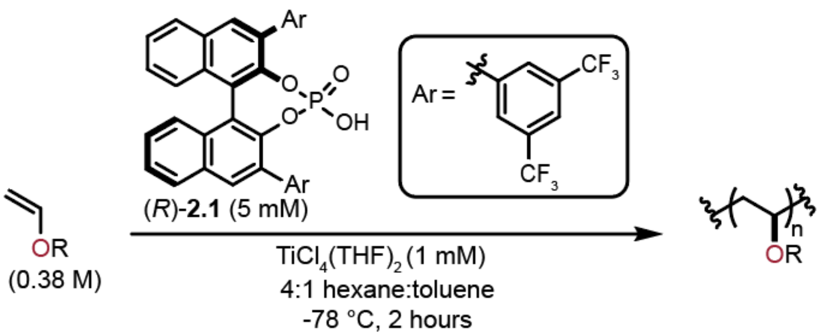

General Homopolymerization Procedure Using (*R*)-2.2 (0.76 mmol scale): Polymerizations were performed in 8 mL septum-capped reaction vials prepared in a N_2-filled glovebox. An oven-dried 8 mL septum-capped vial equipped with a stir bar was charged with vinyl ether monomer (0.76 mmol) and hexane (1.6 mL). A separate 8 mL septum-capped vial equipped with a stir bar was charged with 0.2 mL of a 0.05 M stock solution of **2.1** in MePh (0.01 mmol) and 0.2 mL of a 0.01 M stock solution of $TiCl_4(THF)_2$ in MePh (0.002 mmol). Both vials were removed from the glovebox and cooled to -78 °C in a dry ice/acetone bath. After stirring at -78 °C for 20 min, the entire MePh solution was transferred via dry syringe to the vial containing monomer solution. The reaction was stirred at -78 °C for 2 h, after which 0.33 mL of Et_3N/MeOH solution (10% v/v) was added to quench the polymerization. Upon warming to room temperature, the mixture was washed with 1N HCl, and all volatiles removed in vacuo. The crude polymer was dissolved in minimal (~1 mL) THF and precipitated into 50 mL of cold MeOH, filtered, and washed with cold MeOH. This procedure was repeated two times and the resulting purified polymer was dried under vacuum for at least 12 h to a constant weight.

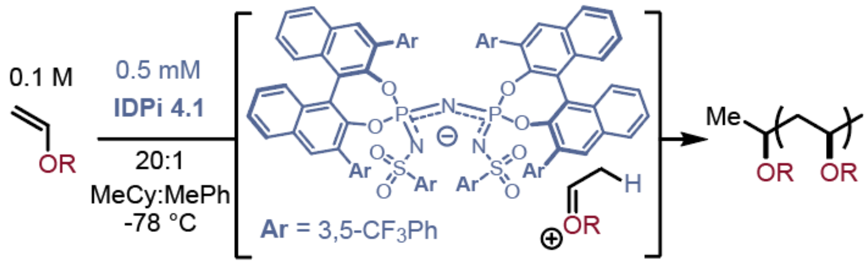

General Hompolymerization Procedure Using IDPi 4.1: In a glove box under inert atmosphere, to an 8 mL septum-capped vial equipped with a stir bar was added 4.2mL of methylcyclohexane and 0.25 mL of 10mM IDPI **4.1** catalyst stock solution in toluene. In a separate 8 mL septum-capped vial equipped with a stir bar was added 50 mg (0.500 mmol) iBVE and 0.5mL of MeCy. Both of these capped vials were then removed from the glove box and cooled to -78 °C in a dry ice/acetone bath over 15 min. A dry syringe was then used to transfer all of the monomer solution to the vial containing catalyst **4.1**. The reaction was allowed to stir at -78 for 1 h. Then, the reaction was quenched with 500 µL of 10% Et_3N in MeOH, washed with 1M HCl, and the volatiles were removed under reduced pressure.

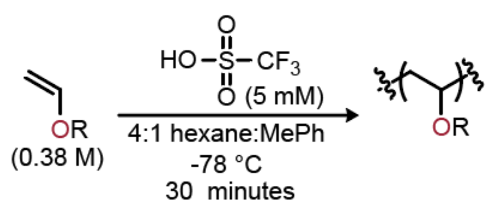

General Homopolymerization Procedure using CF_3SO_3H (0.76 mmol scale): Polymerizations were performed in 8 mL septum-capped reaction vials prepared in a N_2-filled glovebox. An oven-dried 8 mL septum-capped vial equipped with a stir bar was charged with vinyl ether monomer (0.76 mmol), 0.2 mL MePh, and 1.6 mL hexane. The vial was removed from the glovebox and cooled to -78 °C in a dry ice/acetone bath. After stirring at -78 °C for 20 min, 0.2 mL of anhydrous pre-chilled 50 mM trifluoromethanesulfonic acid in MePh was added to initiate the polymerization. The reaction was stirred at -78 °C for 30 minutes, after which 0.33 mL of Et_3N/MeOH solution (10% *v*/*v*) was added to quench the polymerization. Upon warming to room temperature, the mixture was washed with 1N HCl and all volatiles removed in vacuo. The resulting polymer was dried under vacuum for at least 12 h to a constant weight.

REFERENCES

(1) Akiyama, T.; Morita, H.; Itoh, J.; Fuchibe, K. Chiral Brønsted Acid Catalyzed Enantioselective Hydrophosphonylation of Imines: Asymmetric Synthesis of α-Amino Phosphonates. *Org. Lett.* **2005**, *7* (13), 2583–2585.

(2) Manxzer, L. E.; Deaton, J.; Sharp, P.; Schrock, R. R. *Tetrahydrofuran Complexes of Selected Early Transition Metals.*; Fackler Jr., J. P., Ed.; John Wiley & Sons, Ltd, 1982.

(3) Hatada, K.; Kitayama, T.; Matsuo, N.; Yuki, H. C-13 NMR Spectra and Spin-Lattice Relaxation Times of Poly(Alkyl Vinyl Ether)S. *Polym. J.* **1983**, *15* (10), 715–725.

(4) Teator, A. J.; Leibfarth, F. A. Catalyst-Controlled Stereoselective Cationic Polymerization of Vinyl Ethers. *Science.* **2019**, *363* (6434), 1439–1443.

(5) J. Tiegs, B.; Sarkar, S.; M. Condo, A.; Keresztes, I.; W. Coates, G. Rapid Determination of Polymer Stereoregularity Using Band-Selective 2D HSQC. *ACS Macro Lett.* **2016**, *5* (2), 181–184.

(6) Zinna, F.; Pescitelli, G. Towards the Limits of Vibrational Circular Dichroism Spectroscopy: VCD Spectra of Some Alkyl Vinylethers. *Chirality* **2016**, *28*, 143–146.

(7) Luisi, P. L.; Chiellini, E.; Franchini, P. F.; Orienti, M. Stereoregularity and Dipole Moments of Optically Active Poly-Alkyl-Vinyl-Ethers. *Die Makromol. Chemie* **1968**, *112* (2674), 197–209.

(8) Le, P. Q.; Nguyen, T. S.; May, J. A. A General Method for the Enantioselective Synthesis of α-Chiral Heterocycles. *Org. Lett.* **2012**, *14* (23), 6104–6107.

(9) Rueping, M.; Nachtsheim, B. J.; Koenigs, R. M.; Ieawsuwan, W. Synthesis and Structural Aspects of N-Triflylphosphoramides and Their Calcium Salts'highly Acidic and Effective Brønsted Acids. *Chem. - A Eur. J.* **2010**, *16* (44), 13116–13126.

(10) Lee, S.; Bae, H. Y.; List, B. Can a Ketone Be More Reactive than an Aldehyde? Catalytic Asymmetric Synthesis of Substituted Tetrahydrofurans. *Angew. Chemie - Int. Ed.* **2018**, *57* (37), 12162–12166.

(11) Byers, J. A.; Bercaw, J. E. Kinetic Resolution of Racemic α-Olefins with Ansa-Zirconocene Polymerization Catalysts: Enantiomorphic Site vs. Chain End Control. *Proc. Natl. Acad. Sci. U. S. A.* **2006**, *103* (42), 15303–15308.

(12) Teator, A. J.; Leibfarth, F. A. Catalyst-Controlled Stereoselective Cationic Polymerization of

Vinyl Ethers. *Science*. **2019**, *363*, 1439–1443.

APPENDIX D: SUPPORTING INFORMATION FOR CHAPTER 5

General Considerations

The following compounds were prepared according to previously reported literature procedures: squaramide **5.1**,[1] squaramide **5.4**,[2] squaramide **5.9**,[3] squaramide **5.10**,[4] 1-methoxyisochroman,[5] 1-(3,5-bis(trifluoromethyl)phenyl)-3-((*S*)-1-((*R*)-2-(4-fluorophenyl)pyrrolidin-1-yl)-3,3-dimethyl-1-oxobutan-2-yl)thiourea[5], 1-(3,5-bis(trifluoromethyl)phenyl)-3-cyclohexylthiourea,[6] and α-chloroethyl isobutyl ether.[7] Other squaramides reported in the main text were made through similar synthetic approaches as those listed previously. All vinyl ether monomers were dried over CaH_2 and distilled under vacuum prior to storage in a N_2-filled glovebox freezer before further use. Unless otherwise noted, solvents were dried and degassed using a Pure Process Technology solvent purification system and then subsequently stored over molecular sieves (3Å) in a N_2-filled glovebox. Other reagents whose syntheses are not described in Section 1.3 were purchased from commercial sources and used without further purification. All syntheses were performed under inert atmosphere (N_2) using flame-dried or oven-dried glassware unless specified otherwise. NMR spectra were recorded using a Bruker DRX 400 MHz, Bruker AVANCE III 500 MHz, or Bruker AVANCE III 600 MHz CryoProbe spectrometer. Chemical shifts δ (ppm) are referenced to tetramethylsilane (TMS) using the residual solvent as an internal standard (^{1}H and ^{13}C). For ^{1}H NMR: $CDCl_3$, 7.26 ppm. For ^{13}C NMR: $CDCl_3$, 77.16 ppm. Coupling constants (*J*) are expressed in hertz (Hz). The use of ^{13}C NMR to quantify tacticity of several poly(vinyl ethers) has been established and reported previously.[8,9]

Macromolecular Characterization

Gel permeation chromatography (GPC) was performed on a Waters 2695 separations module liquid chromatograph equipped with either four Waters Styragel HR columns (WAT044225, WAT044231, WAT044237, and WAT054460) arranged in series or two Agilent Resipore columns (PL1113-6300) maintained at 35 °C, and a Waters 2414 refractive index detector at room temperature. GPC was also performed on a Tosoh EcoSEC Elite GPC system equipped with a

TSKgel Super HM-M (17392) column maintained at 40 °C with an RI detector. Tetrahydrofuran was used as the mobile phase at a flow rate of 0.5 mL/min (Tosoh GPC) or 1.0 mL/min (Waters GPC). Molecular weight and dispersity data are reported relative to polystyrene standards.

Melting-transition temperature (T_m) and glass-transition temperature (T_g) of precipitated and dried polymer samples were measured using differential scanning calorimetry (DSC) on a TA Instruments Discovery DSC. Unless specifically noted otherwise, values for T_m and T_g were obtained from a second heating scan after the thermal history was removed.

Syntheses and Characterization Data

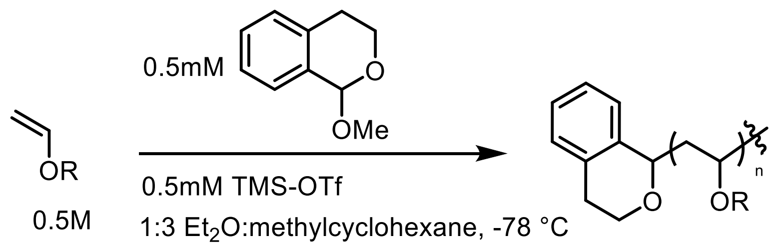

General Procedure for Control Polymerization: Polymerizations were performed in 8 mL septum-capped reaction vials prepared in a N_2-filled glovebox. An oven-dried 8 mL septum-capped vial equipped with a stir bar was charged with 0.75 mmol vinyl ether monomer, 0.225 mL diethyl ether, and 1.125 mL methylcyclohexane. A separate 8 mL septum-capped vial equipped with a stir bar was charged with 0.45 mL of a 5.5 mM stock solution of isochroman acetal in diethyl ether. A separate 8 mL septum-capped vial equipped with a stir bar was charged with 0.2 mL of a 50 mM trimethylsilyl thrifluoromethanesulfonate solution in diethyl ether. The three vials were removed from the glovebox and cooled to -78 °C in a dry ice/acetone bath. After stirring at -78 °C for 20 min, 0.05 mL of the trimethylsilyl thrifluoromethanesulfonate solution was transferred via dry syringe to the vial containing the isochroman acetal solution. To initiate polymerization, 0.15 mL of the newly formed solution (that is now 5 mM with respect to methoxytrimethylsilane, an isochroman-derived cationogen, and trifluoromethanesulfonate) was transferred via dry syringe to the vial containing the monomer solution. The reaction was stirred at -78 °C for 20 minutes, after which 0.20 mL of

Et_3N/MeOH solution (10% v/v) was added to quench the polymerization. Upon warming to room temperature, the mixture was washed with 1N HCl, and all volatiles removed in vacuo. The crude polymer was dissolved in 1‑2 mL CH_2Cl_2 and filtered through a plug of SiO2 (4-5 cm) in a glass pipette eluting with additional CH_2Cl_2. The resulting purified polymer was dried under vacuum for at least 12 h to a constant weight.

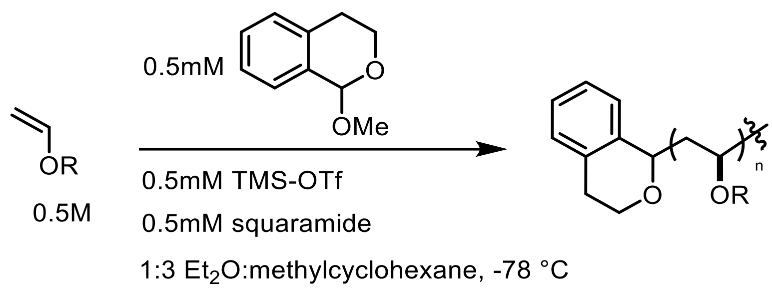

General Procedure for Polymerization with a Squaramide: Polymerizations were performed in 8 mL septum-capped reaction vials prepared in a N_2-filled glovebox. An oven-dried 8 mL septum-capped vial equipped with a stir bar was charged with 0.75 mmol vinyl ether monomer, 0.225 mL diethyl ether, and 1.125 mL methylcyclohexane. A separate 8 mL septum-capped vial equipped with a stir bar was charged with 0.0025 mmol squaramide and 0.45 mL of a 5.5 mM stock solution of isochroman acetal in diethyl ether. A separate 8 mL septum-capped vial equipped with a stir bar was charged with 0.2 mL of a 50 mM trimethylsilyl thrifluoromethanesulfonate solution in diethyl ether. The three vials were removed from the glovebox and cooled to -78 °C in a dry ice/acetone bath. After stirring at -78 °C for 20 min, 0.05 mL of the trimethylsilyl thrifluoromethanesulfonate solution was transferred via dry syringe to the vial containing the isochroman acetal/squaramide solution. To initiate polymerization, 0.15 mL of the newly formed solution (that is now 5 mM with respect to methoxytrimethylsilane, an isochroman-derived cationogen, and trifluoromethanesulfonate-squaramide complex) was transferred via dry syringe to the vial containing the monomer solution. The reaction was stirred at -78 °C for 20 minutes, after which 0.20 mL of Et_3N/MeOH solution (10% v/v) was added to quench the polymerization. Upon warming to room temperature, the mixture was washed with 1N HCl, and all volatiles removed in vacuo. The crude polymer was dissolved in 1‑2 mL CH_2Cl_2 and filtered through a plug of SiO2 (4-5 cm) in a glass pipette eluting with additional CH_2Cl_2. The resulting purified polymer was dried under vacuum for at least 12 h to a constant weight.

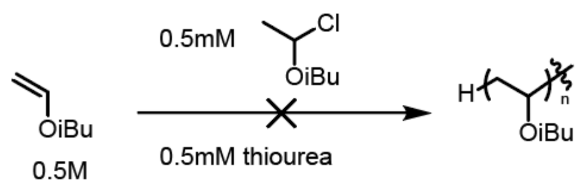

General Procedure for Attempted Polymerization with Thiourea: Polymerizations were performed in 8 mL septum-capped reaction vials prepared in a N_2-filled glovebox. An oven-dried 8 mL septum-capped vial equipped with a stir bar was charged with 0.75 mmol vinyl ether monomer, 1.20 mL solvent, and 0.15 mL of a 5 mM α-chloroethyl isobutyl ether solution. A separate 8 mL septum-capped vial equipped with a stir bar was charged with 0.15 mL of a 5 mM thiourea solution. These two vials were removed from the glovebox and cooled in a cold bath. After stirring at cold temperatures for 20 min, the contents of the thiourea solution vial were transferred via dry syringe to the vial containing the monomer solution. The reaction was stirred at cold temperature for 20 minutes, after which 0.20 mL of Et_3N/MeOH solution (10% v/v) was added to quench the polymerization. Upon warming to room temperature, the mixture was washed with 1N HCl, and all volatiles removed in vacuo.

Optimization Studies

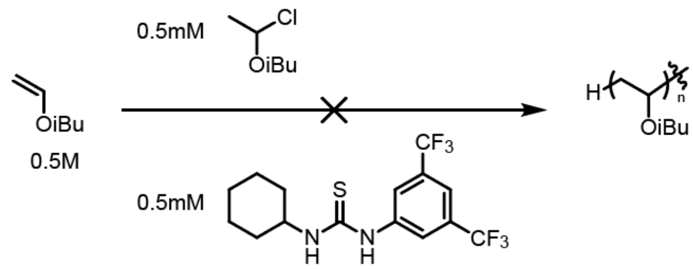

solvent	temperature	reactivity
1:3 Et_2O:methycylohexane	-40 °C	NR
1:3 Et_2O:methycylohexane	-78 °C	NR
methyl *tert*-butyl ether	-40 °C	NR
methyl *tert*-butyl ether	-78 °C	NR

Attempted polymerizations of iBVE using an α-chloroethyl isobutyl ether initiator and a thiourea catalyst. NR = no reaction.

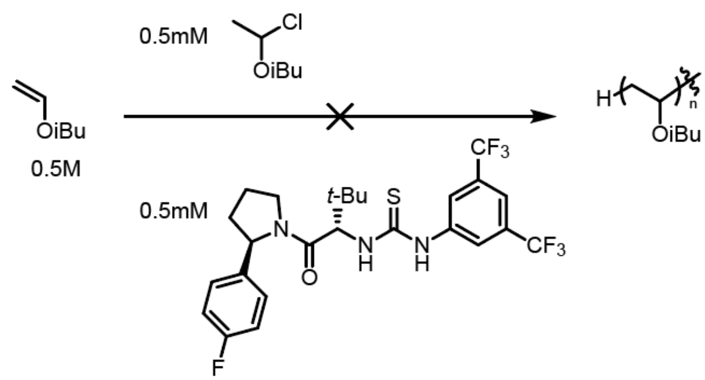

solvent	temperature	reactivity
1:3 Et_2O:methycylohexane	-40 °C	NR
1:3 Et_2O:methycylohexane	-78 °C	NR
methyl *tert*-butyl ether	-40 °C	NR
methyl *tert*-butyl ether	-78 °C	NR

Attempted polymerizations of iBVE using an α-chloroethyl isobutyl ether initiator and a chiral thiourea catalyst. NR = no reaction.

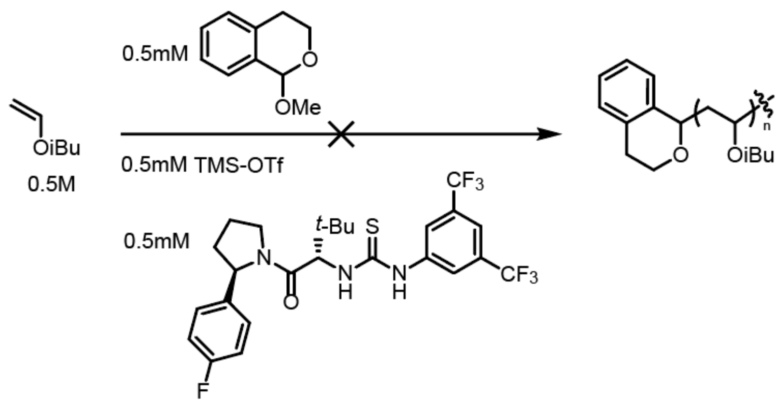

solvent	temperature	reactivity
1:3 Et_2O:methycylohexane	-40 °C	NR
1:3 Et_2O:methycylohexane	-78 °C	NR
methyl *tert*-butyl ether	-40 °C	NR
methyl *tert*-butyl ether	-78 °C	NR

Attempted polymerizations of iBVE interfacing a chiral thiourea with an isochroman acetal derived cationogen. NR = no reaction.

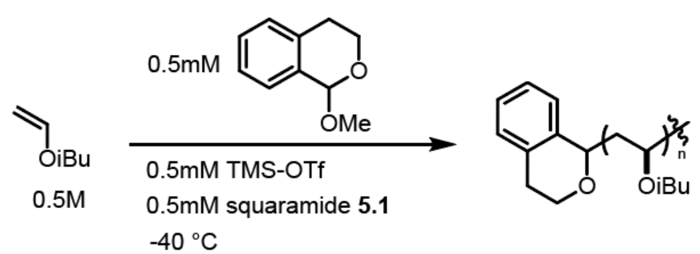

ratio of Et_2O: methylcyclohexane	M_n (kg mol^{-1})	*Đ*	*m* (%)
9:1	35	1.5	71
3:1	52	1.7	71
1:1	55	1.6	74
1:3	45	1.8	75
1:9	56	1.9	71

Screening solvent at -40 °C in the polymerization of isobutyl vinyl ether using squaramide **5.1** and an isochroman acetal derived cationogen.

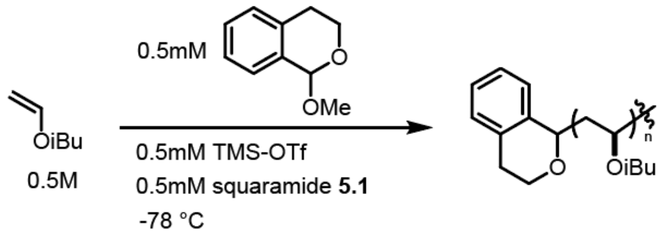

ratio of Et_2O: methylcyclohexane	M_n (kg mol^{-1})	*Đ*	*m* (%)
9:1	50	1.2	75
3:1	61	1.3	75
1:1	82	1.5	76
1:3	77	1.2	77

Screening solvent at -78 °C in the polymerization of isobutyl vinyl ether using squaramide **5.1** and an isochroman acetal derived cationogen.

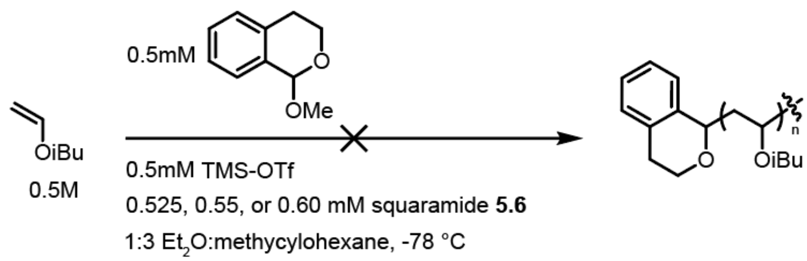

[squaramide **5.6**]	reactivity
0.525 mM	NR
0.55 mM	NR
0.60 mM	NR

Attempted polymerizations of isobutyl vinyl ether with an isochroman acetal derived cationogen and molar excess of squaramide **5.6**. NR = no reaction.

<u>Kinetic Studies</u>

Representative Polymerization & NMR Sample Preparation for Kinetic Analysis:

Polymerizations for kinetic analyses were set up as originally described above. Instead of quenching with 0.20 mL of Et_3N/MeOH solution (10% v/v) after 20 minutes, however, these polymerizations were quenched after 5, 10, 15, or 20 s. The monomer concentration present immediately prior to quenching was found through the following protocol. After quenching (*vide supra*) and allowing the reaction set-up to warm to room temperature, an NMR sample was prepared with 0.1 mL of the quenched reaction solution and 0.5 mL of a 42.6 mM 1,4-dimethoxybenzene solution in $CDCl_3$. The unique proton signals from 1,4-dimethoxybenzene allowed this to serve as an internal standard, against which the vinyl protons of isobutyl vinyl ether were integrated to calculate conversion. Knowing the % conversion allowed for the calculation of the monomer concentration present immediately prior to quenching.

A total of five data points (spanning 20 seconds) were used to calculate a first order rate constant (as represented in **Figure 5.3** in the main text). Analysis of the stereoselective polymerization using squaramide **5.6** ([iBVE]=0.5 M, [isochroman acetal]=0.5 mM, [TMS-OTf]=0.5 mM, [squaramide **5.6**] =0.5 mM) and the control reaction conditions ([iBVE]=0.5 M, [isochroman acetal]=0.5 mM, [TMS-OTf]=0.5 mM) was conducted three times at each 5 s interval.

Pseudo-First Order Kinetics: The cationic polymerization of vinyl ethers, including isobutyl vinyl ether, may be represented as:

$$M + C \longrightarrow P$$

Under the assumption that there are negligible side-reactions taking place in the formation of polymer (P), vinyl ether monomer (M) will always be present in a large excess over the catalyst (C). As such, pseudo-first-order kinetics are valid for rate calculations.[10] In this scenario, the following rate law applies:

$$\frac{d[P]}{dt} = k[M][C]_0 = k[M]$$

The integrated form of the rate equation is represented as:

$$\ln[M] = \ln[M]_0 - kt$$

This equation indicates that plotting -ln[M] versus *t* (s) should give a linear plot where *k* is equal to the slope of the line. **Figure 5.3** in the main text illustrates this relationship.

Temperature Dependence on Stereoselectivity

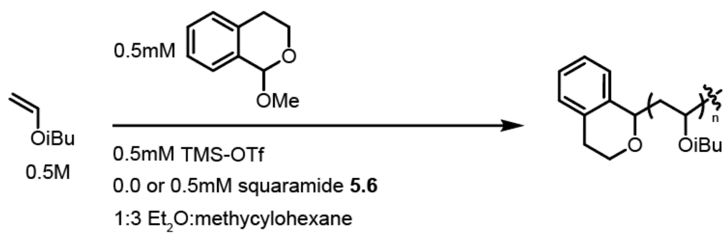

temperature	[squaramide **5.6**]	M_n (kg mol^{-1})	*Đ*	*m* (%)
-40 °C	0.0 mM	6	2.1	65
-61 °C	0.0 mM	27	1.8	69
-78 °C	0.0 mM	51	1.7	71
-40 °C	0.5 mM	38	1.8	74
-61 °C	0.5 mM	49	1.5	75
-78 °C	0.5 mM	90	1.4	83

Temperature dependence on stereoselectivity of both the stereoselective polymerization and the control polymerization. The experimental data seen in **Figure 5.4** in the main text as the data portrayed here.

Substrate Scope

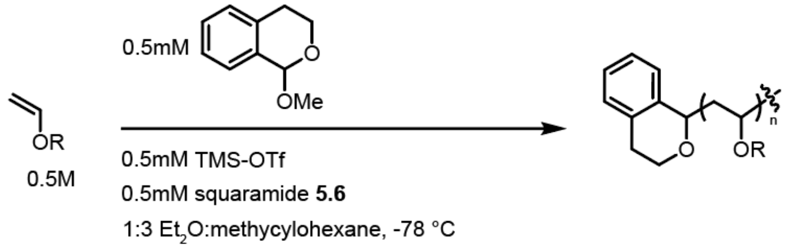

monomer	M_n (kg mol^{-1})	*Đ*	*m* (%)
nPrVE	48	1.6	80
nBVE	57	1.7	82
iBVE	90	1.4	83
iPVE	48	1.9	71
tBVE	11	1.7	65

Representative structure-reactivity profiles for a variety of alkyl vinyl ethers synthesized with the stereocontrolled reaction conditions using squaramide **5.6**.

REFERENCES

(1) Wendlandt, A. E.; Vangal, P.; Jacobsen, E. N. Quaternary Stereocentres via an Enantioconvergent Catalytic SN1 Reaction. *Nature* **2018**, *556* (7702), 447–451.

(2) Banik, S. M.; Levina, A.; Hyde, A. M.; Jacobsen, E. N. Lewis Acid Enhancement by Hydrogen-Bond Donors for Asymmetric Catalysis. *Science.* **2017**, *358*, 761–764.

(3) Liu, R. Y.; Wasa, M.; Jacobsen, E. N. Enantioselective Synthesis of Tertiary α-Chloro Esters by Non-Covalent Catalysis. *Tetrahedron Lett.* **2015**, *56* (23), 3428–3430.

(4) Bendelsmith, A. J.; Kim, S. C.; Wasa, M.; Roche, S. P.; Jacobsen, E. N. Enantioselective Synthesis of α-Allyl Amino Esters via Hydrogen-Bond-Donor Catalysis. *J. Am. Chem. Soc.* **2019**, *141* (29), 11414–11419.

(5) Reisman, S. E.; Doyle, A. G.; Jacobsen, E. N. Enantioselective Thiourea-Catalyzed Additions to Oxocarbenium Ions. *J. Am. Chem. Soc.* **2008**, *130* (23), 7198–7199.

(6) Sun, J.; Kuckling, D. Synthesis of High-Molecular-Weight Aliphatic Polycarbonates by Organo-Catalysis. *Polym. Chem.* **2016**, *7* (8), 1642–1649.

(7) Varner, T. P.; Teator, A. J.; Reddi, Y.; Jacky, P. E.; Cramer, C. J.; Leibfarth, F. A. Mechanistic Insight into the Stereoselective Cationic Polymerization of Vinyl Ethers. *J. Am. Chem. Soc.* **2020**, *142* (40), 17175–17186.

(8) Hatada, K.; Kitayama, T.; Matsuo, N.; Yuki, H. C-13 NMR Spectra and Spin-Lattice Relaxation Times of Poly(Alkyl Vinyl Ether)S. *Polym. J.* **1983**, *15* (10), 715–725.

(9) Teator, A. J.; Leibfarth, F. A. Catalyst-Controlled Stereoselective Cationic Polymerization of Vinyl Ethers. *Science.* **2019**, *363* (6434), 1439–1443.

(10) Teator, A. J.; Varner, T. P.; Jacky, P. E.; Sheyko, K. A.; Leibfarth, F. A. Polar Thermoplastics with Tunable Physical Properties Enabled by the Stereoselective Copolymerization of Vinyl Ethers. *ACS Macro Lett.* **2019**, *8* (12), 1559–1563.